Nuclear Architecture and Chromatin Dynamics in Development and Regeneration

Hannah Arbach

A dissertation

submitted in partial fulfillment of the

requirements for the degree of

Doctor of Philosophy

University of Washington

2021

Reading Committee:

Andrea Wills, Chair

Dana Miller

David Kimelman

Program Authorized to Offer Degree:

Department of Biochemistry

University of Washington

Abstract

Nuclear Architecture and Chromatin Dynamics in Development and Regeneration

Hannah Arbach

Chair of the Supervisory Committee:

Professor Andrea Wills, PhD

Biochemistry

The nucleus and its contents are not just static entities which offer a location and template for transcription. In both development and disease alterations in nuclear structure and/or chromatin architecture can contribute to normal or impaired function. In this study I used *Xenopus tropicalis* to study two processes that alter nuclear structure or chromatin architecture. Fist, to study the impact of nuclear compartment shape I characterized cells with branched nuclei in the tail fin. We found that despite an extreme nuclear shape, cell with branched nuclei had active cell cycles, and marks of active transcription, as well as transcriptional repression. Our characterization also determined that actin and laminb1 were necessary for maintaining branched nuclear structure. Second, I studied how dynamic changes in chromatin structure facilitated by epigenetic modifications enabled tail regeneration. Using ATAC-seq (An Assay for Transposase Accessible Chromatin) we queried changes in chromatin accessibility upon inhibition of Histone deacetylases (HDACs), and the enzymatic component of the polycomb repressive 2 complex, enhancer of zeste 2 (EZH2), both of which serve to close chromatin. We found that HDACs and EZH2 had distinct targets in the first 24 hours post amputation (hpa). Early inhibition of HDAC activity impairs tail regeneration and promoter regions are particularly sensitive. Our analysis uncovered a role for

HDAC activity in regulation of neural regeneration. EZH2 inhibition during the first 24 hpa also impairs regeneration, however gene bodies were much more susceptible to be more accessible upon EZH2 inhibition. We also uncovered a role in early EZH2 activity in regulating the immune response that occurs after injury. Overall, we leveraged the powerful model system *Xenopus tropicalis* to establish a new model for extreme nuclear morphology and identify alterations in chromatin structure that regulate regenerative processes.

TABLE OF CONTENTS

LIST OF FIGURES

LIST OF TABLES

ACKNOWLEDGEMENTS

As I have been writing this thesis and reflecting on my journey to and through graduate school, I feel (yes, if any of my lab mates read this, I said feel) an overwhelming sense of support and privilege to be standing at this point in my life. The Biochemistry Department has been an incredible community for my studies, thank you to all its members for creating this environment and striving to leave it even better than how you found it.

I thank Andrea Wills (Boss) my mentor. Thank you for allowing me to take on a project that was out of both of our previous areas of study and run with it. Thank you for allowing me to have big ideas and reminding me to break those ideas into bite size questions. You have been an incredible mentor, letting me drive my project forward and pursue aspects that interest me and my own hypotheses, all while being there to make sure I did not fall off a cliff. Boss, I am so appreciative of the support both scientifically, and personally, your support of balance and caring for myself in life, inside and outside the lab will be something I hope to emulate as a mentor in the future. Thank you for finding all my spelling mistakes.

Dana Miller, David Kimelman, Trisha Davis, and Steve Henikoff you all have been an incredible committee. Thank you for bringing so many scientific perspectives to the table, and for support through fellowship writing, and project changes. I am so appreciative of your constructive feedback that significantly enhanced my research and encouraged me to expand my skillset beyond wet lab work.

I would like to acknowledge my family as my original scientific mentors and supporters. Thank you to my parents for allowing me to take apart the vacuum cleaner to figure out how it worked. You have encouraged and enabled my curiosity and encouraged me to seek solutions to problems and knowledge. Even if I was very frustrated when I had to look up every single word, I wanted to know the meaning of in the unabridged dictionary. To my sister who has been a role model in pursuing her interest and allowing herself to follow her passions rather than feeling the need to continue something that does not fulfill her. To Sutton my niece and Hayden my nephew for making me smile. To my grandparents thank you for being an active part of my life and always supporting me.

Thank you to my scientific mentors from Mount Holyoke. Especially Wei Chen, who encouraged me to give research a try, and suggesting Katie McMenimen's lab as a potentially good fit. Katie, thank you for teaching me that I needed to label graphs on my slides. I am forever grateful for you providing the foundations for my research career, you were incredibly patient with me and gave me the confidence to try new experiments and not ask permission first. Thank you for continuing to support me through grad school both personally and professionally and calling me out when I am being afraid to commit. Finally, thank you

to Amy Camp for making me write so much, and for providing thoughtful critical feedback, I am a far better science writer for it.

I am incredibly fortunate for the scientific community that has supported me, and my projects through graduate school. To all the current and former Wills Lab members, thank you. I am especially grateful to Meghna Singh, Anneke Kakebeen, Madison Williams, and Jeet Patel for all the helpful discussions, and making the lab accessible for me and helping with experiments after my surgeries. To Marcus Harland-Dunaway, and Ellie Pickering the real MVPs, thank you for working with me on these experiments and adding your creativity and ideas to these projects. To Chris Braden and Alex Chitsazan, thank you for your seemingly limitless patience with me in learning how to computer, and for help and guidance in the bioinformatic analysis. Thank you to the frogs.

I have been fortunate to also participate in MF4 and regeneration super group meetings and a journal club with the Miller and Hoppins labs which have improved my talks, and always left me new experiments to try, thank you to all who participated in those groups.

The frog and developmental biology communities have been a source of support and inspiration, and I am lucky to be a part of this community. I would especially like to thank John Wallingford, Richard Harland, and Laura Anne Lowery; you have gone above and beyond in your support of me as a scientist. Thank you for your feedback, discussions, reagents, whiskey, and encouragement.

While this may be unusual, I would like to thank all my care teams through the six surgeries I have had through graduate school. Especially to Megan Jones DPT, and Dr. Sarah Burns who have not only fixed my feet but listened to and encouraged me in my research.

I would like to acknowledge the Coast Salish peoples of this land, the land which touches the shared waters of all tribes and bands within the Suquamish, Tulalip, and Muckleshoot nations.

To the friends who have become my family throughout my life, thank you. Thank you, Ellie DeLeon, for your limitless support and for being patient with me as the first student I ever mentored. To my Seattle neighborhood family especially, Roberto, Susan, Ryan, Cyanna, Mila, Leo, Mikey, and Abi I cannot express enough gratitude to you all. You have been with me through all the highs and lows these past years and have loved and supported me through it all, thank you for the laughs, beers, adventures, and memories. Thank you to Chris and Lori for supplying me with beer and proving a safe and welcoming space for a community to come together. Thank you to Sharon Blaney and Billie Bear Blaney for being in my COVID family and helping me push through to finish and liking all my culinary experiments.

Big Norm and Little Penelope thank you for being incredible pets and providing comfort, and always listening to any of my complaints, stressors, or feelings without judgement.

Finally, to my incredible wife Megan. The past 6 years have had some of the greatest moments and some of the most painful I have ever experienced. Thank you for everything you have done to support me through all of it, thank you for encouraging me to celebrate my accomplishments. Thank you for the sacrifices you have made to take care of me, and for helping to keep me optimistic even when I was in pain. Thank you for loving all the parts of me.

DEDICATION

This work is dedicated to Laura Murphy (February 11, 1993 – July 16, 2016) who was killed by a drunk driver weeks before she was due to start her doctoral studies at the University of California Berkley.

CHAPTER 1. INTRODUCTION

Long before the discovery of the cell humans have been fascinated by how an organism, any organism, develops. In fact this is a unifying human experience, documented in a plethora of cultures from Aristotle's *On the Generation of Animals* in ancient Greece, to remarkable illustrations and theories of early human development in ancient Asian cultures, and to the documentation of cases of what we now call congenital anomalies in Mexico (Wallingford, 2021). Today, developmental biology reflects the diverse roots upon which it was founded. The field has expanded from observing the embryo to deeply characterizing the cellular and molecular processes that enable a single cell to develop into an organism with a multitude of cell types, and after those multitude of cell types form how they function and respond to an ever-changing environment including damage (Wallingford, 2019). The robust expansion of technologies in the past several decades has allowed present scientists to deeply probe the various mechanisms of regulation that ultimately determine the final form and function of an organism. A hotbed of discovery has been in understanding the role of the regulation of the nucleus and its genomic contents (Lis, 2019; Mattout et al., 2015a).

For my thesis research I sought to characterize nuclear structure and chromatin architecture and their roles in development and regeneration utilizing *Xenopus tropicalis* as a model vertebrate system. In this chapter, I introduce (1) *Xenopus tropicalis* as a powerful model for vertebrate development and regeneration, (2) the role of nuclear structure in biological processes, and finally (3) epigenetic regulation of chromatin accessibility and transcription.

1.1.Xenopus tropicalis: A diploid vertebrate model for development and regeneration

Xenopus has been a critical genus for experimental developmental biology. *Xenopus tropicalis* offers many advantages that I have leveraged throughout this work. First, there are rich resources available and curated by the community through Xenbase (Karimi et al., 2018). *Xenopus tropicalis* develops ex utero allowing for perturbations and manipulation from fertilization. Important to this work is the ability to microinject embryos with mRNA to express fluorescently labeled proteins, which enable live imaging of many biological processes, to induce overexpression of a particular gene, or to induce expression of a dominant negative allele. This is also particularly powerful because the fates of *Xenopus* blastomeres are known, allowing targeted injections to specific presumptive tissues (Moody, 1987; Sive et al., 2010). In addition, explants of developing embryos can be removed and continue to develop in culture (Afouda and Hoppler, 2009; Durand, 2016; Khokha et al., 2002; Sive et al., 2007; Sive et al., 2010). Explants enable the study of cell fate acquisition, cell migration, and importantly identification of cell-autonomous versus non-autonomous processes.

Xenopus are commonly staged by Nieuwkoop and Farber (NF) staging criteria, and by NF 41 (or approximately 3 days post fertilization, dpf) tadpoles have a clearly defined tail, gut, heart, head, and organ systems (Nieuwkoop and Faber, 1994). The tadpole has melanocytes but its tail and axial structures are transparent, which allows for live imaging of complex processes at both the macro and microscales. This transparency can be leveraged with the microinjection of mRNA of fluorescently labeled proteins to image live and dynamic processes in the tadpole with high spatiotemporal resolution (Kieserman et al., 2010; Wallingford, 2010). The transparency of the tadpole also allows for the use of imaging on fixed samples such as immunofluorescence without the need for chemical clearing (Sive et al., 2010). Also, at this stage and other tadpole stages *Xenopus* is highly regenerative in many tissues. Unlike other regenerative species that are commonly used in research settings, *Xenopus* gradually loses the capacity to regenerate over time making it a unique model to explore pro-regenerative versus anti-regenerative responses in the same genetic context (Kakebeen and Wills, 2019; Kawasumi et al., 2013; Phipps et al., 2020).

Robust work has been completed on a variety of regenerative tissues and stages in *Xenopus.* For the purposes of this thesis, I will restrict the scope of discussion to the regeneration of the tail after amputation

at NF stage 41. *Xenopus tropicalis* is able to regenerate all the tissues of the tail by approximately 5 days post amputation (dpa), and even by 3dpa the regenerated tail has all the features of a complete tail (Figure 1-1) (Kakebeen and Wills, 2019). During regeneration of the tail tissues certain aspects of development are recapitulated, such as proliferation to grow new tissues, signaling to coordinate patterning and cell fate decisions to generate a new properly patterned tissue. Anterior Hox transcription factors for example, are important for establishing positional identity during regeneration (Christen et al., 2003). Using small molecule inhibitors, it has been established that the regenerative processes re-utilize established developmental pathways such as BMP, WNT, FGF, Notch, Shh, and Nodal signaling, and that disruption of these pathways leads to defective regeneration (Beck et al., 2003; Ho and Whitman, 2008; Lin and Slack, 2008; Slack et al., 2004; Slack et al., 2008; Taniguchi et al., 2014). Use of heat-shock inducible transgenic lines have furthered these studies to establish epistatic relationships between some of these developmental pathways. Using this approach it is known that BMP signaling is upstream of WNT signaling which is in turn upstream of FGF signaling during both tail and limb bud regeneration (Lin and Slack, 2008).

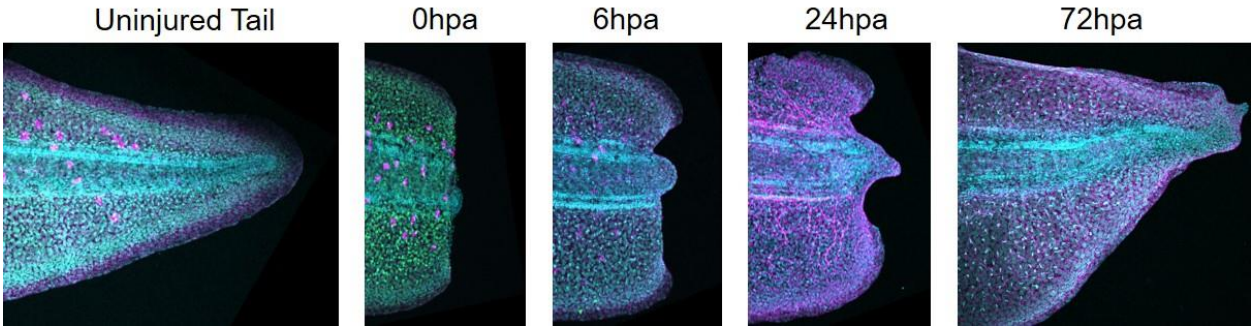

Figure1-1 Regeneration time course of *X. tropicalis* tail
Cyan = DAPI, Magenta = ac-tubulin, Green = H3k27ac

The rapidly evolving spectrum of next-generation sequencing, and *Xenopus tropicalis'* sequenced diploid genome, have sparked a burst in recent studies probing molecular mechanisms enabling regeneration (Grainger, 2012; Hellsten et al., 2010; Karimi et al., 2018). Comprehensive studies of transcriptional dynamics of regeneration using microarray and RNA-seq, including single-cell approaches, have identified biological processes that may differ from other wound healing responses that lead to scarring rather than

regrowth, including reactive oxygen species, metabolic enzymes, innate immune responses, and epigenetic modifications (Aztekin et al., 2019; Chang et al., 2017; Kakebeen et al., 2020; Lee-Liu et al., 2014; Love et al., 2011). Synthesizing the current work in the field has enabled a basic understanding of general phases of whole tail regeneration (Kakebeen and Wills, 2019). Immediately after injury there is an inflammatory response which is required for wound healing and regeneration (Aztekin et al., 2020; Julier et al., 2017). Other early signals in the *Xenopus* regenerative response include reactive-oxygen signaling and bioelectric signaling (Busse et al., 2018; Ferreira et al., 2018). During the first 24 hours post amputation (hpa) the wound epithelium is formed over the injury site which requires coordinated cell migration and communication (Aztekin et al., 2019; Ho and Whitman, 2008; Lin and Slack, 2008). In addition during the first 24 hpa there is critical regulation of the differentiation of neural progenitors (Kakebeen et al., 2020). In contrast to other vertebrate models such as axolotls and zebrafish, a mass of undifferentiated cells known as a blastema does not form in the regeneration bud in *Xenopus* (Gerber et al., 2018; Poss et al., 2000). After formation of the wound epithelium, new tissues need to be grown and properly patterned; this is facilitated by signaling that has been shown to come from cells up to 500 µm from the amputation plane along with a burst of proliferative activity (Lee-Liu et al., 2014; Lin et al., 2007).

1.2. The role of nuclear structure in biological processes

The nucleus is an important organelle that serves to store and organization of the genome. Changes in both the shape of the nuclear compartment and the organization of the genome within the nucleus can alter cellular function (Bertero et al., 2019; Davidson and Lammerding, 2014; Fraser et al., 2015; Gilsbach et al., 2018; Mattout et al., 2015a; Peric-Hupkes et al., 2010; Pillay et al., 2013; Ramdas and Shivashankar, 2015; Rowat et al., 2013; Shah et al., 2013). While nuclear shape is generally round or ellipsoid in most cell types across the animal kingdom, a few healthy cell types exhibit non-ellipsoid morphologies, including neutrophils, which have a distinct lobular structure that allows them to extravasate to areas with damaged tissue (Pillay et al., 2013; Rowat et al., 2013). However, neutrophils are one of the exceptions; perturbations in nuclear morphology are frequently associated with diseases, such as progeria, Pelger-Huet anomaly, forms of muscular dystrophy, cardiomyopathies, and cancers (Bonne et al., 1999; Davidson and Lammerding, 2014; Frost et al., 2016; King and Lusk, 2016; Webster et al., 2009). In the past decade it has become clear that these changes in nuclear shape can have not only biophysical implications but also can cause changes in the structure and packaging of the genome (Bertero et al., 2019; Perovanovic et al., 2016; Shah et al., 2013).

Nuclear morphological variation is associated with changes in the composition or in the functionality of the nucleoskeleton (Davidson and Lammerding, 2014; Goldman et al., 2004; Rowat et al., 2013; Solovei et al., 2013). The nucleoskeleton is a complex network of lamins and associated proteins, the LINC (linker of nucleoskeleton and cytoskeleton) complex, and cytoskeletal components, including actin (Chang et al., 2015; Davidson and Lammerding, 2014; King and Lusk, 2016; Ramdas and Shivashankar, 2015; Webster et al., 2009; Wiggan et al., 2017). Variation in the components of the nucleoskeleton also have consequences both for the biophysical function of the associated tissue and for genomic organization (Bertero et al., 2019; Dahl et al., 2006; Jevtić et al., 2015; Lammerding et al., 2006; Perovanovic et al., 2016; Pillay et al., 2013; Shah et al., 2013; Solovei et al., 2009; Solovei et al., 2013; Verstraeten et al., 2008; Zwerger et al., 2013).

Alterations in heterochromatin propagation is linked to changes in nuclear morphology caused by perturbations to lamin proteins, known as laminopathies (Davidson and Lammerding, 2014; Perovanovic

et al., 2016; Shah et al., 2013). Hutchinson-Gilford Progeria Syndrome (HGPS) is a laminopathy that causes premature aging, and is associated with mutations in *LMNA* that lead to nuclear envelope ruffling (Shah et al., 2013). As cultured cells with *LMNA* mutations undergo more passages, they acquire progressively more nuclear ruffling and alterations of heterochromatin, resembling senescent cells rather than proliferative cells. Similar alterations in heterochromatic regions are seen in LMNB1-depleted cells and cancer cells (Perovanovic et al., 2016; Shah et al., 2013). This suggests that alteration of the nucleoskeleton can contribute to large-scale chromatin reorganization and gene expression contributing to aging or pathologies.

Despite lack of a dramatic change to nuclear envelope morphology, major chromatin remodeling occurs throughout development, cellular differentiation and aging (Krumm and Duan, 2019; Mattout et al., 2015a; Shah et al., 2013; Stergachis et al., 2013). One type of remodeling event that has been studied well is how regions of chromatin change association with the nuclear lamina during differentiation of neuronal cell types (Fraser et al., 2015; Peric-Hupkes et al., 2010). During differentiation, the genetic programs needed to carry out cellular function change and genes need to be precisely activated and silenced. Heterochromatin is strongly associated with the nuclear lamina (Fraser et al., 2015; Mattout et al., 2015b; Solovei et al., 2013; Towbin et al., 2012). It has been shown through differentiation of a variety of cell-types, regions of chromatin that are inactive early in development and later become active lose association with the nuclear lamina just before they are expressed. In contrast, regions that are initially expressed and then later become repressed gain association with the nuclear lamina (Dixon et al., 2012; Dixon et al., 2015; Guelen et al., 2008). These dynamic remodeling events are critical for proper development, and our understanding of the nuances of these changes are expanding (Peric-Hupkes et al., 2010).

Changes in association with the nuclear lamina are not the only important and dynamic reorganization events that regulate chromatin. In studies which map the interactions between large topologically associated domains (TADs) of chromatin that can be distant in sequence space, TADs are classified as belonging to the A or B compartment of the nucleus. The A compartment which is generally associated with less compact chromatin and higher gene expression, and the B compartment which is generally associated with chromatin compaction and decreases in gene expression (Dixon et al., 2012; Krumm and Duan, 2019).

In cardiomyocyte differentiation and disease both epigenetic states as well as changes between A and B compartments have been shown to be integral to regulating gene expression (Bertero et al., 2019; Gilsbach et al., 2018). Both RNA-seq and ATAC-seq (assay for transposase accessible chromatin) confirmed that transitions from the B to A compartment resulted in increased chromatin accessibility and increased gene expression of the genes in the associated region generally, and vice-versa. Loss of specific trans-interacting chromatin domains were also shown to be deleterious to cardiomyocyte differentiation (Bertero et al., 2019). In addition, changes in both methylation and acetylation state of DNA and histones have been shown to be critical in development of cardiomyocytes, and loss of these patterns results in failure to properly differentiate. If these states are not maintained in the mature tissue it can also lead to disease states (Gilsbach et al., 2018).

Re-organization of the genome is not only critical from a gene regulatory viewpoint but can also confer advantageous properties for a tissue's function. In rod photoreceptors, more compact chromatin that in most other cell types would be generally associated with the nuclear periphery is pushed to the center of the nucleus. This reversal of organizational strategies prevents the distortion of incoming light enabling greater vision clarity. In fact, loss of this organizational pattern is associated with aging and decreased visual acuity (Solovei et al., 2009).

Overall, it is unclear what changes in nuclear envelope shape, and chromatin architecture that are advantageous to function, such as the structures found in neutrophils or rod photoreceptors. On the other side of this, it is unclear what environments or triggers cause changes in nuclear structure and organization that lead to diseases? In Chapter 2 I detail my work describing a population of epidermal cells in the *Xenopus* tail fin that have elaborately branched nuclear morphologies and investigate the role of components of the nucleoskeleton in maintaining their structure.

1.3. Epigenetic regulation of chromatin accessibility and transcription

Understanding gene regulatory mechanisms of regeneration has been at the forefront of the regeneration field across many model organisms. In particular the use of RNA-seq and single-cell RNA-seq has caused an explosion in the understanding of gene expression states during the regenerative response in a variety of organisms (Aboobaker, 2011; Aztekin et al., 2019; Chang et al., 2015; Gehrke et al., 2019; Jorstad et al., 2017; Kakebeen et al., 2020; Lee-Liu et al., 2014; Love et al., 2011; Oulhen et al., 2016; Siebert et al., 2019; Storer et al., 2020; Wu et al., 2013). While these studies show the differentially expressed genes during regeneration, they can lack information on what facilitates the changes in gene expression for individual target genes. There are many facets to changes in gene expression, but I will focus my discussion on how changes in chromatin accessibility due to epigenetic modifications can alter gene expression, and the role of these accessibility changes in regeneration.

Over the last several years work in *Xenopus*, axolotl, and zebrafish has shown that the activity of histone deacetylases (HDACs) is necessary for regeneration (Beck et al., 2003; Pfefferli et al., 2014; Slack et al., 2004; Taylor and Beck, 2012; Tseng et al., 2011; Voss et al., 2019; Wang et al., 2019). Generally, histone acetylation is associated with open, transcriptionally active chromatin. HDACs play a role in closing chromatin by removing acetylation groups from histone tails, allowing for chromatin compaction. In axolotls HDAC activity plays a critical role in regulating early transcriptional responses as shown by microarray analysis. What is striking though, is that changes in gene expression upon HDAC inhibition are not limited to only increases in gene expression, which is what would be predicted by more regions of open chromatin, but decreases in gene expression are also observed (Voss et al., 2019). One interpretation of this is that the indirect effects of changing a class of epigenetic modifications are also critical to our understanding of their role in regeneration. Other possibilities are that some acetyl marks may serve to help close chromatin rather than open, especially when associated with other epigenetic modifications. There are many positions on histone tails that can be acetylated or otherwise modified and not all these modifications have defined functions.

It is also clear that the role of HDAC activity likely has tissue-specific roles and regulation. While inhibition of HDAC activity is detrimental to appendage regeneration in some species, in the mouse retina

it has been shown that inhibition of HDAC activity enhances regeneration by maintaining an open chromatin state at pro-neural enhancers (Jorstad et al., 2017; VandenBosch et al., 2020). It has also been shown that the injury response of neurons in the axolotl limb induces increased expression of *HDAC1* in the wound epidermis. Denervation of limbs prior to amputation causes a loss of HDAC1 activity, and failure to regenerate. The loss of HDAC1 can be rescued with the addition of the three neural factors BMP7, FGF2, and FGF8, restoring the regenerative response (Wang et al., 2019).

As with many of the common signaling pathways in development, timing and context are important factors that regulate pathways such as FGF, WNT, BMP etc. In *Xenopus* HDAC activity is necessary for maintaining pluripotency of blastula cells in early embryogenesis as well as the pluripotent state of neural crest cells (Rao and LaBonne, 2018). HDAC activity however, has been argued to be not necessary for the development of the tail (Taylor and Beck, 2012). Whether HDAC activity is used for similar mechanisms during regeneration as it is during development, such as maintaining pluripotency, is largely unknown.

Another common epigenetic modification that serves to close chromatin is deposition of trimethylation on H3K27. This is deposited by the polycomb repressive complex 2 (PRC2), specifically through the enzymatic activity of EZH2 (Czermin et al., 2002; Rastelli et al., 1993). EZH2 activity has also been shown to be necessary for regeneration in multiple species including *Xenopus, Drosophila,* and zebrafish (Beck et al., 2003; Ben-Yair et al., 2019; Harris et al., 2020; Hayashi et al., 2015; Hirose et al., 2013; Yakushiji et al., 2007). In *Xenopus* limb regeneration it has been show through ChIP-seq that H3k27me3 is similar in the limb before injury and at 5 dpa. However chemically inhibiting EZH2 activity inhibits limb regeneration suggesting that perhaps other genomic regions are affected, or that more temporal resolution is required (Hayashi et al., 2015). Supporting the idea that the dynamics of EZH2 activity may be necessary in certain genomic regions is imaginal disk regeneration in *Drosophila.* In this system it has been established that the methylation state at H3K27 of damage versus developmental enhancers aides in regulation of the regenerative response, specifically at WNT targets (Harris et al., 2016; Harris et al., 2020).

In a developmental context EZH2 activity is critical for lineage specification. It has extensive known roles for craniofacial development in mice as a transcriptional repressor at promoter regions (Schwarz et al., 2014). In addition to its role in inactivating promoters, EZH2 activity and the deposition of H3k27me3

on gene bodies serves to compact chromatin into facultative heterochromatin, and in some cases target these regions towards the nuclear periphery (Mattout et al., 2015a). Similar to the findings in the wing imaginal disk, H3K27me3 is enriched at enhancers along with H3K4me, and H3K27ac is depleted at enhancers in human embryonic stem cells (hESCs). This is termed a “poised” chromatin state and this combination of epigenetic marks is enriched on genes that orchestrate early embryogenesis events such as gastrulation (Creyghton et al., 2010; Rada-Iglesias et al., 2011). It is unclear if EZH2 is utilized in similar fashions during regeneration. The work in the wing disk suggests that this may be the case, but the poised state may be restricted to damage-specific promoters and enhancer regions.

In Chapter 3 I describe my studies on the role of HDAC and EZH2 activity in early appendage regeneration. To gain insight into how chromatin accessibility dynamics are altered by inhibiting EZH2 activity or HDAC activity we utilized ATAC-seq to profile genome-wide accessibility changes over the first 24hpa in the tail of *Xenopus tropicalis* (Buenrostro et al., 2015). We analyzed these datasets and discovered that early EZH2 activity leads to an increased proportion of accessible gene bodies during regeneration whereas HDAC activity leads to persistent accessibility of promoter regions. We also identified distinct Gene Ontology (GO) terms when inhibiting EZH2 activity or HDAC activity, which for the first time suggests these modifications have at least some distinct regulatory targets during appendage regeneration.

CHAPTER 2. EXTREME NUCLEAR BRANCHING IN HEALTHY EPIDERMAL CELL OF THE *XENOPUS* TAIL FIN

Chapter 2 is adapted with modification from:

Arbach, H.E., Harland-Dunaway, M., Chang, J.K., Wills, A.E. (2018) Extreme nuclear branching in healthy epidermal cells of the *Xenopus* tail fin. *Journal of Cell Science*. **131(18)**.

2.1.Abstract

Changes in nuclear morphology contribute to regulation of complex cell properties, including differentiation and tissue elasticity. Perturbations of nuclear morphology are associated with pathologies that include, progeria, cancer, and muscular dystrophy. The mechanisms governing nuclear shape changes in healthy cells remain poorly understood, partially because there are few healthy models of nuclear shape variation. Here, we introduce nuclear branching in epidermal fin cells of *Xenopus tropicalis* as a model for extreme variation of nuclear morphology in a diverse population of healthy cells. We find that nuclear branching arises and elaborates during embryonic development. They contain broadly distributed marks of transcriptionally active chromatin and heterochromatin and have active cell cycles. We find that nuclear branches are disrupted by loss of filamentous actin and depend on epidermal expression of the nuclear lamina protein Lamin B1. Inhibition of nuclear branching disrupts fin morphology, suggesting that nuclear branching may be involved in fin development. This study introduces the nuclei of the fin as a powerful new model for extreme nuclear morphology in healthy cells to complement studies of nuclear shape variation in pathological contexts.

2.2.Introduction

Nuclear shape is highly conserved across cell types and species. Most healthy cells have round or ellipsoid nuclei. A few healthy cell types exhibit non-ellipsoid morphologies, including neutrophils, which have a distinct lobular structure that allows them to extravasate to areas with damaged tissue (Pillay et al., 2013; Rowat et al., 2013). Frequently, perturbations in nuclear morphology are associated with disease. Well-studied examples include progeria (Dahl et al., 2006; Goldman et al., 2004; Schirmer et al., 2001;

Verstraeten et al., 2008), muscular dystrophy (Bertero et al., 2019; Bonne et al., 1999), neurodegeneration (Frost et al., 2016), and cancers (Denais and Lammerding, 2014; Fu et al., 2012; Shah et al., 2013). HeLa cells in particular are a model for nuclear morphological variation, which includes blebbing and ruffling of the nuclear membrane and dysregulation of multiple nucleoskeletal components (Wiggan et al., 2017). However, it is largely unclear what general mechanisms allow cells to acquire non-ellipsoid nuclear morphologies or how these morphologies could influence tissue and cellular function. One barrier to understanding extreme morphological variation of the nucleus is the dearth of models where nuclear morphology varies without being associated with a disease. Here we characterize epidermal cells in the fin margin of *Xenopus tropicalis* tadpoles that have a non-ellipsoid, branched nuclear architecture. These striking nuclear morphologies arise during tail development and persist late into metamorphosis.

The nucleus derives its shape from interactions between the nucleoskeleton and the actin cytoskeleton. The nucleoskeleton is a complex network of Lamin filaments, associated proteins, and the LINC (**LI**nker of **N**ucleoskeleton and **C**ytoskeleton) complex (Chang et al., 2015; Chen et al., 2014; Davidson and Lammerding, 2014; Denais and Lammerding, 2014; Fu et al., 2012; Goldman et al., 2004; Schirmer et al., 2001; Vergnes et al., 2004; Zwerger et al., 2013). Alterations in nuclear lamina composition, particularly the relative levels of A-type and B-type Lamins, enable changes in not only nuclear shape but also nuclear deformability (Swift et al., 2013). Changes in this ratio allow the formation of nuclear lobes and a highly deformable nuclear envelope in neutrophils, which in turn enable passage through small capillaries. Perturbation of B-type Lamins or their receptors has deleterious effect on neutrophil migration (Dreesen et al., 2013; Rowat et al., 2013). More recent studies of interactions between perinuclear actin and the nuclear envelope have also clarified that the rigidity of the actin cap and degree of actin polymerization directly affect nuclear shape and tissue stiffness (Swift et al., 2013; Wiggan et al., 2017). Variation in nuclear morphology is therefore predicted to have consequences for the biophysical function of the associated tissue, although relatively little is known about the mechanism by which other nuclear functions are modulated or constrained by extreme shape change (Dahl et al., 2006; Pajerowski et al., 2007; Rowat et al., 2013; Zwerger et al., 2013).

The structural organization of the nuclear lamina scaffolds functional domains within chromatin and serves to protect the genome (Peric-Hupkes et al., 2010; Shah et al., 2013; Solovei et al., 2013). Chromatin-lamina interactions are important for appropriate gene regulation. Canonically, heterochromatin or repressed regions of the genome are associated with the nuclear lamina (Fraser et al., 2015; Mattout et al., 2015a; Peric-Hupkes et al., 2010). Alterations in heterochromatin propagation are linked to changes in nuclear morphology caused by laminopathies (Davidson and Lammerding, 2014; Dreesen et al., 2013; Perovanovic et al., 2016; Shah et al., 2013). Hutchinson-Gilford Progeria Syndrome (HGPS) is a laminopathy that causes premature aging and is associated with mutations in LMNA that disrupt prelamin A cleavage, leading to gross changes in nuclear morphology (Chen et al., 2014; Dahl et al., 2006; Goldman et al., 2004; Verstraeten et al., 2008). As cultured cells with HGPS *lemma* mutations undergo more passages, they acquire progressively more nuclear ruffling and alterations of heterochromatin, resembling senescent cells rather than proliferative cells. Similar alterations in heterochromatic regions are seen in Lamin B1-depleted cells and cancer cells (Perovanovic et al., 2016; Shah et al., 2013). This suggests that alteration of the nucleoskeleton can contribute to large-scale changes in chromatin reorganization and gene expression that contribute to aging or other pathologies.

In this study we have characterized nuclear branching in the fin epithelium of *Xenopus* tadpoles. The thin epithelium of the tadpole is made up of flattened epidermal cells that overlie a mesenchymal core (Tucker and Slack, 2004). Its specialized cell biological and biophysical properties allow rapid regeneration and sinusoidal swimming movements. We show that branched morphologies of the nuclear lumen, chromatin, and nuclear lamina arises during development in a heterogenous population of epidermal cells that make up the fin periphery. Cells with branched nuclei contain epigenetic marks of active enhancers and inactive chromatin throughout the nucleoplasm, additionally these cells have active cell cycles. We find that actin filaments, but not polymerized microtubules are necessary to maintain branched nuclear morphology. We also find that functional epidermal Lamin B1 is required for both nuclear branching and for proper development of the fin and tail.

2.3.Results

2.3.1.Nuclei in the tail of Xenopus tropicalis *are branched*

Although *Xenopus* has long served as a model for epidermal cell biology and nuclear composition, there has been little examination of nuclear morphology in the differentiated fin. We conducted whole-embryo DAPI stains of the *Xenopus tropicalis* tadpole fin, which revealed an unexpected elaborately branched distribution of DNA in the fin marginal cells (Figure 2-1A). Although examples of potentially branched nuclear morphologies can be observed in earlier literature, these have not been described in detail (Davis and Kirschner, 2000). Our first goal was to establish whether branching was confined to chromatin or was shared by the nuclear lumen and envelope (Figure 2-1B). To this end, cleavage-stage embryos were injected with either a cocktail of *h2b-rfp* and *lmnb3-gfp* mRNA to label histones (chromatin) and the nuclear lamina respectively, or with GFP bearing a nuclear localization signal (Nuclear GFP) (Figure 2.1C). Tadpoles were reared to NF stage 41 and then live images were taken in the anterior-most third of the fin margin. Nuclear GFP confirmed that the nuclear lumen in cells of the fin margin is also highly branched structure (Figure 2.1D). Consistent with our observations for DAPI, we find that H2B-RFP has a branched distribution in the nuclei of fin margin cells. Lamin B3-GFP localization showed that the nuclear compartment is also branched (Figure 2.1E). Thus, the entire nucleus of fin marginal cells is branched, including the lamina, lumen, and chromatin.

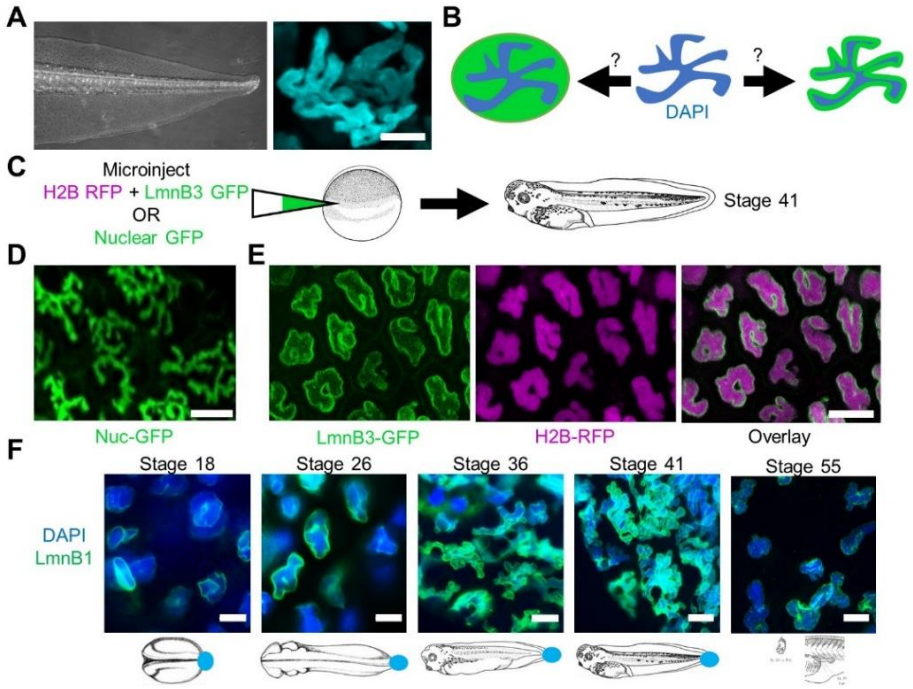

Figure 2-1 Nuclei in the tail fin of *Xenopus tropicalis* are branched.
A) Bright field image of a stage 41 tadpole tail. Immunofluorescence of DAPI (cyan) in a single nucleus. The scale bar represents 5 μm. B) Two models of nuclear structure, branched chromatin in an ellipsoid nuclear compartment or branched chromatin in a branched nuclear compartment. C) Experimental design to address B). D) Fluorescent images of the nuclear lumen, periphery, and chromatin. Scale bar represents 10μm. E) Immunofluorescence of nuclear branches during development. Scale bar represents 10 μm.

We next asked what the spatiotemporal distribution of nuclear branching is during *Xenopus* development. Because injected mRNAs have a limited lifetime, we utilized immunohistochemistry to explore endogenous nuclear structure in the epidermis and other tissues through development. Tadpoles were fixed at various stages and stained for Lamin B1 to show the nuclear periphery and, DAPI to label chromatin. We find that by late neurula stages (NF stage 18), the nuclear envelope is ruffled and irregular, though the chromatin distribution is still largely ellipsoid (Figure 2-1F). We note that ruffling of the nuclear envelope is found in several epidermal cell types at this stage, including secretory cells, multiciliated cells, and the goblet cells surrounding them (Figure 2-2A). At NF stage 22, ruffling of the nuclear envelope is more pronounced, though chromatin distribution as shown by DAPI remains ellipsoid. As the embryo enters tailbud stages, the distribution of both chromatin and the nuclear lamina becomes gradually more branched, with defined branches appearing by NF stage 26, multiple branches evident per nucleus by NF stage 35,

and the most elaborate degree of branching reached by NF stage 41 (Figure 2-1E). The absolute number of branches per nucleus is quiet variable, ranging dramatically from 2-13 (Figure 2-2C, D). All nuclear branching is lost shortly before the onset of tail reabsorption, and epidermal cells of the adult frog are not branched (data not shown). While non-ellipsoid nuclear structures are also visible in some other cell types, notably granulocytes/neutrophils, nuclear branching was only observed in epidermal cells. Epidermal cells of the head at stage 41 showed some minor lobulation, while nuclei of other tissues such as the heart and somites were ellipsoid (Figure 2-2B). The only structure in which we identified branched nuclei outside of the tail was the surface epithelial cells covering the retina (Figure 2-2B).

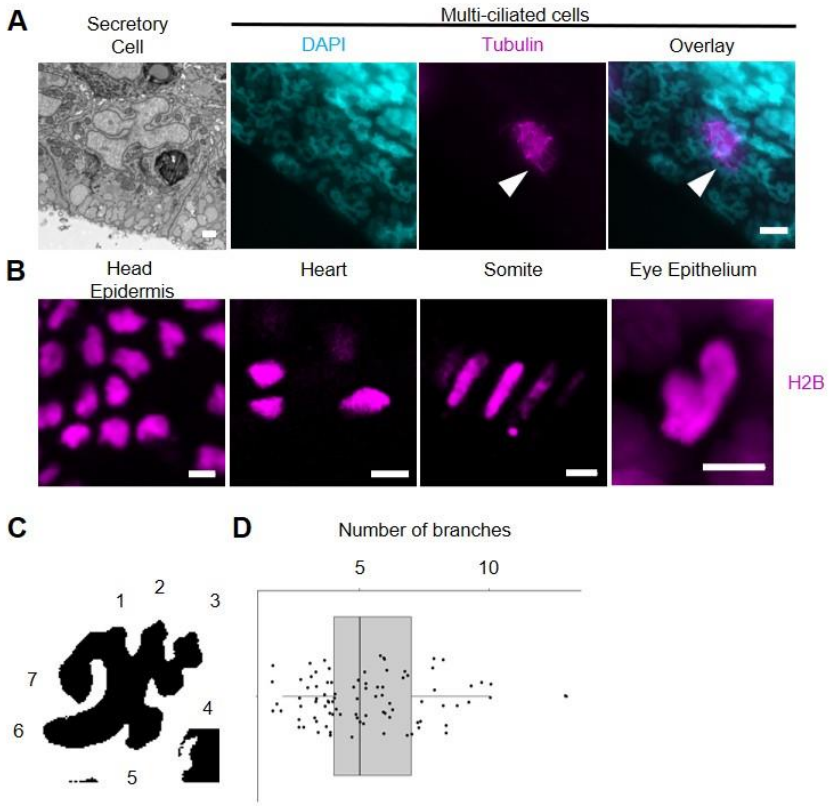

Figure 2-2 Cell types of branched and non-branched nuclei

A) Transmission electron micrograph of a secretory cell with a branched nucleus. Scale bar represents 250 nm. Immunofluorescence of DAPI and Tubulin show a heterogeneous cell population of multiciliated cells (white arrow heads), and presumably goblet cells. Scale bar represents 10 µm. B) Live images of H2B of cells with non-branched nuclei from the head epidermis, gut, heart, and somites. Scale bars represent 10 µm. C) Example of single nucleus with 7 branches. D) Box plot of the number of nuclear branches (n=89 nuclei; 11 tadpoles)

2.3.2. *Branched nuclei have intact envelopes, and contain normal mitochondria, nucleoli, and marks of active enhancers*

Because perturbations of nuclear morphology are associated with pathology in many cell types (Li et al., 2016; Wang et al., 2008), we asked whether epidermal cells with branched nuclei showed hallmarks of cellular damage or senescence. These could include nuclear envelope rupture, mitochondrial damage, or cell cycle exit. To assess subcellular signs of cell damage, we utilized TEM (Transmission electron microscopy) to assess nuclear envelope integrity and mitochondrial abundance. Micrographs reveal diverse nuclear structures (Figure 2-3A), including clearly demarcated branched nuclei enclosed by bilayer nuclear envelopes. Upon close examination of the nuclear envelope, we see that it is a continuous bilayer in cells with branched nuclei, with an average of 18 nm between the inner and outer leaflets and containing nuclear pores with a mean diameter of 60 nm (Figure 2-3B). The integrity of the nuclear envelope is also supported by the even distribution of Nuclear GFP within the nuclear lumen and by the continuous distribution of LaminB1 in branched nuclei, with no evidence of leaks, partitions, or ruptures (Figure 2-1D, E). Cells with branched nuclei also contain numerous mitochondria with abundant cristae (Figure 2-3A). These observations suggest cells with branched nuclei are not undergoing apoptotic or senescent processes that would be reflected in nuclear envelope breakdown, low mitochondrial numbers, or loss of mitochondrial cristae.

TEM did reveal some atypical features in branched nuclei, including a lack of well-defined regions of perinuclear increased electron density in micrographs that would be indicative of heterochromatic regions, or of clear identifiable nucleoli (Figure 2-3A). To determine if there were nucleoli present in nuclear branches, we analyzed localization of the nucleolar marker fibrillarin (Brangwynne et al., 2011). We found that cells with branched nuclei did contain foci of fibrillarin (Figure 2-3C), suggesting the presence of nucleoli, and that the average number of foci per nucleus did not change between branched (1.60) and unbranched nuclei (1.69) (Figure 2-3D). We did note that foci of fibrillarin did not correspond to apparent foci of H2B.

To better understand whether cells with branched nuclei contain both active and inactive chromatin domains, we used immunofluorescence and live imaging to examine the distribution of histone

modifications associated with active enhancers (H3K27ac and H3K4me1), and heterochromatin (H3K9me3 and HP1β).Using immunofluorescence we find H3K27ac, H3K4me1, and H3K9me3 are all distributed broadly in branched nuclei at NF stage 41 (Figure 2-3E); the distribution appears uniform for H3K27ac, but H3K9me3 appeared more concentrated in foci, and H3K4me1 may be excluded from some regions of the nuclear periphery. To better characterize the distribution of heterochromatin, we used a GFP fusion of the heterochromatin binding protein HP1β (Mattout et al., 2015b). We find that HP1β-GFP broadly co-localizes with H2B (Figure 2-3F). Although heterochromatin is typically enriched at the nuclear envelope, we did not observe a clear enrichment of HP1β at the nuclear periphery, however, we observe foci of HP1β-GFP fluorescence in the nucleus corresponding to foci in H2B. Taken together this suggests that active enhancers and heterochromatin are found throughout nuclear branches.

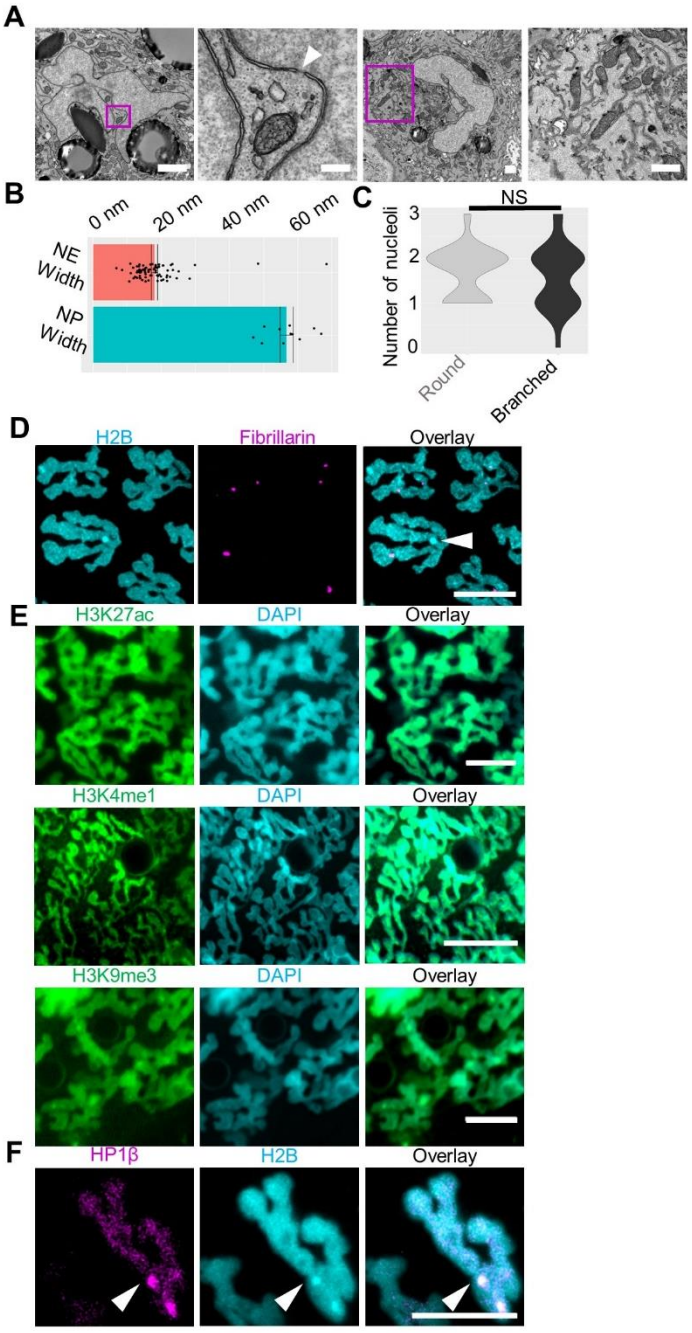

Figure 2-3 Epidermal cells with branched nuclei appear healthy and contain active enhancers.

Transmission electron micrographs of cells with branched nuclei. Upper left panel shows a single nucleus, Scale bar represents 1µm. Magenta box indicates region depicted in second panel. Arrowhead shows nuclear pore. Scale bar represents 250nm. Third panel shows a single nucleus, scale bar represents 1 µm. Magenta box indicates region depicted in fourth panel. Fourth panel shows mitochondria of a cell with a branched nucleus, with visible cristae. Scale bar represents 1 µm. B) Quantification of nuclear envelope (NE) width and nuclear pore (NP) width from TEM micrographs. C) Violin plots of the distribution of nucleoli in round (n=38 nuclei, 3 tadpoles) and branched nuclei in the

tadpole (n=46 nuclei, 3 tadpoles) (p=0.49, two-tailed student's t-test). D) Fluorescent images of H2B and nucleoli labeled by fibrillarin, scale bar represents 10 μm. E) Distribution of chromatin marks in branched nuclei. Immunofluorescence of H3K27ac (active transcription), H3K4me3 (active enhancers) H3K9me3 (heterochromatin). Scale bars represent 10 μm. F) Live image of HP1β (heterochromatin), white arrow heads indicate foci. Scale bars represent 10 μm.

2.3.3.Cells with branched nuclei have active cell cycles

In many cell types, breakdown of ellipsoid nuclear morphology is a hallmark of senescence, cell cycle dysregulation, or genomic instability (Dahl et al., 2006; Goldman et al., 2004; Schirmer et al., 2001; Wang et al., 2008). In particular, keratinocytes are known to acquire aberrant nuclear morphologies following terminal differentiation and cell cycle exit, and in premature aging syndromes (Gdula et al., 2013; McKenna et al., 2014). We therefore wanted to determine if cells with branched nuclei in the keratin-rich tadpole epidermis were undergoing an active cell cycle. We utilized immunofluorescence of Phosphorylated-Histone H3 (PH3) to mark mitotic nuclei, and Lamin B1 to mark the nuclear periphery. We find numerous examples of PH3-positive cells that retain branched nuclei (Figure 2-4A). Examination of chromatin morphology in PH3-positive cells suggests that nuclei remain branched and are still enclosed by a branched nuclear envelope through prophase but form a condensed metaphase plate while the nuclear envelope breaks down. Chromatin remains condensed through anaphase. Daughter cells establish independent branching patterns and re-form the nuclear envelope at late telophase.

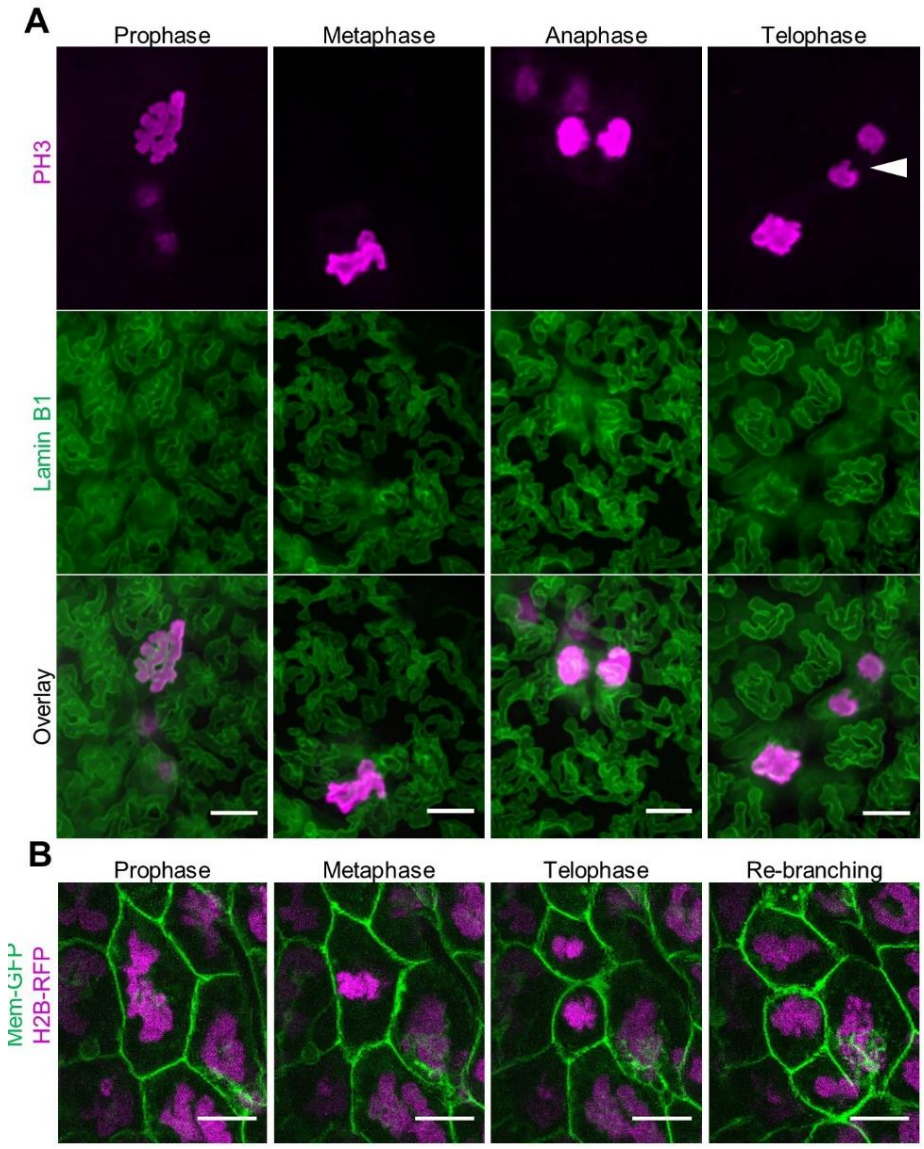

Figure 2-4 Cells with branched nuclei have active cell cycles.
A) Immunofluorescence of phospho-H3 (PH3) and Lamin B1 cells in various stages of mitosis. B) Various stages of mitosis in live cells. Asterisk shows potential vesicles being from the cell. Scale bars represent 10 µm.

To better characterize nuclear envelope and chromatin dynamics through mitosis, we conducted live imaging using H2B-RFP and membrane-GFP to track individual nuclei throughout mitosis (Figure 2-4B). These confirmed our initial observations that nuclei are initially branched, formed morphologically normal metaphase plates that segregate into two well-defined populations at anaphase, and are re-enclosed by the nuclear envelope following telophase, with the nucleus beginning to re-form branches

approximately 21 minutes after cytokinesis. Nuclear branching patterns in daughter cells do not typically recapitulate those of the mother cell, nor do both daughters show the same branching patterns. Additionally, branches did not appear to be reabsorbed once formed after the completion of mitosis but did exhibit some dynamic motion within the branches. In nuclei not undergoing mitosis, the number and relative positions of branches can remain stable for two hours or more. Both fixed and live imaging therefore demonstrate that branched nuclei can undergo mitosis.

2.3.4.Perturbations of Actin and not Microtubules disrupt nuclear branching

We next sought to determine what molecular mechanisms enabled nuclear branching in the fin margin. In mammalian cells, perturbations of nucleoskeleton components lead to nuclear shape deformation. These include mutations in LMNA, which lead to nuclear blebbing in progeroid syndromes (Chen et al., 2014; Dahl et al., 2006; Goldman et al., 2004; Perovanovic et al., 2016; Verstraeten et al., 2008), mutations or duplications of LMNB1 or its receptor, which disrupt nuclear flexibility and extravasation in neutrophils (Dreesen et al., 2013), perturbations of the Sun and Nesprin components of the LINC complex (Chang et al., 2015; Hatch and Hetzer, 2016; Hatch et al., 2013; Kim and Wirtz, 2015), or alterations in the abundance, orientation, or phosphorylation of actin, which contribute to nuclear morphological disruption in HeLa cells (Hatch et al., 2013; Kim and Wirtz, 2015; King and Lusk, 2016; Ramdas and Shivashankar, 2015; Webster et al., 2009; Wiggan et al., 2017; Zwerger et al., 2013). Therefore, we decided to pursue whether similar components were required for nuclear branching in the fin margin.

First, we observed actin localization in cells with branched nuclei. We found no apparent bias of actin localization to tips or bases of branches (Figure 2-5A). To determine if actin filaments were necessary for nuclear branches, we incubated stage 41 tadpoles with Latrunculin B (Lat B), which disrupts actin filament formation. Lat B has been found to disrupt other actin-dependent processes in *Xenopus* at non-lethal doses (Lee and Harland, 2007). To monitor the effect of this inhibitor on actin filaments and nuclear morphology, we injected embryos at cleavage stages with mRNAs encoding H2B-RFP and the actin binding protein Utrophin-GFP. We find that treatment with Lat B results in breakdown of the actin cytoskeleton beginning at 25 minutes post treatment. Concurrently, foci of Utrophin-GFP were visible (Figure 2-5B). Nuclear branches were gradually lost after actin destabilization and were lost more slowly in nuclei that

initially had more numerous or complex branches. Nuclear branches reformed after wash-out of Lat B. Actin filaments visualized by LifeAct began to be visible 25 minutes after Lat B removal along with some nuclear deformation, similar kinetics to what was observed for the loss of actin filaments. By 125 minutes after Lat B removal new branches were fully formed although the branching patterns were not conserved relative to their initial pre-treatment distribution (Figure 2-5C).

Because actin has known roles in compressing nuclei (Versaevel et al., 2012; Vishavkarma et al., 2014; Wiggan et al., 2017) and nuclear branches are in an extremely flattened epithelium, we next measured changes in nuclear depth and surface area -to- volume ratios of nuclei with intact and Lat B perturbed actin networks. Both WT (wild type) and Lat B-treated tadpoles had comparable nuclear depths (5.6 and 4.1 µm respectively) (Figure 2-5D). However, the nuclear surface area -to- volume ratio decreased from 1.405 in WT to 1.134 in Lat B treated animals (Figure 2-5E). Nuclear volume also decreased by approximately 7.5% and the surface decreased by approximately 25.4% in Lat B treated animals (Data not shown). Together this suggests that loss of branches decreases the amount of nuclear membrane (surface area) relative to the volume. However, the lack of change in nuclear depth suggests that actin is not supplying a compressive force causing branches to form, but rather pushing, or pulling forces.

To confirm that loss of nuclear branches was not specific to Lat B treatment we utilized Cytochalasin D (Cyto D), which inhibits actin polymerization and has also been shown to disrupt other actin-dependent processes in *Xenopus* (Lee and Harland, 2007). Treatment with either Cyto D or Lat B results in a rapid loss of nuclear branching in the fin margin, as revealed by LamnB3-GFP and H2B-RFP (Figure 2-5F).

We next asked whether microtubules contributed to nuclear branches, as they have been shown to play a role in maintaining nuclear morphology (Tariq et al., 2017). We utilized the microtubule polymerization inhibitor nocodazole at non-lethal doses (Dutta and Kumar Sinha, 2015). While nocodazole

treatment noticeably disrupts spindle formation in tadpoles, it does not affect nuclear morphology relative to DMSO-treated controls (Figure 2-5G).

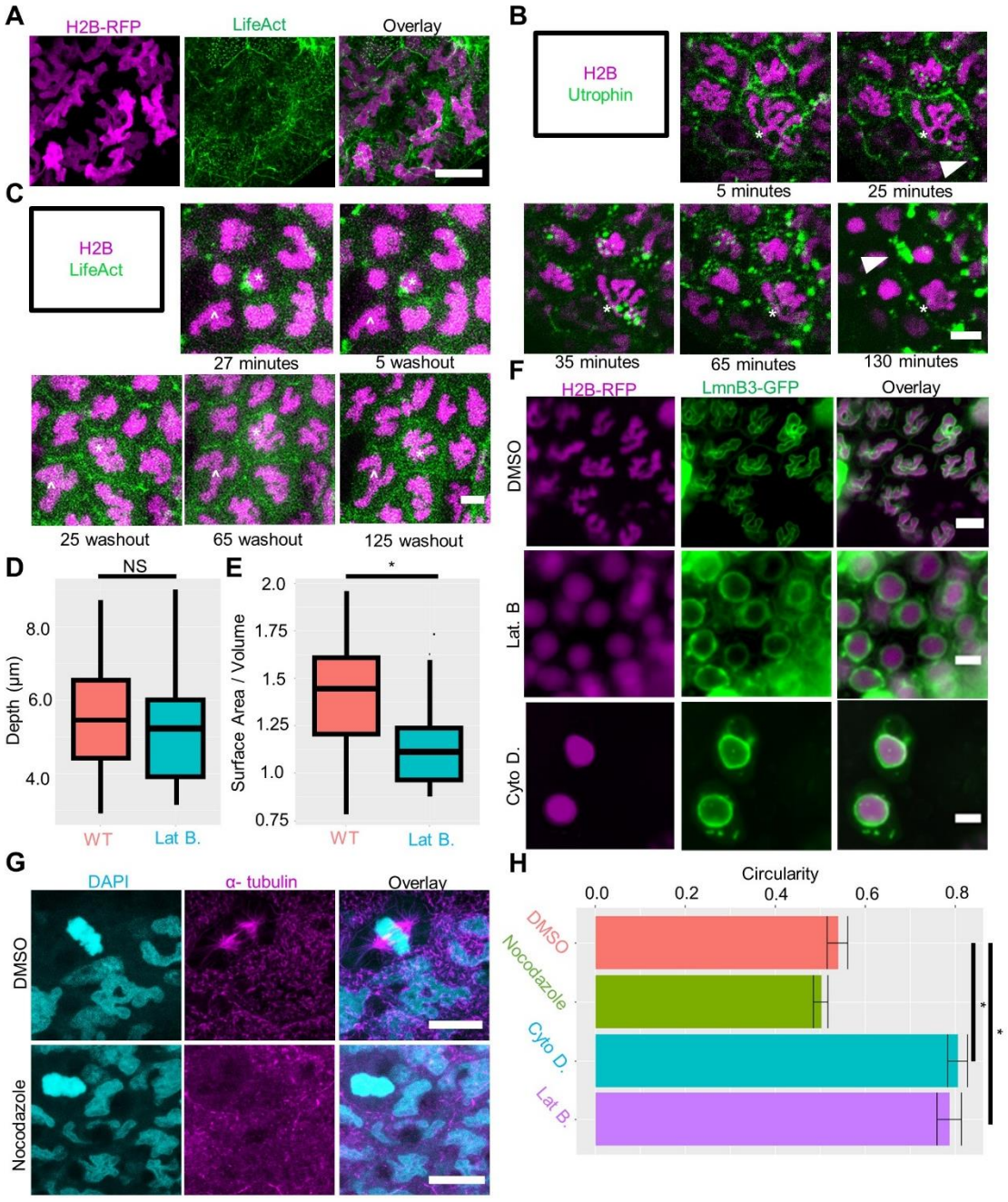

Figure 2-5 Perturbations of Actin but not microtubules disrupt nuclear branching.

Actin localization in cells with branched nuclei, H2B (magenta) and LifeAct (green) Scale bar = 10 µm. B) Latrunculin B treatment causes loss of actin filaments (utrophin-GFP, green), and nuclear branches (H2B, magenta). White arrow heads show depolymerized actin, asterisk denotes a single nucleus. Times denote length of treatment. Scale bar = 10 µm. C) Nuclear branches (H2B, magenta) and actin

filaments (LifeAct, green) reform after Lat B wash-out. White arrow heads show changes in actin. Asterisk and carrot show single nuclei. Scale bar = 10 µm. D) Nuclear height (µm) of Wildtype (n=14 nuclei, 3 tadpoles) and Lat B treated tadpoles (n=17 nuclei, 4 tadpoles) (E) Nuclear surface area / volume ratios in Wildtype (n=21 nuclei, 3 tadpoles) and Lat B treated tadpoles (n=19 nuclei, 3 tadpoles) ($p<0.05$, one-tailed student's t-test) F) Treatment with Cytochalasin D (Cyto D) and latrunculin B (Lat B) disrupt nuclear branches, branches remain intact in DMSO vehicle control. Scale bars =10 µm. G) Nocodazole treatment disrupts microtubules, but not nuclear branches. Scale bars =10 µm. H) Quantification of nuclear circularity in actin and microtubule drug treatment, Cyto D (n=50; 7 tadpoles) and Lat B (n=45; 6 tadpoles) significantly increase circularity compared to DMSO (n=168; 10 tadpoles), Nocodazole (n=90; 3 tadpoles) had no change compared to DMSO ($p<0.01$, one-way ANOVA and Tukey's post-hoc, error bars are s.e.m)

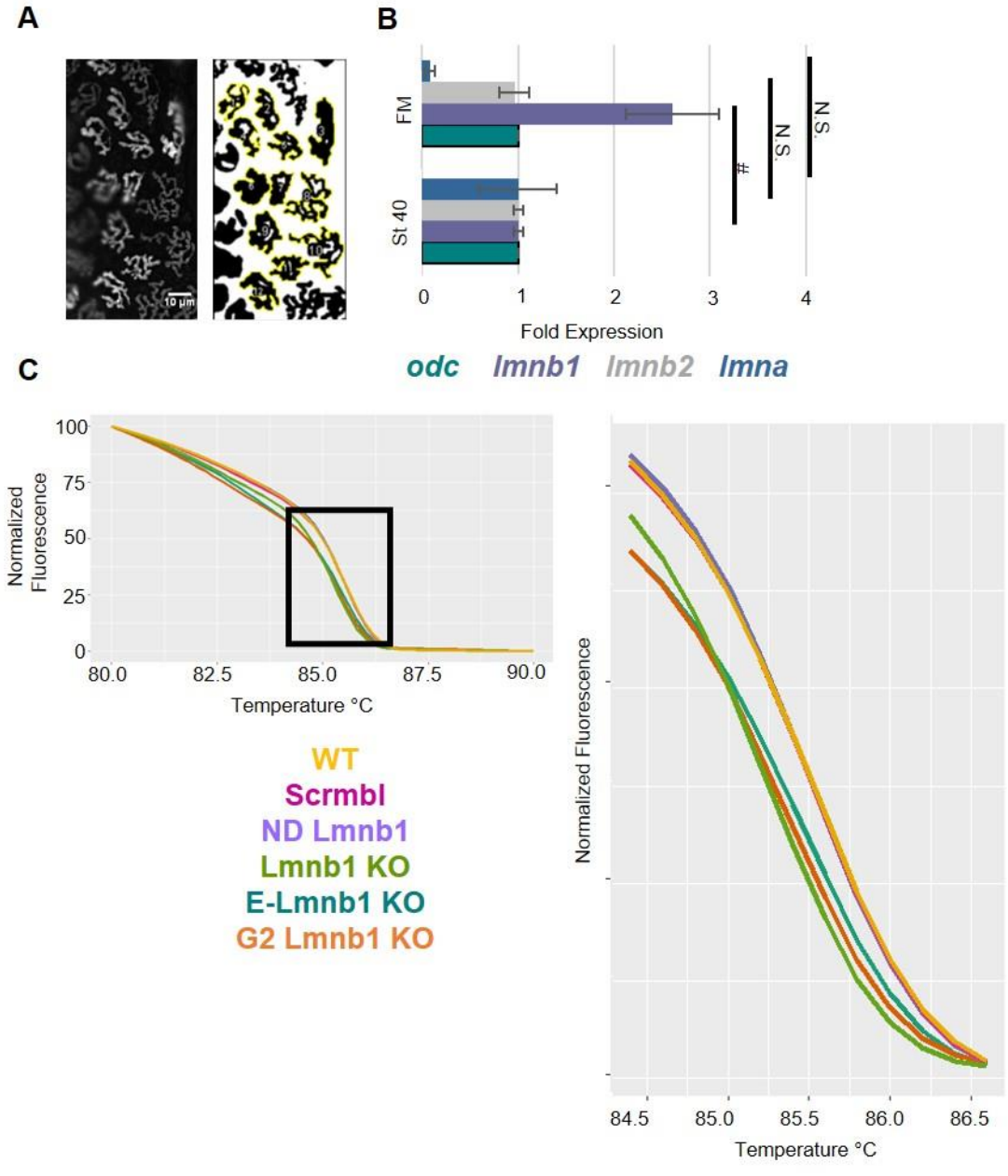

Figure 2-6 Quantification of nuclear morphology, gene expression, and genotype.

A) Particle selection using ImageJ to calculate nuclear circularity (see methods). B) RT-qPCR fold expression of lamins relative to ornithine decarboxylase (*odc)* in whole stage 40 tadpoles (St 40), and isolated stage 40 fin margins (FM) data represents the mean ± SEM. (#p=0.56, N.S. = not significant, *p=0.0045 two-way heteroscedastic T-test) C) High resolution melt analysis of *lmnb1* mutations.

We quantified changes in nuclear morphology for all cytoskeleton perturbations using the circularity measurement on ImageJ (see methods, Figure 2-6A). We found there was a statistically significant increase in epidermal nuclear circularity when tadpoles were treated with either Cyto D or Lat B, but not Nocodazole (Figure 2-5H). These results indicate that nuclear branches require intact actin filaments for their maintenance, but not polymerized microtubules.

2.3.5.LaminB1 is necessary for nuclear branches

We next asked whether nuclear branching relies on specific components of the nuclear lamina. Modulation of nuclear lamina components has been shown to regulate tissue elasticity in mammals: greater levels of Lamin A lead to an increase in tissue stiffness, while Lamin B is critical for nuclear envelope flexibility in neutrophils (Mattout et al., 2015b; Mattout et al., 2015a; Peric-Hupkes et al., 2010; Perovanovic et al., 2016; Solovei et al., 2013; Towbin et al., 2012). *Xenopus tropicalis* contain one Lamin A/C homolog, as well as three Lamin B homologs: Lamin B1, Lamin B2 and the germline specific Lamin B3 (Session et al., 2016). We first sought to determine whether any of these components were preferentially enriched or depleted in fin marginal cells containing branched nuclei. To this end, we isolated fin margin tissue or whole embryo tissue, and quantified expression of *lmnb1*, *lmnb2,* and *lmna* using qRT-PCR (Figure 2-6B). We find that expression of *lmnb1* is significantly upregulated in the fin margin relative to the whole embryo (2.6-fold increase), whereas *lmnb2* and *lmna* are unchanged. To determine whether this upregulation reflected a functional role for *lmnb1* in the fin margin or in nuclear branching, we used CRISPR/Cas9 to create mutations in *lmnb1* by co-injecting gene-specific sgRNAs together with humanized Cas9 protein in F0 tadpoles (Bhattacharya et al., 2015; Nakayama et al., 2013). To track nuclear and cell morphology, we again co-injected these embryos with mRNAs encoding H2B-RFP and Membrane-GFP. We used high-resolution melt analysis to confirm gene-specific mutations (Figure 2-6C). Upon analyzing nuclear morphology in F0 tadpoles at stage 41, we find that only *lmnB1* mutant embryos (*Lmnb1* CRISPR) have

markedly reduced branching, instead exhibiting crescent or elongated obloid shapes (Figure 2-7A). This effect is confined to *lmnB1* mutants and is not induced by injection of a scrambled version of the *lmnB1* sgRNA (Scrmbl) (Figure 2-7A).

To confirm that these effects were intrinsic to epidermal cells, and not secondary to any effect of whole-embryo perturbation, we next targeted our injections specifically to the ventral animal blastomeres at the 8-cell stage, which give rise to the epidermal lineage (Bauer et al., 1994; Moody, 1987). These epidermal-only *lmnB1* mutant embryos (E- Lmnb1 CRISPR) also exhibited reduced nuclear branching in the fin epidermis (Figure 2-7A). As a further confirmation, we generated a *Xenopus* form of dominant-negative Lamin B1, following the domain structure used in mammals (Goldman et al., 2004). This dominant negative LaminB1 (Lmnb1-rod) contains only the rod domain, which is thought to disrupt the lamin network and LINC complex interactions when overexpressed (Goldman et al., 2004). We co-injected this into epidermal blastomeres at the 8-cell stage, together with H2B-RFP and Membrane-GFP. Epidermal cells injected with Lmnb1-rod also exhibited reduced nuclear branching at stage 41 (Figure 2-7A). We quantified nuclear circularity in LmnB1 perturbed tadpoles and found that epidermal cells in LmnB1 CRISPR, E-LmnB1 CRISPR, and Lmnb1-rod tadpoles had statistically significant increase in nuclear circularity, where there was no difference between WT and Scrmbl tadpoles (Figure 2-7B). Together these results argue that nuclear branching depends on functional Lamin B1 in the epidermis.

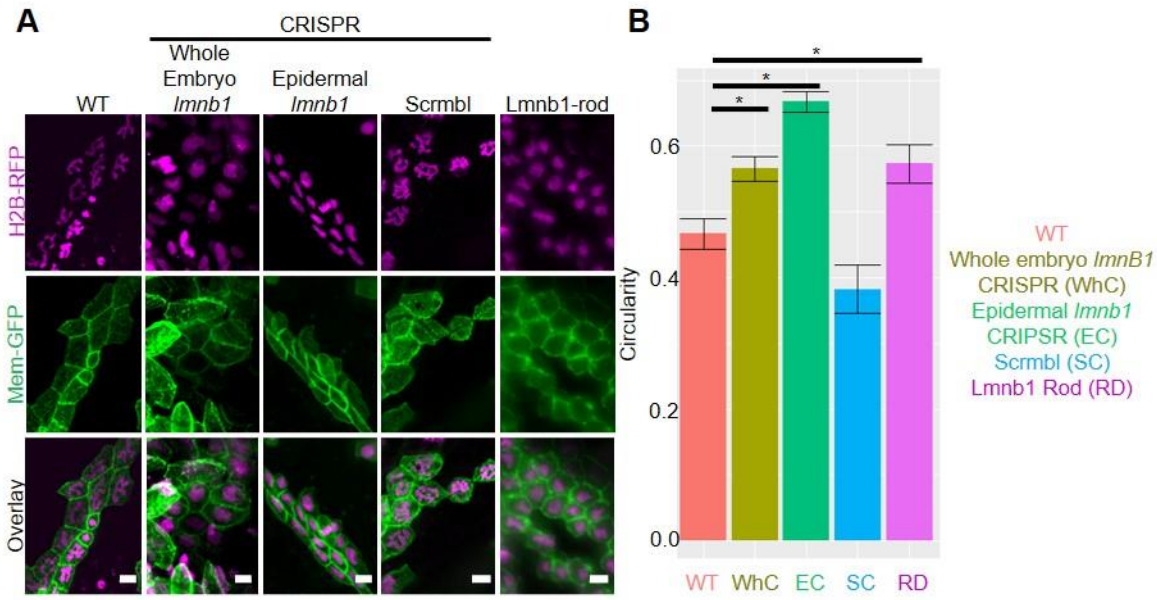

Figure 2-7 LaminB1 is necessary for nuclear branches.

A) Mosaic Crispr Cas9 knock-out of lamin B1 (Whole embryo lmnb1 CRISPR, Epidermal lmnb1 CRISPR), and dominant negative lamin B1 disrupt nuclear branches. Scale bars represent 10 μm. B)) Quantification of nuclear circularity in lamin B1 perturbed nuclei. Whole embryo *lmnb1* CRISPR (n=86 nuclei; 7 tadpoles) and Epidermal *lmnb1* CRISPR (n=51 nuclei; 6 tadpoles), and laminB1 dominant negative (n=50 nuclei; 5 tadpoles) increase circularity significantly relative to wildtype (n=82 nuclei; 7 tadpoles) ($p<0.01$, ANOVA and Tukey's post hoc, error bars are s.e.m.). Scrambled CRISPR/Cas9 guide (n=40 nuclei; 5 tadpoles) does not change nuclear circularity relative to wildtype.

2.3.6.Nuclear morphology arises independently from swimming motions and contributes to fin morphology

One potential source of nuclear morphological variation derives from the physical forces exerted against the nucleus either by intracellular compression, such as through perinuclear actin, or by extracellular compression, such as that exerted by endothelial cells during neutrophil extravasation. The tadpole fin encounters a unique extracellular force profile as it undergoes swimming movements. We therefore tested if the mechanical forces sustained by the fin from swimming were required for nuclear branching in the fin. To this end, we utilized dorsal posterior explants at the neurula stage. These explants give rise to tails with fins that lack muscle (Tucker and Slack, 2004). We then compared the circularity of nuclei in the fin margin of stage matched tadpoles and nuclei in the fin of explants and found no change in

circularity (Figure 2-8A). This suggests that the mechanical forces from swimming are not necessary to induce nuclear branching.

We concluded by investigating the relationship between nuclear branching and development. We observed that tadpoles with *lmnb1* mutations had tail defects, sloughing of the fin epidermis, were inefficient swimmers, and developed edema, likely due to decreased locomotion (Figure 2-8B, C). We found that nuclear morphology and fin morphology were correlated; *imnb1* sgRNA-injected tadpoles that had no tail defect, did not lose nuclear branching (Figure 2-6). Tails were statically significantly shorter and narrower in tadpoles with *lmnb1* mutations compared to wild type (Figure 2-8D, E). This suggests that *lmnb1*-dependent nuclear branching may be necessary for proper tail formation and function but does not rule out the possibility that the contribution of the function of LaminB1 on gene regulation affects tail formation.

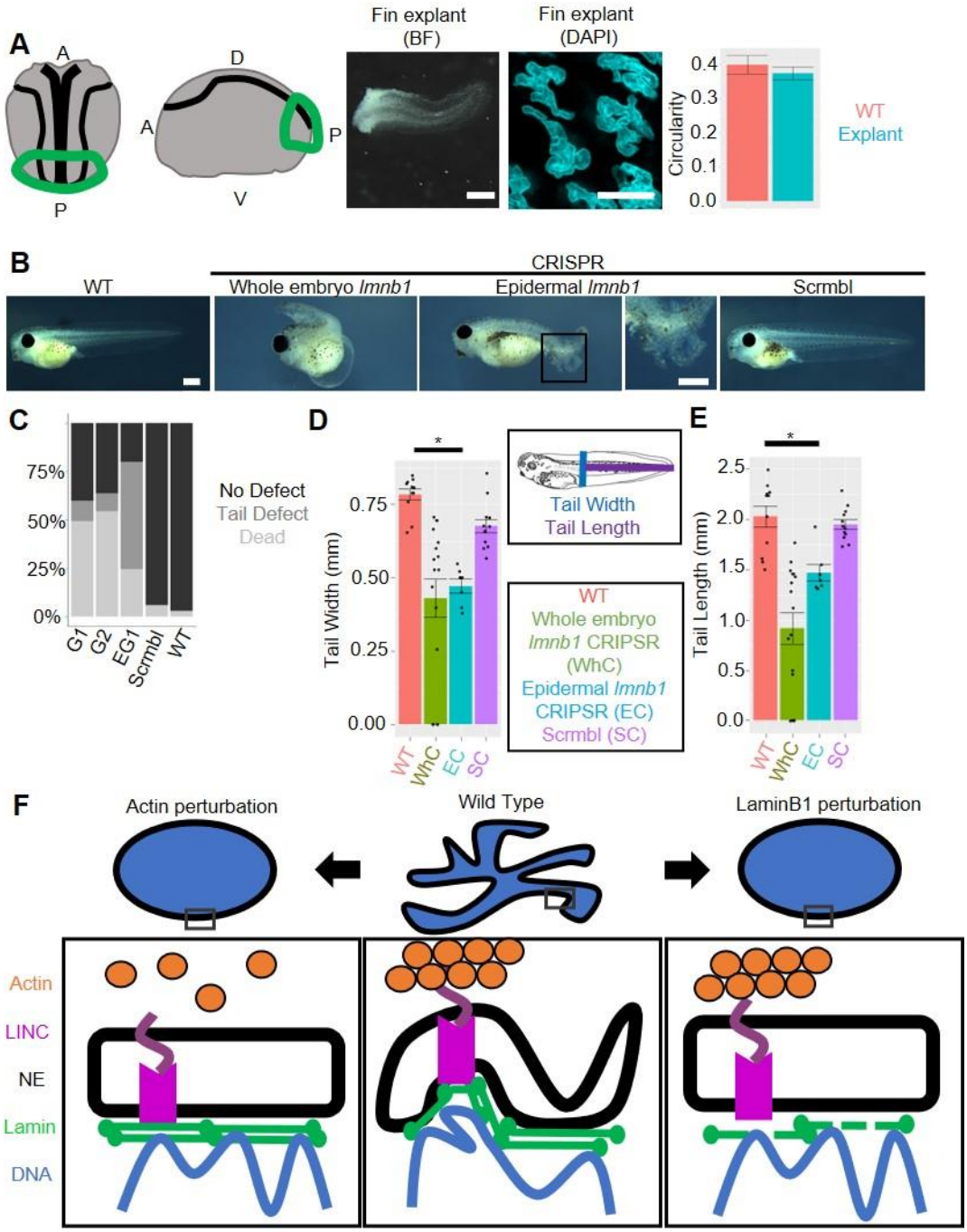

Figure 2-8 Nuclear morphology in arises independently from swimming motions and contributes to fin morphology

Dorsal posterior explants develop a stationary tail (scale bar indicates 1 mm) which retains nuclear branching (Scale bars represent 10 μm).). Circularity is unchanged between explants (n= 86 nuclei; 5 explants) and stage matched tadpoles (n= 32 nuclei; 4 tadpoles) (p>0.05, ANOVA and Tukey's post-hoc, error bars are s.e.m.). B) Stage 41 tadpoles with and without Lmnb1. Boxed area of Epidermal *lmnb1* CRISPR tadpole shown. Scale bars indicate 1mm. C) Tadpole phenotypes G1 = Whole embryo *lmnb1* CRISPR with guide 1, G2 = Whole embryo *lmnb1* CRISPR with guide 2, 8G1 = Epidermal *lmnb1* CRISPR with guide 1 (G1 n= 409 tadpoles; 5 clutches, G2 n=22 tadpoles; 1 clutch, 8G1 n= 155 tadpoles; 3 clutches, scrmbl n= 149 tadpoles; 3 clutches, WT n= 201 tadpoles; 4

clutches). D) Tail width of tadpoles is significantly decreased in *lmnb1* perturbed tadpoles E) Tail length of tadpoles are significantly decreased in *lmnb1* perturbated tadpoles (For D-E; WT n=11, Whole embryo LmnB1 CRISPR n= 16, Epidermal-LmnB1 CRIPSR n=6, Scrmbl n=12, $p<0.01$ one-way ANOVA and Tukey's post hoc). F) Perturbations of actin filaments and LaminB1 alter nuclear morphology.

2.4.Discussion

2.4.1.Xenopus epidermal branching as a model for extreme variation in healthy tissue

Across tissues and species, nuclear morphology is generally ellipsoid. There are very few cases of healthy epithelial cell types with highly irregular nuclear morphologies; the mandibular gland epithelium of the wax moth *Ephestia kuehniella* is a notable example, which is exhibits a branched nuclear morphology like the morphology of the tadpole fin (Buntrock et al., 2012). Here we describe an epithelial epidermal tissue, the *Xenopus* tadpole fin margin, which exhibits a highly branched nuclear morphology. In this epithelial tissue, a heterogenous population of cell types including secretory cells, goblet cells and multiciliated cells displays highly irregular branched nuclear morphology. The degree of nuclear branching we describe is more extreme than in most other instances of nuclear morphological changes among both healthy and diseased vertebrate cells. Like neutrophils, these fin margin cells develop branched nuclear morphology over the course of development, but unlike neutrophils appear to decrease branching to some degree as tadpoles age.

Xenopus has long served as a model organism for nuclear morphology, including molecular and cell biological characterization of nuclear envelope components and the cell biological consequences of their perturbation. Overexpression of specific Lamin components has been observed to alter both nuclear shape and size in oocyte nuclei from *Xenopus laevis,* and nuclear size scaling in early *Xenopus* embryos is dependent on cytoplasmic volume as well as the nuclear transport factors Importin a and NTF2 (Good et al., 2013; Jevtić and Levy, 2015; Jevtić et al., 2015; Levy and Heald, 2010). More recently, *Xenopus* has served as a source model for proteomic studies of nuclear composition (Wühr et al., 2015). Morphological variation in nuclei later in embryogenesis has not been examined in depth. We find that nuclear branching begins late in neurulation, well after the initial specification of epidermal fate at the stage when multiciliated cells begin to undergo apical emergence (Sedzinski et al., 2016). Nuclear branching is dramatically

elaborated as the tail elongates, and by late tailbud stages highly branched nuclei are found both in multiciliated cells and their goblet cell neighbors. Our data suggest that nuclear branching is a general property of the fin margin epithelium in *Xenopus*. The extremity of morphological variation observed suggests that these nuclei may represent a valuable model for nuclear diversity: they are easily imaged, in a whole organism system that is easily modulated both genetically and through small molecules.

2.4.2.Branched nuclei do not interfere with cell health or mitosis

Xenopus epidermal fin cells exhibit branched nuclear morphologies while maintaining an active cell cycle. This contrasts with many cases of non-ellipsoid nuclear morphologies, which occur in post mitotic cells. In the epidermis, keratinocytes are known to undergo nuclear flattening and to acquire irregularities in their nuclear envelope after cell cycle exit, and these become more extreme with aging or in specific disease scenarios (Yang et al., 2011). Among actively cycling cells, nuclear morphological perturbations such as blebbing or nuclear ruffling are common in cancer cells but very infrequent in healthy cell types (Denais and Lammerding, 2014; Fu et al., 2012; Pillay et al., 2013; Shah et al., 2013). We find that nuclear branching is common in mitotic epidermal cells in the *Xenopus* tail fin, with rapid collapse of nuclear branching approximately 7 minutes before metaphase and re-formation of nuclear branches becoming apparent 21 minutes after cytokinesis. Branched nuclei do appear to undergo complete nuclear envelope breakdown, and we have not found evidence of karyomeres or chromosome-specific nuclear envelopes as are seen in the early mitoses of zebrafish and *Xenopus* (Lemaitre et al., 1998; Schoft et al., 2003). Following mitosis, the branched structure formed by the two daughter cells are distinct and do not faithfully recapitulate the mother cell's nuclear morphology.

In cells with branched nuclei, we find that both active enhancers and heterochromatin are distributed continuously throughout the nucleus. Normally, regions of chromatin that are transcriptionally repressed are associated with the nuclear lamina and the periphery of the nucleolus (Mattout et al., 2015b; Mattout et al., 2015a; Peric-Hupkes et al., 2010; Perovanovic et al., 2016; Solovei et al., 2013; Towbin et al., 2012). In TEM of branched epidermal nuclei, we see no increase in electron density around the nuclear periphery, nor do we find evidence of increased electron density representing a nucleolus in most nuclei. However, we found that cells with branched nuclei did contain foci of fibrillarin, a component of the

nucleolus, in regions distinct from the densest chromatin as represented by H2B fluorescence. Interestingly we do see puncta of increased intensity of HP1β and H3K9Me3 but have not yet seen corresponding regions of increased density on TEM. Taken together this suggests that cells with branched nuclei may partition heterochromatin without anchoring these regions to the nuclear lamina. Future research will examine the organization of heterochromatin in branched nuclei, and the organization of specific chromatin domains within these nuclei.

2.4.3.Nuclear branching in tail fin is dependent on nucleoskeleton components

Previous work has shown a role for the nuclear lamina, LINC complex, and cytoplasmic actin in the shaping of the nucleus (Chen et al., 2014; Hatch and Hetzer, 2016; Hatch et al., 2013; Ho et al., 2013; Kim and Wirtz, 2015; King and Lusk, 2016; Lammerding et al., 2006; Ramdas and Shivashankar, 2015; Webster et al., 2009; Wiggan et al., 2017). Here we have shown that both an intact actin network and Lamin B1 are necessary to maintain nuclear branches. Our working model therefore suggests that actin and LaminB1 filaments serve to maintain nuclear branches by stabilizing curvature across the nuclear envelope. Loss of either filamentous actin or LaminB1 results in a broken bridge across the nuclear envelope disrupting local curvature without envelope blebbing (Figure 2-8F). Additional experiments will be needed to clarify how the loss of Lamin B1 may indirectly affect the localization of other Lamin sub-types or how binding partners affect nuclear branching.

Actin is known to play a role in compressing the nucleus with stress fibers during migration or passage through narrow openings (Versaevel et al., 2012; Vishavkarma et al., 2014; Wiggan et al., 2017). In laminopathies nuclei lose rounded morphologies and adopt more irregular architectures. Previous studies have also shown that gaps in the nuclear lamina allow blebbing (Hatch et al., 2013). Conversely, the fin margin nuclei appear to have a fully functional lamina network with no apparent gaps. There was no obvious localization of actin to the base or tips of nuclear branches indicative of actin pushing or pulling on the nucleus, but loss of actin caused nuclei to increase in circularity, suggesting that by some other mechanism they contribute to nuclear branching. We also found that the loss of actin did not increase nuclear depth suggesting that the extra-cellular matrix or other force transmitting molecules cause the flattening of this tissue. We did find that there was a decrease in nuclear surface are to volume ratio when

f-actin was lost, as well as a modest decrease in total nuclear volume. These observations both suggest that nuclear envelope distribution, and possibly size, are closely linked to f-actin in these nuclei. While it is clear f-actin is necessary to maintain nuclear branches, it is unclear how nuclear actin or actin binding proteins contribute to maintenance, and establishment of nuclear branches. Previous studies have shown a relationship between cell-spreading and nuclear actin polymerization raising the possibility that in this flattened epithelium nuclear actin may contribute to nuclear branch formation (Keeling et al., 2017; Plessner et al., 2015). Another possibility that we have not yet been able to test explicitly is the role for intra-nuclear actin filaments (Baarlink et al., 2017; Kalendová et al., 2014; Oda et al., 2017), which may also contribute to nuclear branching. Our time-lapse imaging show that nuclear morphological change tracks closely in time with cytoplasmic f-actin disruption. We therefore favor the hypothesis that cytoplasmic f-actin is required for nuclear morphology, but intranuclear actin may also contribute to the formation or stabilization of branches.

2.4.4.A potential biological function for nuclear branching

Perturbations of nuclear branching have deleterious effects on the formation of the fin and consequently on its downstream function. While we have been able to show that specific nucleoskeletal components are required for nuclear branching, the ultimate role of branched nuclear morphologies in tail fin cell and tissue function remains open. Nuclear branching may play a role in genomic organization or gene regulation, as discussed above, or in fin biomechanics.

The thin epithelium of the tadpole fin is made up of flattened epidermal cells that overlie a mesenchymal core. Its specialized cell biological and biophysical properties allow rapid regeneration and sinusoidal swimming movements (Tucker and Slack, 2004). To accommodate this structure, a flattened nuclear structure would be advantageous, and nuclear branching could impart biophysical properties necessary for tissue function. The elastic modulus of the nucleus has been shown to be different than that of the cytoskeleton. The irregular nuclear structure could aid in creating a more uniform elastic modulus of the tissue, as opposed to localized regions of differential stiffness (Guilak et al., 2000; Kha et al., 2004; Pajerowski et al., 2007). The requirement of Lamin B1 to maintain nuclear branches suggests that nuclear

branching could be modulating tissue stiffness (Kha et al., 2004; King and Lusk, 2016; Pajerowski et al., 2007; Swift et al., 2013; Verstraeten et al., 2008; Zwerger et al., 2013).

In conclusion, we have shown that the fin epithelium of the *Xenopus tropicalis* tadpole tail contains a heterogenous population of cells that have branched nuclear structures. These cells with branched nuclei are healthy and have active cell cycles. Additionally, we have shown that nuclear branching depends on an intact actin network and Lamin B1. We determined that forces incurred from swimming are not necessary to induce nuclear branches, however, loss of nuclear branching through *lmnb1* mutations decreases swimming efficiency and impede tail and fin development. These cells offer a novel system to study extreme nuclear morphological variation in a healthy tissue.

2.5.Methods

2.5.1.Ovulation, in vitro fertilization, and rearing of embryos

Use of *Xenopus tropicalis* was carried out under the approval and oversight of the IACUC committee at UW, an AALAC-accredited institution. Ovulation of adult *X. tropicalis* and generation of embryos by in vitro fertilization according to published methods (Khokha et al., 2002; Sive et al., 2010). Fertilized eggs were de-jellied in 3% cysteine in 1/9x modified frog ringer's solution (MR) for 10-15 minutes. Embryos were reared as described (Khokha et al., 2002). Staging was assessed by Nieuwkoop and Faber (Nieuwkoop and Faber, 1994).

2.5.2.mRNA synthesis and injections

DNA plasmids were linearized at appropriate restriction sites (Table 1) and mRNA was transcribed with Sp6 mMessage mMachine kits (Ambion). mRNAs were injected into embryos at the 1-8 cell stage at a dose of 100 pg/ embryo, depending on experiment. The following constructs were generated in pCS2+ and linearized with NotI: Nuclear-GFP*, H2B-RFP*, Membrane-GFP*, Utrophin-GFP**, LifeAct-GFP**, LmnB3-GFP***. Lmnb1 Rod only and Fibrillarin-GFP**** were generated from pCS107 that was KpnI linearized. Finally, GFP-HP1β (Mattout et al., 2015b) was linearized with KpnI from pBCHGN.

*Generous gifts from Richard Harland, University of California Berkeley

** Generous gift from John Wallingford, University of Texas Austin

***Generous gift from Daniel Levy, University of Wyoming

****Generous gift from Clifford Brangwynne, Princeton University

2.5.3.Immunohistochemistry

X. tropicalis embryos were fixed for 20 minutes in MEMFA at room temperature. Embryos were permeabilized by washing 3X 20 minutes in PBS + 0.01% Triton x-100 (PBT). Embryos were blocked for 1 hour at room temperature in 10% CAS-block (Invitrogen #00-8120) in PBT. Then embryos were incubated in primary antibodies (see Supplemental table 2) in 100% CAS-block overnight at 4°C. Embryos were then washed 3X 10 minutes at room temperature in PBT and re-blocked for 30 minutes in 10% CAS-block in PBT. Secondary antibodies (see table below) were diluted in 100% CAS-block and incubated for 2 hours. Embryos were then washed 3X 20 minutes in PBT. Whole embryos or isolated tails were mounted on slides in Vectashield containing DAPI (Vector Laboratories #H-1500). Images were acquired with a Lecia DM 5500 B and ORCA-flash 4.0LT camera. LaminB1 (Abcam 16048), and Phospho-H3 (Abcam 14955) were utilized at a 1:1000 dilution. H3K27ac (Abcam 4729), β-tubulin (Sigma T8535), H3K27Me3 (Abcam 6002-100), H3K4Me (Abcam 8895), H3K9Me3 (Active Motif 39162), Anti-Mouse (Life Technologies A21422), and Anti-Rabbit (Life Technologies A11008) were utilized at a 1:500 dilution. α- tubulin (Invitrogen 62204) was utilized at a 1:250 dilution.

2.5.4.Quantification of the number of nuclear branches

Branches were counted as the number of termini of the nucleus (Figure 2-2), Branches were counted from images of tadpoles with nuclear markers of H2B, DAPI, or Nuclear localized GFP.

2.5.5.Live imaging conditions

Tadpoles were imaged sedated in 0.01% tricaine in 1/9th MR. Tadpoles were mounted for imaging as previously described (Kieserman et al., 2010; Wallingford, 2010) with the following modifications for Actin and Lamin B1 perturbation (Figure 2-5,5): A perimeter of vacuum grease was made on a glass slide. A tadpole was placed in the center of the vacuum grease perimeter with several drops of media containing

drug. A glass cover slip was gently pressed into the vacuum grease perimeter over the tadpole. Images were acquired with a Lecia DM 5500 B. Mitosis and Actin perturbation movies were acquired with a Zeiss 880. Gross tadpole morphologies were acquired with a Lecia M205 FA.

2.5.6.Transmission electron microscopy

Stage 41 tadpoles were fixed in 2.5% glutaraldehyde/0.1M sodium cacodylate buffer. Samples were washed 4 times in sodium cacodylate buffer, postfixed in osmium ferrocyanide (2% osmium tetroxide/3% potassium ferrocyanide in buffer) for 1 h on ice, washed, incubated in 1% thiocarbohydrazide for 20 min, and washed again. Samples were washed and *en bloc* stained with 1% aqueous uranyl acetate overnight at 4°C. Samples were finally washed and *en bloc* stained with Walton's lead aspartate for 30 min at 60°C, dehydrated in a graded ethanol series, and embedded in Durcupan resin. Serial sections were cut at 60 nm thickness and viewed on a JEOL-1230 microscope with an AMT XR80 camera (Giarmarco et al., 2017).

2.5.7.qPCR

Total RNA was isolated from embryos (3-5 per experiment) or fin margin (15-20 per experiment) (Sive et al., 2010). RNA was treated with DNAse 1 (Invitrogen #18068015). cDNA was synthesized using SuperScript III first strand synthesis kit (Intivrogen #18080-051). Quantitative PCR analysis was preformed using BioRad iCycler PCR machine, iQ Sybr Green mix (BioRad #1708862) and analysis software. Primer sequences are as follows:

lmnb1-forward AACCAGAACTCATGGGCAAC, reverse ACTGTTGTGCGCTGTGCTAC

lmnb2-forward ACAGGCATTGGATGAACTCC, reverse TCAAGCTTGGCCTGATAGGT

lmna-forward ACTGTACCGATTCCCACAGC, reverse GAGGAGCTGAGCTGGACAGT

odc (orthithine decarboxylase)- forward TTTGGTGCCACCCTTAAAAC, reverse CCCATGTCAAAGACACATCG.

2.5.8.Nuclear circularity quantification

A gaussian blur was applied to all images in a data set and a threshold was applied to images. Particles were selected using FIJI (ImageJ) and manually refined. Particles were discarded if the whole nucleus was not in the field of view, if a partial particle was selected based on the original image, if a particle selected was comprised of two nuclei in the original image, or if a particle selected did not appear on the original image. After manual refinement circularity of particles were measured using FIJI (ImageJ) (Schöchlin et al., 2014).

2.5.9.Pharmacological inhibitors

Latrunculin B (Sigma, L5288) and Cytochalasin D (Sigma, C8273), Nocodazole (CalBiochem, 31430-18-9) were resuspended using DMSO as a vehicle. Latrunculin B and Cytochalasin D were equilibrated at room temperature for 1 hour prior to use. For experiments inhibitors were diluted to the following final concentrations in 1/9 MR: 1µM Latrunculin B, 10µM cytochalasin D (Lee and Harland, 2007), 150 µM Nocodazole.

2.5.10.Surface area and volume measurements

IMARIS was utilized to create the 3D renderings and perform the surface area and volume calculations, with a surface area detail level for all treatments of 0.25 µm. Nuclei were excluded if volumes were below 100 μm^3 or above 1000 μm^3, as these were determined to be incomplete nuclei or fused nuclei respectively when images were examined.

2.5.11.CRISPR guide design and injection

CRISPR guides were designed from the V7.1 or V8 gene models on Xenbase and CRISPRscan. Target sites were chosen from UCSC tracks. Guides were chosen using the following criteria: no off targets predicted, a score greater than 50, and in a region in or as close to exon 1 as possible. We generated site specific sg-RNA by ordering a single oligo 5' - CTAGCTAATACGACTCACTATAGG-(n18) target sequence GTTAGGAGCTAGAAATAG-3' (Table below). PCR was performed as described in Bhattacharya et al. (Bhattacharya et al., 2015). SgRNA was transcribed using T7 mMachine kit (Ambion). Guides were injected

into 1 or 2 cell embryos (dose in table below) with 1.5ng Cas9 (Bhattacharya et al., 2015; Nakayama et al., 2013). All guides were injected at a dose of 400 pg/embryo, the targeting sequences are as follows:

LmnB1 G1-GGGAAGAGGTGCGGAGCC

Lmnb1 G2- GCGGAGCCGGGAAGTGAG

Scrmbl – GGGAAGAGGGCGTGAGCC

2.5.12.Dominant negative LmnB1

Lamin B1 dominant negative constructs were constructed following a similar strategy to Schrimer et al. (Schirmer et al., 2001), beginning with *X. laevis* Lamin B1 (Xenbase ORFeome clone XICD00712670) with the following primers: Rod only left primer: GGATCCATGGCCACTGCCACA and right primer: GAATTCCAGTGGCAGAGG.

2.5.13.High-resolution melt analysis

To extract genomic DNA individual tadpoles were lysed by heating at 95°C in 25mM NaOH and 0.2mM EDTA. Samples were cooled to RT and equal volume of TRIS-HCl 40 mM buffer was added. 2µL of extracted genomic DNA was utilized in PCR reactions containing HRM master mix (GoTaq Flexi buffer (Promega #M8901), dNTPs, $MgCl_2$, DMSO, EvaGreen (Biotium #31000), taq polymerase (Quiagen #201203), nuclease free water). The region of interest was amplified (Left primer GATCTGCAGGAGCTGAATGAC, right primer TGTTCCACGGAGATCTTACTGA) for 35 cycles and melted from 60 - 95°C at 0.1°C increments with EvaGreen fluorescence measured after each temperature change.

2.5.14.Explants

Dorsal posterior explants were dissected between stage 15-17 as previously described (Tucker and Slack, 2004). Explants were cultured in Danilchik's for Amy (DFA) buffer without antibiotics. Sibling tadpoles were reared in 1/9th MR as described above.

2.5.15.Statistical analysis

R studio was utilized in generating statistics. One-way ANOVA, with Tukey's post hoc was utilized to calculate P-values for circularity and tail morphometric measurements, for qPCR, nucleoli number, and surface area and volume measurements P-values were calculated with a two-tailed student's t-test assuming unequal variance.

2.6.Acknowledgements

We thank Ed Parker for assisting with TEM imaging, and the UW vision core facility (NEI P30EY001730). We acknowledge support from the W. M. Keck Center for Advanced Studies in Neural Signaling (NIH S10 OD016240) and the assistance of center manager Dr. Nathaniel Peters. We are grateful to Nathaniel Ng of the Enrique Amaya lab for testing staging conditions for time-lapse analysis and preliminary movies. Alexander Chitsazan helped with training in R and advised on statistical methods. We thank the Molecular and Cell Biology of Xenopus Course at Cold Spring Harbor for embryology and microscopy training, the Xenopus Quantitative Imaging Course at the Marine Biological Laboratories for training in imaging and statistical analysis. We thank Xenbase for curation of genomic and literature information used to generate materials and conduct analysis. We thank Wills lab members, Emily Hatch of FHRC and John Wallingford of UT Austin for comments on the manuscript. Finally, we thank Daniel Levy University of Wyoming, Richard Harland UC Berkley, Cliff Brangwynne Princeton University, and John Wallingford UT Austin for materials

CHAPTER 3. CHROMATIN ACCESSIBILITY ANALYSIS REVEALS DISTINCT FUNCTIONS FOR HDAC AND EZH2 ACTIVITIES IN EARLY REGENERATION

3.1.Abstract

Xenopus tropicalis tadpoles have the capability to scarlessly regenerate appendages including the limb and tail. Following injury, complex genetic processes must be activated and inactivated with high spatial and temporal resolution to result in a properly patterned appendage. Functional studies have established that histone modifying enzymes that act to close chromatin are required for regeneration, but the genomic regions sensitive to these activities are not established. Here we show that early inhibition of HDAC or EZH2 activity results in incomplete regeneration. To identify the impact that each of these perturbations has on chromatin accessibility, we applied an assay for transposase accessible chromatin (ATAC-seq) to HDAC or EZH2 inhibited regenerating tadpoles. We find that neither perturbation results in a global increase in chromatin accessibility, but that both inhibitors have targeted effects on chromatin accessibility and gene expression. Upon HDAC inhibition, promoter regions and regulatory regions neighboring genes associated with neuronal regeneration are more accessible, whereas following EZH2 inhibition we find gene bodies and regulatory regions associated with regulation of the immune response and apoptosis are preferentially accessible. Together this suggests distinct roles for EZH2 activity and HDAC activity in appendage regeneration.

3.2.Introduction

Xenopus tadpoles have the remarkable capacity to scarlessly heal after a wide variety of injuries including, limb amputation, spinal cord transection, and tail amputation (Beck et al., 2009; Kakebeen and Wills, 2019; Lee-Liu et al., 2017). While many animals regenerate after injuries, including zebrafish, axolotl, planaria, acoels, and hydra, these animals are lifelong regenerators, while *Xenopus* have stage specific-regenerative competency (Edwards-Faret et al., 2021; Gehrke et al., 2019; Kawasumi et al., 2013; Mitogawa et al., 2018; Siebert et al., 2019; Suzuki et al., 2006). This places *Xenopus* as a particularly powerful model to study changes in gene regulation that are either pro-regenerative, or inhibitory to regeneration.

After injury in *Xenopus,* it is well established that dynamic changes in transcriptional activity help to close the wound, pattern, and grow new tissue. Many classical developmental pathways are known to function in regulating the regenerative response, including Wnt, Shh, TGFβ, BMP, Notch, and FGF (Beck et al., 2003; Ho and Whitman, 2008; Slack et al., 2008; Taniguchi et al., 2014). In addition, the advances in genomic sequencing has enabled large scale studies of transcriptional dynamics of the regenerative process of bulk tissue and at the single-cell level in *Xenopus* (Aztekin et al., 2019; Chang et al., 2017; Kakebeen et al., 2020) and other regenerative species (Gerber et al., 2018; Siebert et al., 2019; Wu et al., 2013). These studies all point to complex and dynamic changes in regulation of the transcriptional landscape, but also highlight that we still know relatively little about the gene regulatory landscape underlying and enabling transcriptional changes.

There are many points of possible regulation that would modulate changes in gene expression. Work over the last several years has begun to probe the contributions of specific histone modifying enzyme activities to gene expression dynamics but has also illustrated that these enzymatic activities can have effects not easily parsed by overall regeneration outcomes. Histone deacetylase (HDAC) activity is well documented to be required in early regeneration of multiple species, including *Xenopus* and axolotls (Taylor and Beck, 2012; Tseng et al., 2011; Voss et al., 2019). By contrast, in the mouse retina, inhibition of HDAC activity serves to enhance regeneration and cell reprogramming, specifically be increasing chromatin accessibility at neuronal enhancers (Jorstad et al., 2017; VandenBosch et al., 2020). The effects of HDAC perturbations on axonal regeneration are also complex and even sometimes opposing (Cho and Cavalli, 2014). Additional enzymatic activities that modulate chromatin accessibility, including the histone methyltransferase EZH2 and DNA methylase, are required for regeneration of structures such as the *Xenopus* hindlimb and zebrafish fin (Hayashi et al., 2015; Hirose et al., 2013). Approaching the same problem from the other side by considering genomic target loci rather than the chromatin modifier, multiple studies have also identified regeneration-specific enhancer elements that are activated following injury, as in the *Drosophila* imaginal disc (Harris et al., 2016), or have highlighted sets of genes with increased chromatin accessibility following injury, as in *Xenopus* neural progenitors (Kakebeen et al., 2020). Thus, while there is abundant evidence that histone-modifying-enzymatic activities impact regeneration, and that changes in chromatin accessibility either at specific regions or genome-wide impact regeneration.

In *Xenopus*, both HDAC activity and EZH2 activity have been shown to be required for appendage regeneration (Hayashi et al., 2015; Taylor and Beck, 2012; Tseng et al., 2011). These enzymes both act to render chromatin less accessible (Figure 3-1). However, the effect of either of these modifications on chromatin accessibility has not been directly assayed in this context, leaving open several questions. Among these are whether either or both activities maintain inaccessible chromatin globally across the genome, or whether they act at a specific subset of loci. If they act predominantly at specific loci, are their targets shared, or do HCACs and EZH2 target different gene sets? We also sought to establish greater temporal resolution over when each of these activities is required. By addressing these questions directly, we can gain greater insight into how the multiple independent chromatin modifying activities that contribute to regeneration are regulated across the genome. To address these gaps, we used ATAC-seq (Buenrostro et al., 2015) to capture chromatin accessibility states of regenerating *Xenopus* tails in the first 24 hours post amputation (hpa) while inhibiting histone deacetylase (HDAC) activity or the PRC2 complex via inhibition of EZH2 with the goal of identifying distinct roles for these two modes of epigenetic modification in regulating regeneration in *Xenopus tropicalis*. We find that both HDAC and EZH2 inhibition have relatively minor effects on global patterns of chromatin accessibility, and that each targets different subsets of genes, affecting distinct processes required for overall regeneration success.

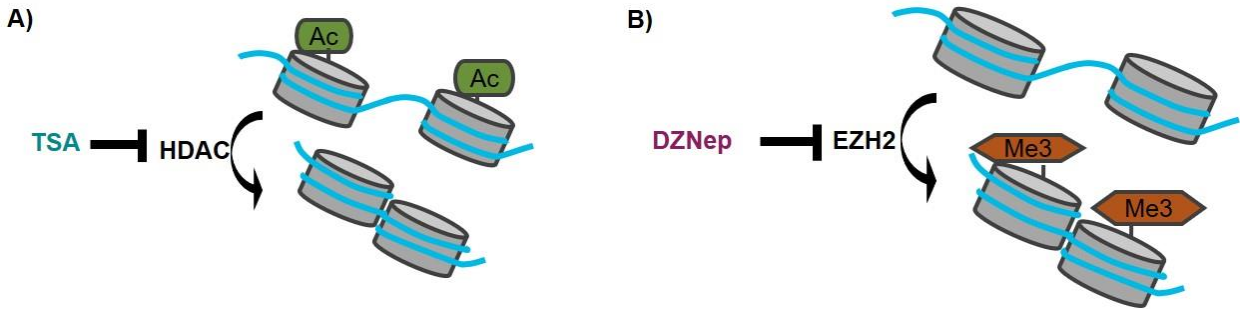

Figure 3-1 HDAC and EZH2 activity aide in chromatin closure.
A) Schematic of HDAC activity B) Schematic of EZH2 activity.

3.3.Results

3.3.1. HDAC and EZH2 activity are required during the first 24 hours of appendage regeneration

To determine if perturbations of HDAC or EZH2 activity affected regenerative outcomes during specific time periods of *Xenopus tropicalis* tail regeneration, we amputated stage 41 tadpoles and treated with the HDAC inhibitor TSA, or the EZH2 inhibitor DZNep (3-Deazaneplanocin) for various windows of time from 0-72 hours post amputation (Figure 3-2 A). Both these inhibitors have been well-validated in previous studies of *Xenopus,* including appendage regeneration (Hayashi et al., 2015; Rao and LaBonne, 2018; Taylor and Beck, 2012; Tseng et al., 2011). We found that for TSA, progressively longer treatment windows resulted in progressively shorter regenerated tails (Figure 3-1B). However, with DZNep treatment we found that animals treated for only the first 24 hpa had significantly shorter regenerated tails than their control counterparts, whereas a longer treatment from 24-72 hpa had a milder defect, suggesting that EZH2 activity is most critical in the first 24 hours of regeneration (Figure 3-1C). For both treatments treating from 0-72hpa produced the strongest decrease in regenerate length. Interestingly, during the shorter treatment windows, we observed for many regenerates that even if the tissue was regrowing to the same length as their counterpart controls that not all the tissues were present. To quantify this, we binned animals in 5 categories: full regeneration in which all tissues were present; 1 fin in which either the dorsal or ventral fin were absent; no fins in which only an axial tissue spike regenerated; wound closure in which there was no outgrowth of tissue after wound closure, or dead (Figure 3-3A). We found that fin regeneration was particularly sensitive to loss of HDAC activity, and that treatment with TSA for just the first 24 hpa caused almost all animals to fail to regenerate both fins (Figure 3-3B). Likewise, for animals treated with DZNep we found that fin regeneration seemed particularly susceptible to defects. Even short windows of DZNep treatment led to a loss of either the dorsal or ventral fin (Figure 3-3C). Based on these observations we concluded that both HDAC activity and EZH2 activity are required for tail regeneration in *X. tropicalis* and set out to define their chromatin accessibility targets.

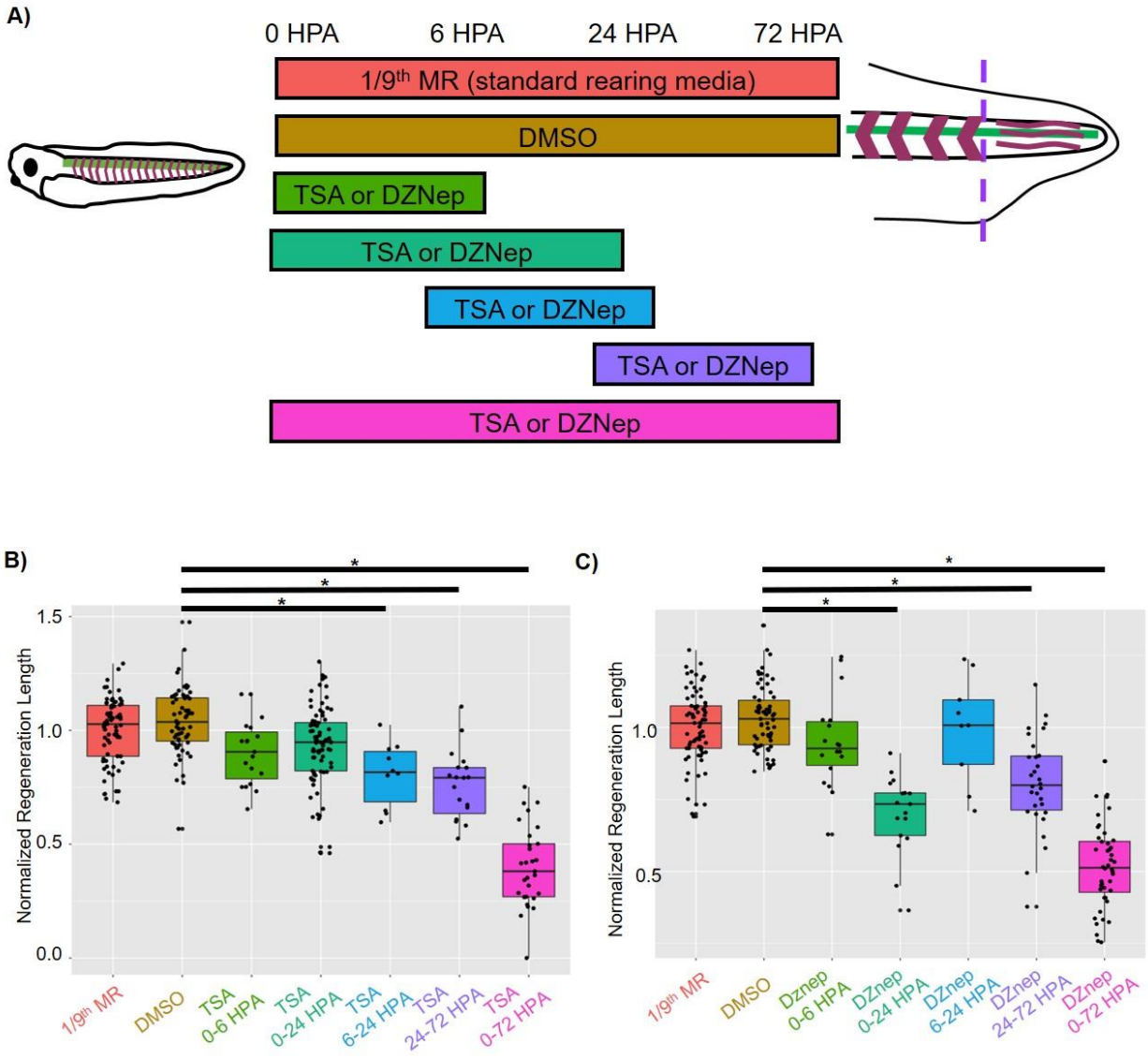

Figure 3-2 HDAC and EZH2 activity is necessary for *X. tropicalis* tail regeneration.

A) Experimental schematic of treatment windows during regeneration. 1/9th MR is tadpole rearing media, DMSO is the vehicle control. B) Tail regeneration length during windows of TSA treatment. B) Tail regeneration length during windows of DZNep treatment. B-C) * p<0.05 ANOVA with Tukey's post hoc.

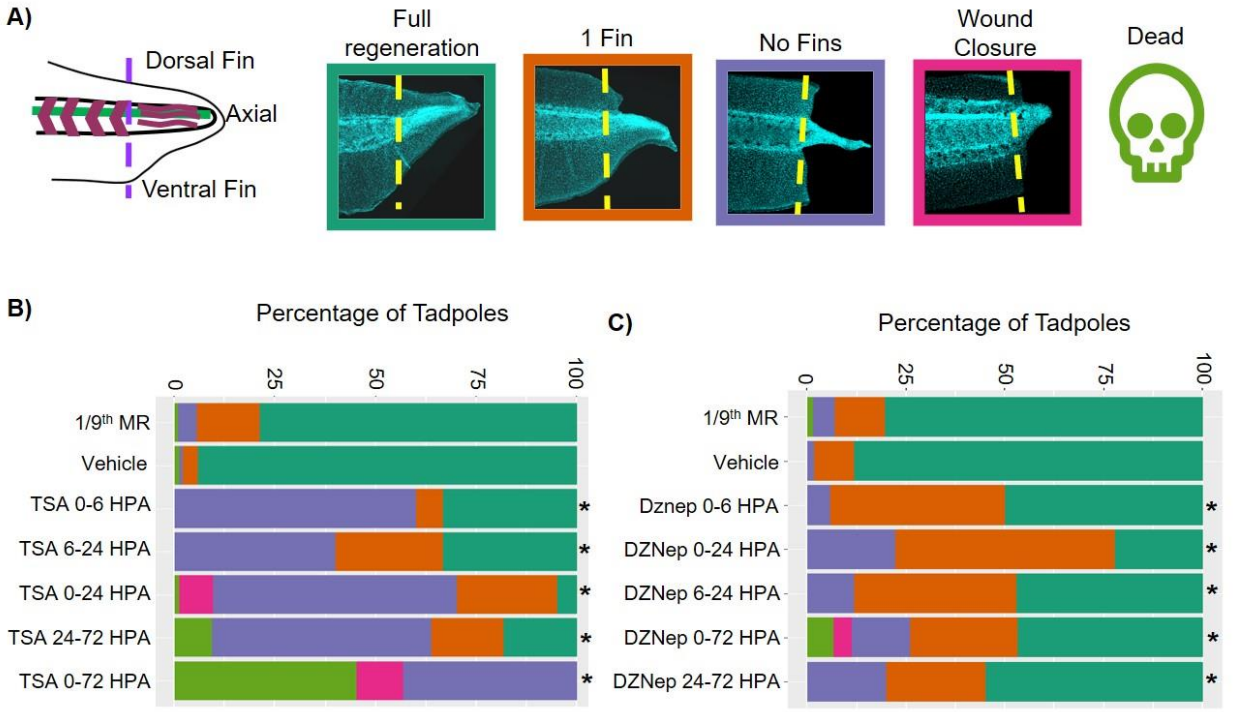

Figure 3-3 HDAC and EZH2 activity are necessary for regeneration of tissues.

A) Phenotypic classifications of regenerated tissues. B) Proportions of phenotypic classifications of regenerated tadpoles treated with TSA (* = p <0.05 compared to 1/9th MR and Vehicle, ANOVA with Tukey's post-hoc). C) Proportions of phenotypic classifications of regenerated tadpoles treated with DZNep (* = p <0.05 compared to 1/9th MR and Vehicle, ANOVA with Tukey's post-hoc).

3.3.2.Promoters are sensitive to inhibition of HDAC activity during regeneration

We next set out to identify the genomic targets of HDAC activity during regeneration utilizing ATAC-seq. TSA is a broad deacetylase inhibitor, and so identifying its effects on each possible histone acetylation site would require multiple rounds of ChIP-seq, CUT&RUN, or other epigenetic profiling techniques (Kaya-Okur et al., 2019; Skene and Henikoff, 2017). By using ATAC-seq we can identify all differentially accessible regions regardless of specific acetylation site(s). A caveat, however, is that we will also identify indirect effects of inhibiting HDAC activity. To identify chromatin accessibility changes resulting from TSA treatment over a regenerative time course, we first isolated uninjured control tissue from the posterior third of stage 41 tadpole tails and prepared this tissue for ATAC sequencing libraries. In parallel, we isolated the newly regenerated tissue at 0, 3, 6, and 24 hpa in both vehicle and TSA treated cohorts (Figure 3-4 A), collecting the tissue from the 250um adjoining the amputation plane as previously described (Kakebeen et al., 2020). Libraries for each timepoint were made in duplicate, multiplexed, and sequenced on the Illumina Next-seq

platform. Read alignment and peak calling methods were performed using a pipeline described in Materials and Methods (Appendix A). Sequenced libraries were selected for analysis if they met the minimum ENCODE standards for ATAC-seq (Figure 3-5).

A first possibility was that treatment with this broad deacetylase inhibitor would result in global increases in chromatin accessibility as all acetylated lysines were maintained. To determine if inhibiting HDAC activity resulted in a global gain in accessibility of chromatin, we compared the number of peaks called at each time point between TSA treatment and the stage matched DMSO vehicle control and found that similar numbers of peaks were called at each time point (Figure 3-5). We next determined which peaks were differentially accessible between TSA and vehicle regenerates at each time point and determined the proportion of peaks that either gained or lost accessibility when treated with TSA compared to the control. Approximately 50% of differentially accessible peaks gained accessibility when treated with TSA relative to the vehicle treated regenerates at 3hpa (Figure 3-5 B). This proportion subtly increased at 6hpa and 24hpa (Figure 3-4 B), suggesting that the proportion of open chromatin regions increases with time. Thus, TSA is not just causing a global gain in accessibility across the entire genome, and suggests that we are capturing both direct gains in accessibility and indirect losses as regeneration proceeds.

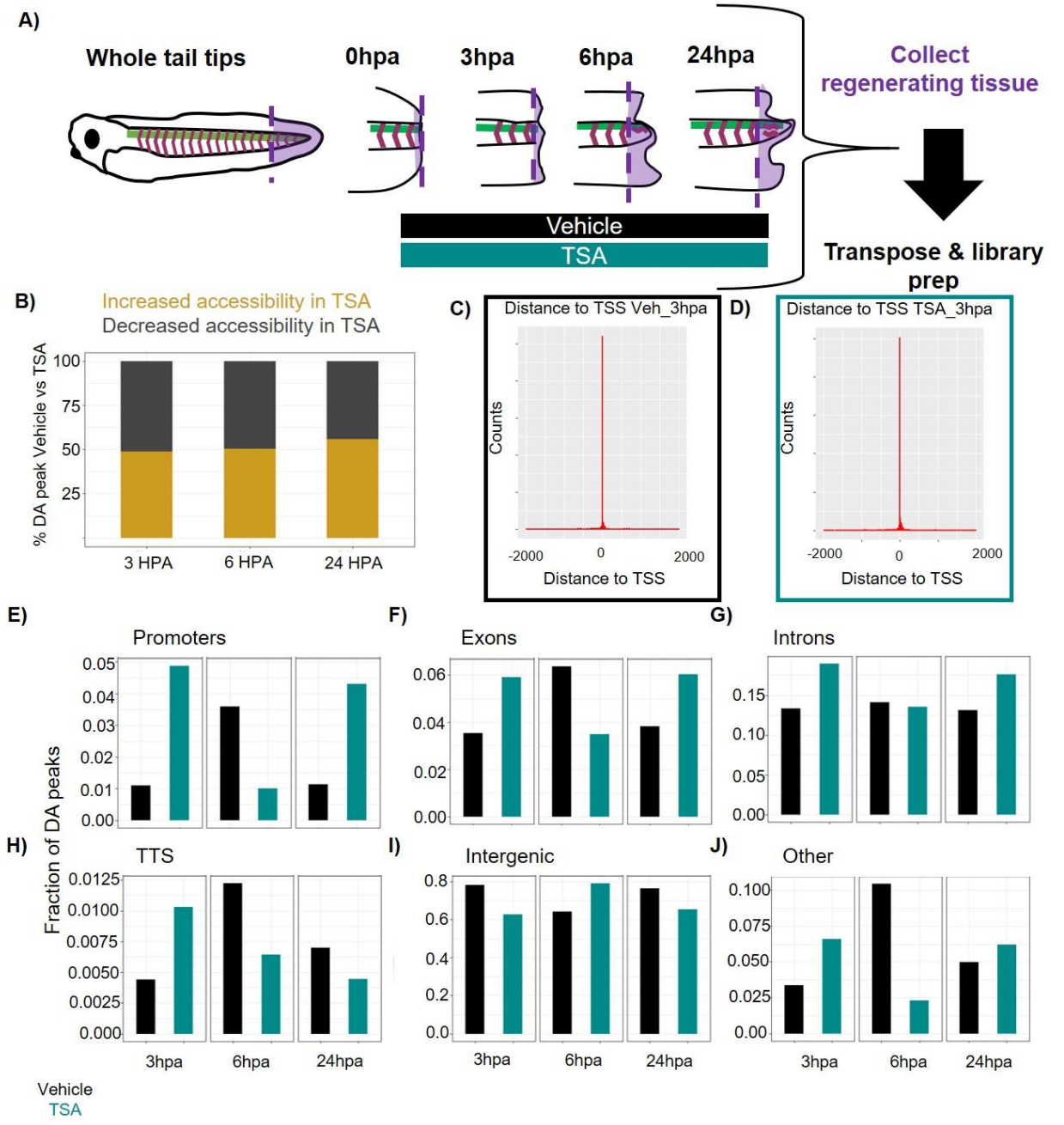

Figure 3-4 HDAC inhibition alters chromatin accessibility during *X. tropicalis* tail regeneration. A) Schematic of ATAC-seq experimental design. B) Proportions of differentially accessible peaks that have increased accessibility in TSA relative to the vehicle (gold) or decreased accessibility in TSA relative to the vehicle (black) at each regeneration timepoint. C) Representative histograms show distance of peaks calls to the transcription start site (TSS) in vehicle treated tadpoles. D) Representative histograms show distance of peaks calls to the transcription start site (TSS) in TSA treated tadpoles. E-J) Peaks flagged as having increased accessibility in the vehicle relative to TSA treatment (black), or in the TSA treatment relative to the vehicle (teal) for each time point were annotated to genomic features. The proportion of these differentially accessible peaks assigned to each genomic feature are plotted at 3, 6, and 24hpa. E) Promoters F) Exons G) Introns H) Transcription termination site (TTS). I)Intergenic regions J) Other genomic features.

We next examined the genomic distribution of peaks called in vehicle control and TSA-treated samples. As is typical for ATAC-Seq, most peaks called in either treatment condition were located within 500bp of a transcription start site, which is typical of ATAC-seq data, however there are still peaks that correspond to regions outside promoter regions (Figure 3-4 C, D). Since histone acetylation has been shown to be enriched near the transcription start site (TSS) and in enhancers during development (Bogdanović et al., 2012; Esmaeili et al., 2020; Rada-Iglesias et al., 2011; Wang et al., 2008), we hypothesized that we would find a bias in the proportion of differentially accessible peaks that were annotated to those features. We identified peaks that gained accessibility in TSA versus controls at each time point, as well as peaks that gained accessibility in controls versus the TSA treatment. We utilized HOMER (Heinz et al., 2010) to annotate peaks to genomic features and to determine based on the coverage of the peaks if there was an enrichment or depletion of any genomic feature (Figure 3-4E-J). We found that at TSA treatment was associated with an increase in accessible peaks at promoters, exons, and introns at both 3 and 24hpa, but not at 6hpa (Figure 3-4 E-G). The early increase in peaks that are more accessible when HDAC activity is inhibited suggests that one possibility of altering gene expression patterns in the first 3 hpa is make promoters less accessible by removing acetyl groups from histones, thereby preventing transcription factor binding.

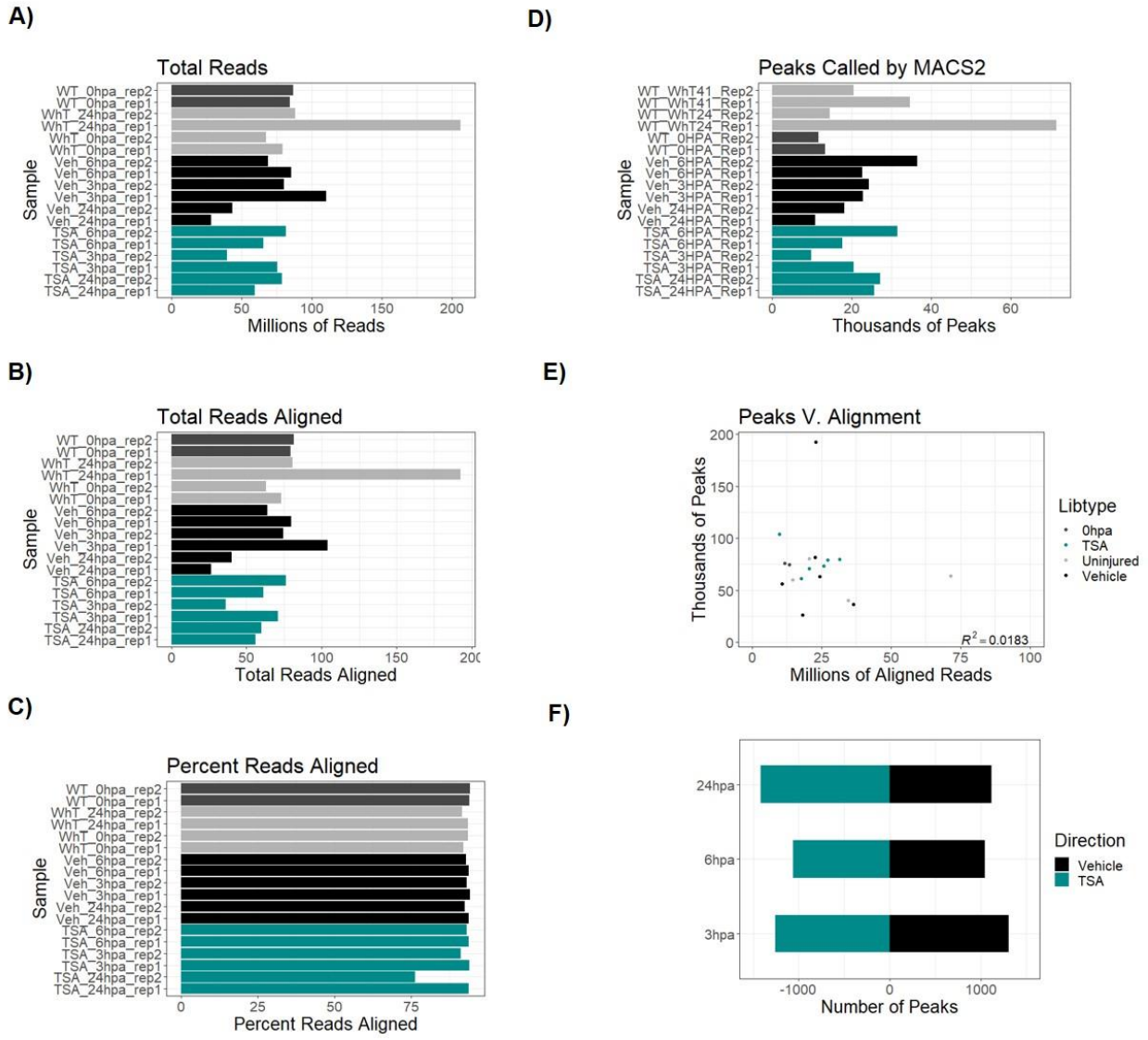

Figure 3-5 Quality control metrics of TSA and Vehicle control ATAC-seq datasets

A-F) 0hpa dark grey, uninjured tails dark grey, vehicle black, TSA treated teal. A) Total reads for each sequencing library. B) total reads aligned for each library. C) percentage of reads aligned. D) number of peaks called by MACS2. E) Peak versus alignment. F) Number of peaks during regeneration time points.

3.3.3. Inhibition of HDAC activity preferentially affects neuronal outgrowth early in regeneration

Next, we aimed to identify what types of biological processes were regulated by HDAC activity. We annotated all peaks to the nearest TSS to associate each peak with the closest gene. Next we identified regions of chromatin that gained accessibility in TSA treated versus vehicle control tadpoles at each time

point, and vice-versa, and used the associated gene name for gene ontology (GO) analysis using the GOrilla platform (Eden et al., 2007; Eden et al., 2009). We utilized the complete list of genes assigned to any peak in the analysis as the background gene set. We found that at 3hpa, peaks that the GO term negative regulation of transcription by polII was called, whereas the term positive regulation of transcription by polII was called in the TSA treated group (Figure 3-6A,B). This suggests that inhibiting HDAC activity is associated with increased transcriptional activity, as would be expected. While many GO terms were called we were most interested in two terms negative regulation of neuron death, and negative regulation of dendrite morphogenesis (Figure 3-6A,B). These terms suggested that we may expect the persistence of damaged neurons or neuronal structures that would normally lead to cell death or other cellular maintenance cues when HDACs are inhibited. Likewise, at 6 hpa in TSA treated tadpoles, genes were enriched for regulation of axon regeneration. No specific neural GO terms were identified in the TSA treatment at 24 hpa however, angiogenesis terms were called (File S1). We chose to focus on testing possible functional consequences of alterations in chromatin structure in HDAC inhabitation at 3 hpa reasoning that at this time point we were most likely to identifying direct target of HDAC activity and due to the strong phenotype of regenerating no fins, and only an axial spike.

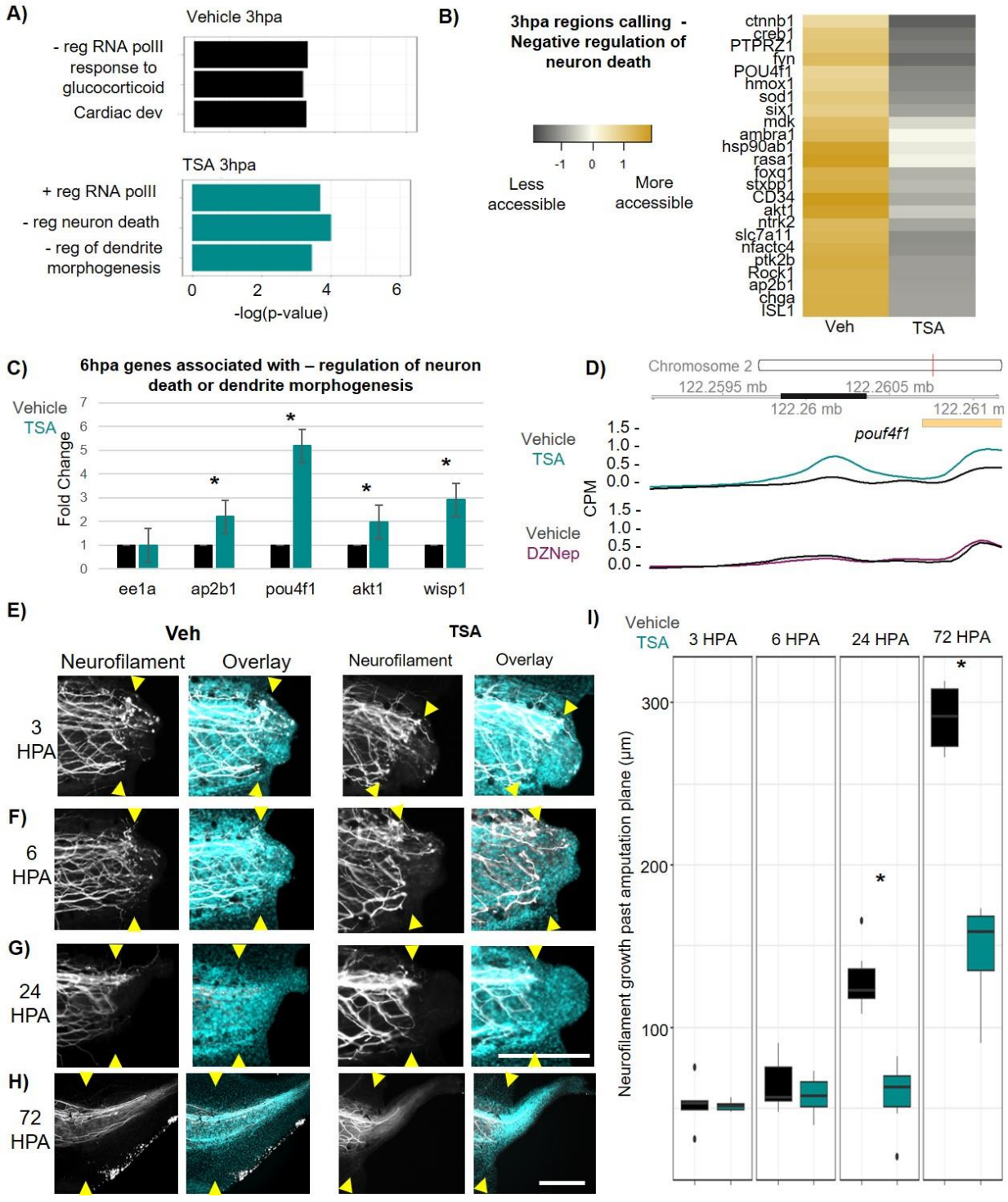

Figure 3-6 Neuronal regeneration is impaired by early HDAC inhibition.

Selected GO terms enriched at 3hpa called from regions with increased accessibility in the vehicle relative to TSA (black) or called from regions that had increased accessibility in TSA relative to the vehicle (teal). B) Differential accessibility heat map of genes assigned to the GO term negative regulation of neuron death or dendrite morphogenesis at 3hpa. C) RT-qPCR fold expression of selected

genes assigned to neural associated GO terms relative to *ee1a* in regenerating tissue. Data represents the mean +/- SEM (* p<0.05 tailed t-test). D) Representative gviz track of both TSA (teal) and DZNep (maroon) treated regenerates with their respective vehicle controls (both sets of controls are black but should be noted they are separate data sets) at 3hpa showing a differentially accessible ATAC-seq peak (dark bar) associated with a gene with differential expression in the TSA treatment. E-H) Time course of neurofilament immunofluorescence (white) in vehicle control tadpoles or TSA treated tadpoles at 3 (E), 6 (F), 24 (G), and 72 hpa (H). Yellow arrow heads indicate amputation plane. Scale bars = 250 µm, panel H shows a region double the size of E-G to show full regeneration of neurofilament. I) Box plots of neurofilament outgrowth past the amputation plane in vehicle (black), or TSA treated tadpoles (teal) (* p< 0.05, two tailed t-test n = 5-7 for each condition).

Having found that TSA-treated tadpoles had open chromatin at genes associated with neuronal maintenance and regeneration at 3 and 6 hpa, we decided to explore the possible role for HDAC activity in neuronal regeneration. We used RT-qPCR to determine if the increase in accessibility of the ATAC-seq peak was accompanied by an increase in gene expression. We looked at 4 of the genes associated with the GO terms negative regulation of neuron death and negative regulation of dendrite morphogenesis: *ap2b1*, *akt1*, *wisp1 (ccn4* in *Xenopus)*, and *pou4f1* and found these all had increased expression by 6 hpa, but not at 3hpa (Figure 3-6C). This suggests that the increased chromatin accessibility in peaks assigned to these genes does indeed precede an increase in their expression. To explore if the changes in accessibility were specific to HDAC inhibition we asked if EZH2-inhibited tadpoles also had increased accessibility at the same genomic loci. We found that these regions of increased accessibility were specific to HDAC inhibition and were not seen in EZH2-inhibited tadpoles. In the genes that we confirmed had both increased accessible peaks and increased gene expression (Figure 3-6D).

Next, to determine if there was a change in neuronal morphology during regeneration, we stained vehicle and TSA treated animals with neurofilament to visualize axon morphogenesis. Neurofilament stains show similar patterns of staining between vehicle and TSA treated groups at 3 and 6 hpa. However, by 24 hpa there was a decrease in the length of axons originating from the spinal cord growing into the regenerating tissue in the TSA treated group. (Figure3-6 E-I). By 72 hpa there is almost no regeneration of axons into the axial tissue spike that regrows in TSA treated animal while there is robust outgrowth of axons into the new tissue in the control suggesting that early HDAC inhibition prevents axon outgrowth (Figure3-5I, J). This suggests that HDAC activity is necessary for early mediation of the transcriptional response of neuronal cells during regeneration that lead to axonal outgrowth after injury.

3.3.4. Gene bodies are sensitive to EZH2 inhibition during early regeneration

We set out to use the same strategy to identify targets of EZH2 activity during regeneration utilizing ATAC-seq. As for TSA, the posterior third of stage 41 tadpole tails were amputated and prepared for sequencing libraries as well as the newly regenerated tissue at 0, 3, 6, and 24 hpa in both vehicle and DZNep treated cohorts (Figure 3-7 A), with libraries made in duplicate and sequenced as above. As we had found for TSA, approximately 50% of differentially accessible peaks had increased accessibility in tadpoles treated with DZNep, relative to the vehicle treated controls (Figure 3-7 B), a proportion that also increased slightly over regenerative time. Additionally, a similar number of peaks was called in DZNep treated samples and controls (Figure 3-8). Thus, DZNep also does not cause a global increase in chromatin accessibility, but rather likely has more localized effects.

In DZNep treated tadpoles we found that most peaks were located near transcription start sites, as expected (Figure 3-7 C, D). The methylation mark H3K27me3, which is deposited by EZH2 activity, is associated heavily with bivalent or facultative heterochromatin in promoters and gene bodies (Bernstein et al., 2006; Bogdanović et al., 2012; Mattout et al., 2015a; Rada-Iglesias et al., 2011; Wang et al., 2008) so we hypothesized that there would be an enrichment of accessible peaks annotated to those regions. We found at all time points there was an enrichment of differentially accessible peaks in exons in the DZNep treatment group suggesting the gene body accessibility may be regulated by EZH2 activity during regeneration. Additionally, we found at 6hpa that there was an enrichment for peaks falling in promoter regions in the DZNep treatment suggesting that EZH2 activity may be affecting promoter accessibility slightly later in the regenerative response (Figure3-7 E-J).

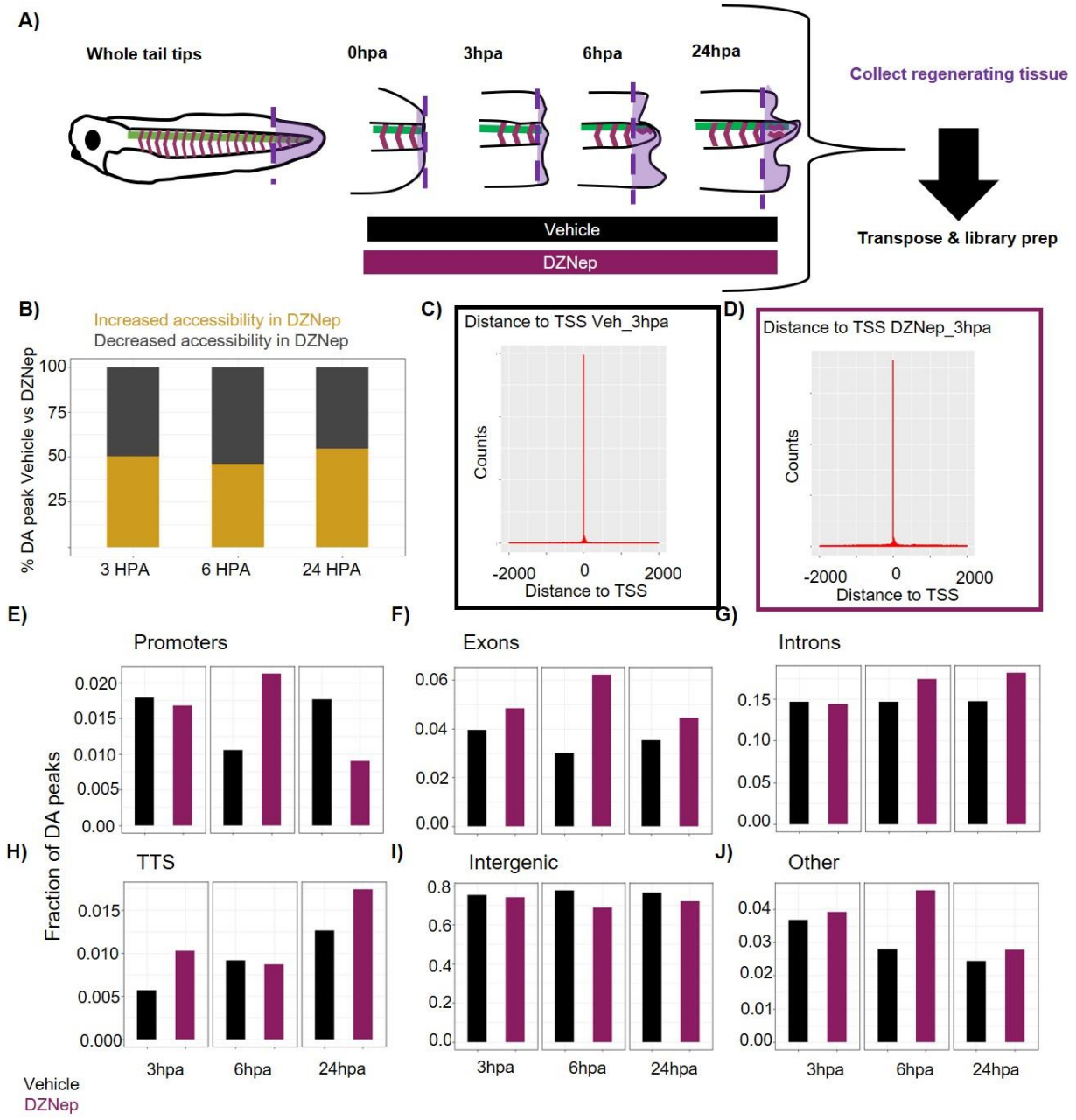

Figure 3-7 EZH2 inhibition alters chromatin accessibility during *X. tropicalis* tail regeneration. A) Schematic of ATAC-seq experimental design. B) Proportions of differentially accessible peaks that have increased accessibility in DZNep relative to the vehicle (gold) or decreased accessibility in DZNep relative to the vehicle (black) at each regeneration timepoint. C) Representative histograms show distance of peaks calls to the transcription start site (TSS) in vehicle treated tadpoles. D) Representative histograms show distance of peaks calls to the transcription start site (TSS) in DZNep treated tadpoles. E-J) Peaks flagged as having increased accessibility in the vehicle relative to DZNep treatment (black), or in the DZNep treatment relative to the vehicle (maroon) for each time point were annotated to genomic features. The proportion of these differentially accessible peaks assigned to each genomic feature are plotted at 3, 6, and 24hpa. E) Promoters F) Exons G) Introns H) Transcription termination site (TTS). I)Intergenic regions J) Other genomic features.

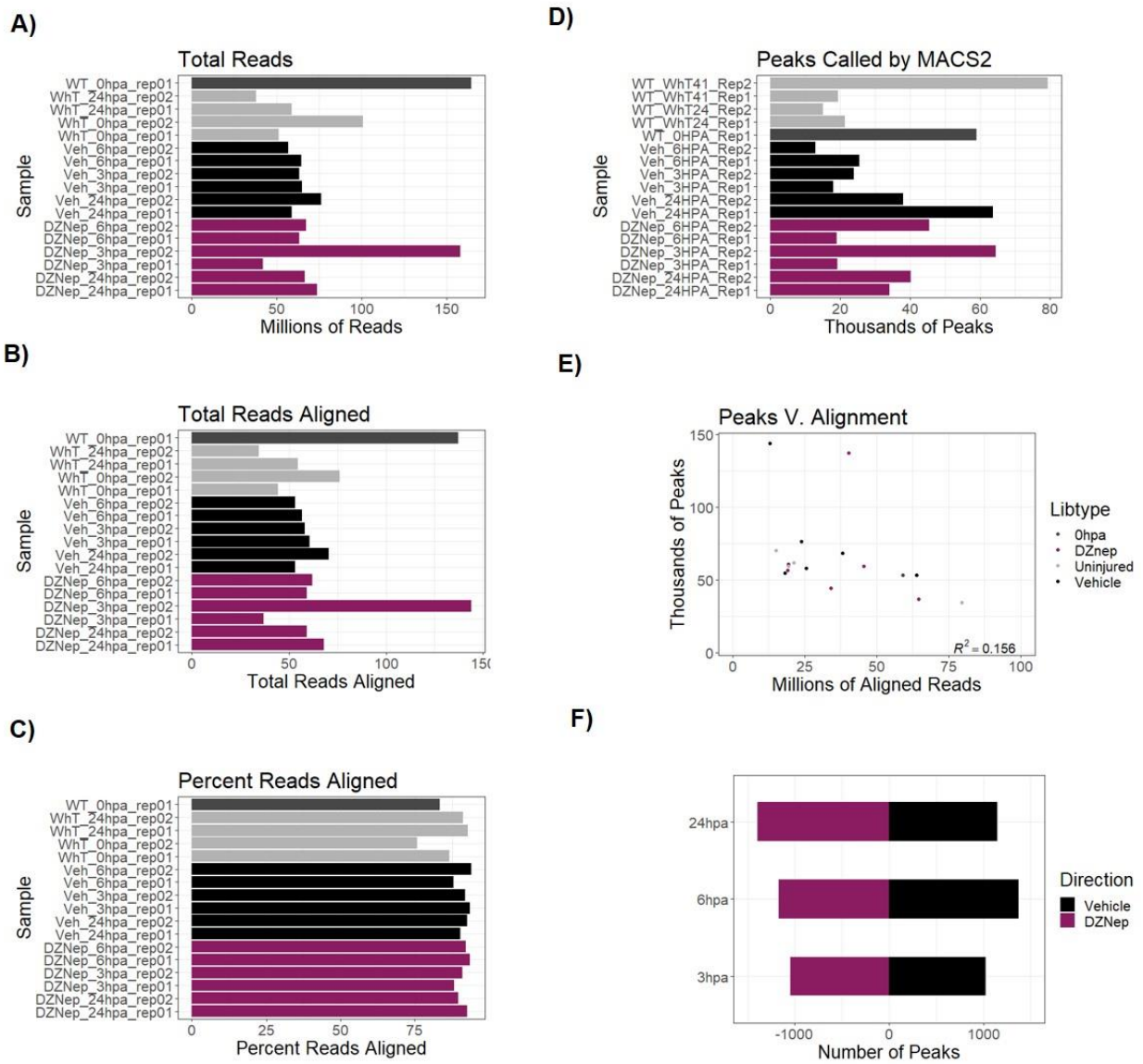

Figure 3-8 Quality metrics of DZNep and Vehicle control ATAC-seq datasets

A-F) 0hpa dark grey, uninjured tails dark grey, vehicle black, DZNep treated maroon. A) Total reads for each sequencing library. B) total reads aligned for each library. C) percentage of reads aligned. D) number of peaks called by MACS2. E) Peak versus alignment. F) Number of peaks during regeneration time points.

3.3.5.EZH2 inhibition perturbs the innate immune response in early regeneration

Our next goal was to identify biological processes regulated by EZH2 activity. We identified regions of chromatin that gained accessibility in DZNep versus the vehicle treated at each time point or vice-versa, annotated these peaks to their nearest neighboring gene, and used the associated gene name for gene ontology analysis, using the same pipeline we established for TSA analysis. At 3 hpa we found multiple GO

terms associated with innate immune function, most notably negative regulation of myeloid cell differentiation in the DZNep treatment condition (Figure 3-9 A,B). Recent work has shown the importance of the immune response in regeneration and showed that early immune response was upstream of regulating levels of apoptosis later in the regenerative response (Aztekin et al., 2020; Godwin et al., 2013). This led us to hypothesis that DZNep treatment may also cause changes in chromatin accessibility at genes associated with regulating apoptosis. We did not find any apoptosis GO terms enriched at 6hpa, but at 24hpa positive regulation of apoptosis was called. We first explored if EZH2 activity regulates the early immune response.

We tested if a subset of genes called in the GO terms that are differentially accessible between DZNep and the control were also differentially expressed at the RNA level. We indeed found upregulation of a subset of genes related to myeloid differentiation at 3hpa, which suggests that the immune response may be perturbed by loss of EZH2 activity (Figure 3-9 C). To confirm that the changes in chromatin accessibility and gene expression were specific to inhibition of EZH2 activity we compared peaks of TSA and DZNep treated tadpoles and their controls at genes that were confirmed to have increased chromatin accessibility and gene expression when treated with DZNep. We visually confirmed that TSA did not cause an increase in chromatin accessibility in these regions (Figure 3-9 D). Based on these called terms and changes in gene expression we hypothesized that EZH2 activity is specifically regulating the early gene expression patterns required for an appropriate immune response during regeneration. To test this, we utilized the macrophage stain neutral red to determine if there was a change in the number or localization of macrophages during regeneration when EZH2 activity is inhibited. We found a decrease in macrophages in the regenerating tissue when EZH2 was inhibited relative to the vehicle control, suggesting that EZH2 activity is necessary for proper macrophage response in the regenerating tissue (Figure 3-9 E-F).

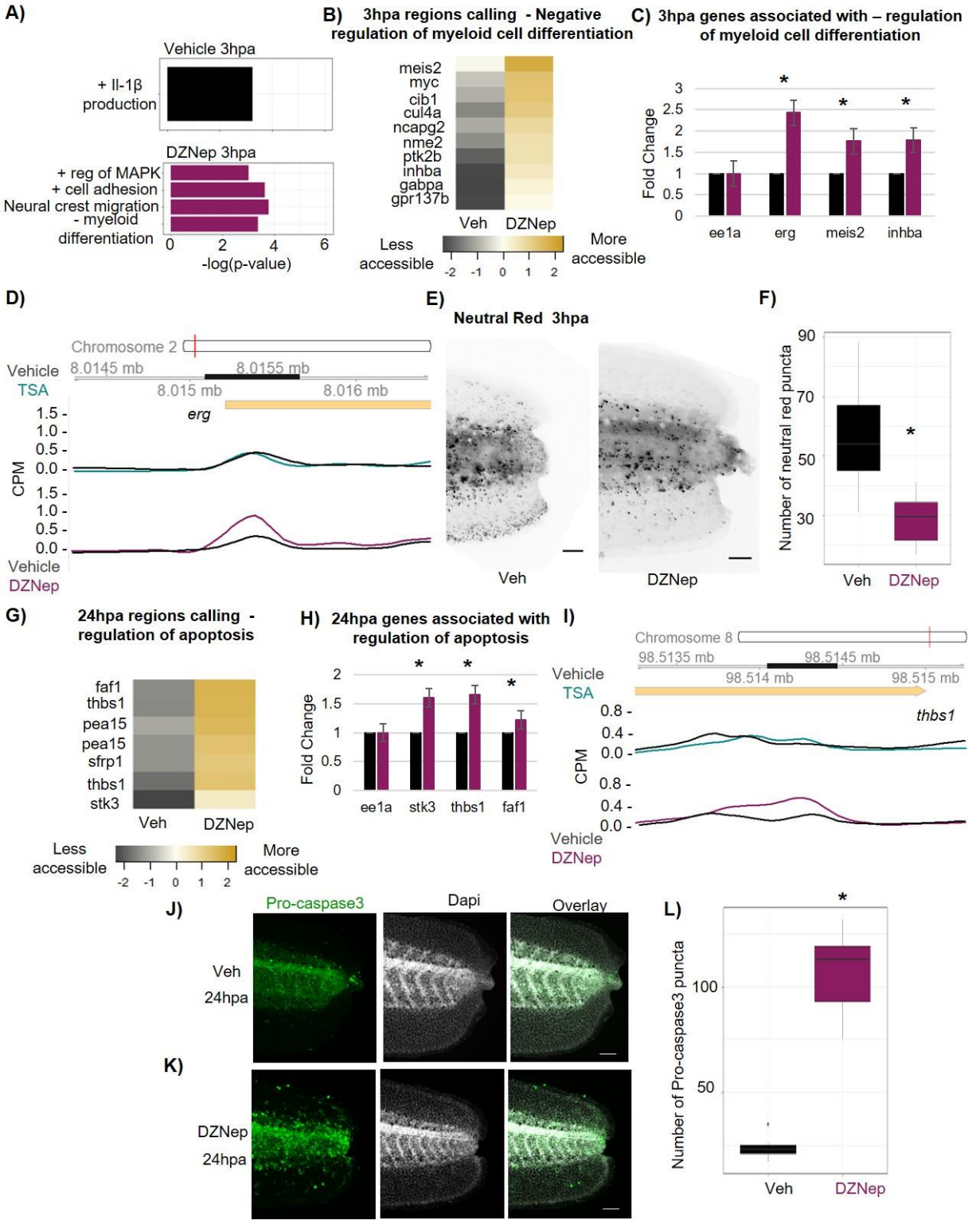

Figure 3-9 EZH2 inhibition regulates early immune response in regeneration which alters later apoptosis levels.

A) Selected GO terms enriched at 3hpa called from regions with increased accessibility in the vehicle relative to DZNep (black) or called from regions that had increased accessibility in DZNep relative to

the vehicle (maroon). B) Differential accessibility heat map of genes assigned to the GO term negative regulation of myeloid cell differentiation at 3hpa. C) RT-qPCR fold expression of selected genes assigned to negative regulation of myeloid differentiation GO terms relative to *ee1a* in regenerating tissue. Data represents the mean +/- SEM (* $p<0.05$ two tailed t-test). D) Representative gviz track of both TSA (teal) and DZNep (maroon) treated regenerates with their respective vehicle controls (both sets of controls are black but should be noted they are separate data sets) at 3hpa showing a differentially accessible ATAC-seq peak (dark bar) associated with a gene with differential expression in the DZNep treatment. E) Neutral red stain of live tadpoles at 3hpa in vehicle or DZNep treated regenerates (scale bar = 250 µm). F) Box plots of the quantification of Neutral red puncta in vehicle or DZNep treated regenerates at 3hpa (* $p<0.05$ two tailed T-test n= 8 for each condition). G) Differential accessibility heat map of genes assigned to the GO term regulation of apoptosis at 24hpa. H) RT-qPCR fold expression of selected genes assigned to regulation of apoptosis GO term relative to *ee1a* in regenerating tissue. Data represents the mean +/- SEM (* $p<0.05$ two tailed t-test). I) Representative gviz track of both TSA (teal) and DZNep (maroon) treated regenerates with their respective vehicle controls (both sets of controls are black but should be noted they are separate data sets) at 24hpa showing a differentially accessible ATAC-seq peak (dark bar) associated with a gene with differential expression in the DZNep treatment. J-K) Cleaved Pro-caspase3 immunofluorescence of 24hpa regenerates (scale bar = 250 µm) J) Vehicle K) DZNep L) Quantification of Cleaved Pro-caspase3 puncta (* $p<0.05$ two tailed T-test n= 7 for each condition).

Having verified that the early immune response was misregulated when EZH2 was inhibited we asked if there were changes in apoptosis upon EZH2 inhibition. We confirmed visually that the peaks called to the GO term positive regulation of apoptosis had increased accessibility when treated with DZNep compared to controls (Figure 3-9 G). We tested several such genes and found that they were indeed upregulated (Figure 3-9 H). To confirm that this change in chromatin architecture was specific to DZNep treatment we compared the same regions that were differential expressed to the chromatin accessibility is TSA treatments, and found that TSA did cause an increase in accessibility (Figure 3-9 I). We next used immunostaining for activated caspase to ask whether cell death was increased in DZNep-treated tadpoles and found increased levels of pro-caspase3 in DZNep-treated tadpoles at the 24hpa timepoint (Figure 3-9 J-L). We conclude that inhibition of EZH2 activity with DZNep results in reduced myeloid cell differentiation early in regeneration, followed later in regeneration by increased apoptosis.

3.4. Discussion

3.4.1. Regulation of epigenetic modifications during early phases of regeneration is critical to enhance regenerative outcome

Coordinated changes in gene expression across heterogenous tissue populations are necessary to regenerate lost tissues. While bulk and single-cell RNA-seq studies in a variety of systems have given

insight into what gene expression profiles are required for regeneration the mechanism of how those gene expression patterns is achieved is relatively understudied (Aztekin et al., 2019; Gerber et al., 2018; Kakebeen et al., 2020; Siebert et al., 2019; Voss et al., 2019). Several studies have interrogated a functional requirement for specific histone modifications using the same pharmacological approaches we have applied here. These have shown that HDAC activity is required for tail regeneration in *Xenopus laevis* and axolotls tail regeneration (Taylor and Beck, 2012; Tseng et al., 2011; Voss et al., 2019) as well as axon regeneration in mammals (Cho and Cavalli, 2014). Similarly, PRC activity is required for regeneration in tissues ranging from the Drosophila imaginal disc to the Xenopus limb bud (Harris et al., 2016; Harris et al., 2020; Hayashi et al., 2015). While these enzymatic activities are therefore well established as being required, few studies have established the precise temporal intervals during which they are required. Here we find that the window of disruption of either HDAC activity or EZH2 activity alters regenerative outcome. Additionally, the disparate phenotypes between HDAC or EZH2 regenerates points to distinct targets of the activities of these histone modifying enzymes. We find that inhibition of HDAC activity with TSA causes a reproducible loss of fin regeneration, while and axial spike regenerates to similar overall length to vehicle treated tadpoles. In contrast when EZH2 activity is inhibited for the first 24 hpa we see that regenerated tails are overall shorter than vehicle treated animals and lack either the dorsal or ventral fin. These differences highlight the importance of temporal resolution in studies such as these: prolonged inhibition of either EZH2 activity or HDAC activity ultimately results in regeneration failure, but shorter treatments highlight that alterations in epigenetic modifications likely have different dynamics in different tissues. One important caveat to HDAC activity is that it also serves an important role in maintaining metabolites, particularly acetyl-CoA by removing acetyl groups from histones and freeing them to be used elsewhere in the cell. In cancer cells it is know that HDAC inhibition can effect metabolic flux due to alterations in the acetyl-CoA pool (Srivatsan et al., 2020). It is unclear if alterations in metabolic state as well as alterations in epigenetic state are contributing to the phenotypes we describe.

3.4.2.HDAC and EZH2 perturbation do not result in a global increase of chromatin accessibility

One of the primary motivators of our study was to contrast the consequences of inhibiting HDAC activity with inhibiting EZH2 activity on genome-wide chromatin accessibility. Both enzymatic activities serve to close chromatin; HDACs by neutralizing the DNA-repulsive negative charges introduced by acetyl groups, and EZH2 by contributing to the formation of facultative heterochromatin. Because TSA is a promiscuous inhibitor of acetyltransferase activity, we predicted that inhibiting all HDAC activity would result in much more accessible chromatin across the entire genome. It is striking, therefore, that although the phenotypic consequences of TSA and DZNep treatment are strong, we observe a relatively modest overall effect in global chromatin accessibility with either treatment, with a bias towards increasing accessibility over time. Although this outcome is perhaps not immediately intuitive, it agrees with other direct interrogations of chromatin accessibility in which similar reagents have been used. For example, in the mouse retina, treatment with TSA dramatically increases the reprogrammability of Muller glia cells to neurons, but its effects on chromatin accessibility are confined to relatively few loci (Jorstad et al., 2017; VandenBosch et al., 2020). There are several possible implications of this finding. One is that genomic patterns of chromatin accessibility may be quite robust to individual pharmacological perturbations, perhaps through independent compensatory mechanisms. On this point we do note that although global chromatin accessibility remains fairly intact during TSA treatment, the levels of H3K27ac increase markedly, arguing that it is not that this mark is unaffected, but rather that the accompanying chromatin accessibility is not globally perturbed.

3.4.3.HDAC and EZH2 perturbation have distinct genomic targets during early appendage regeneration

HDAC and EZH2 inhibition resulted not only in differing phenotypes, but also caused changes in accessibility in different genomic regions. In HDAC inhibited tadpoles there is a highly dynamic enrichment and depletion of accessible promoter peaks in the HDAC inhibited tadpoles (Figure 3-5). The rapid enrichment for peaks in promoters by 3hpa suggests that HDAC's serve to dampen gene expression quickly after injury by targeting promoter regions rather than more distal regulatory elements. This is in contrast to many developmental studies which have shown that histone acetylation state is important for maintaining

pluripotency and regulating early gene expression changes in development (Bogdanović et al., 2012; Creyghton et al., 2010; Dovey et al., 2010; Gupta et al., 2014; Jamaladdin et al., 2014; Karmodiya et al., 2012; Rada-Iglesias et al., 2011; Rao and LaBonne, 2018). In addition, HDAC activity also have several requirements in the early embryo, acting during blastula stages to modulate the responsiveness of promoters to maternally deposited factors (Esmaeili et al., 2020) , and later to direct the establishment and maintenance of neural crest fate (Rao and LaBonne, 2018). HDAC activity has also been shown to In addition studies in *Xenopus* development have shown that HDAC activity is important for the establishment and maintenance of the neural crest population, and lack of HDAC activity allow cells to maintain a more pluripotent cell state (Rao and LaBonne, 2018). However, many of these studies point to the critical role for the acetylation state of enhancers, whereas our analysis showed the strongest early effect in promoters, suggesting that perhaps the large dynamic changes in promoter acetylation state may be specific to injury response. EZH2 treatment, by contrast, results in enrichment of more accessible accessible peaks in exons that persists throughout the first 24hpa, whereas there seems to only be an increase in more accessible accessible promoters at 6hpa (Figure 3-7). This suggests that EZH2 activity may not “prime” promoters as is seen in early embryonic development, but is instead serving to methylate gene. Both functions have been observed in early embryonic development (Bogdanović et al., 2012; Prokopuk et al., 2017; Rada-Iglesias et al., 2011). The data we present here does suggest that methylation states are perhaps not as static as previously suggested in *Xenopus* (Hayashi et al., 2015).

3.4.4.HDACs early role in regulating neuronal regeneration

We found that many accessible genes in the HDAC inhibited groups were called to GO terms associated with negative regulation of neuron death, and maintenance or neuronal structures. When we assayed for axon length, we did see that there was a decrease in axon regeneration suggesting that HDAC activity is necessary for directing early regenerative responses that are conducive for neuronal regeneration (Figure 3-6). Wallerian degeneration is a process in which injured neurons are degraded and cleared from injured tissue. The process of Wallerian degeneration is important for successful regeneration, and incomplete or inhibited Wallerian degeneration results in poor neuronal regeneration and is also associated with peripheral neuropathies (Coleman, 2005; Moreau and Boucher, 2020; Yi et al., 2017). We and others

have demonstrated that HDAC activity is necessary for axon regeneration (Aztekin et al., 2020; Pillay et al., 2013). Our data suggests that the hypothesis that part of the requirement for HDAC activity lies in regulating Wallerian degeneration. Direct measurement of changes in acetylation and gene expression changes would be necessary to test this hypothesis.

3.4.5.EZH2 activity's role in the immune response and its downstream consequences

It has been widely reported on the requirement for a precisely regulated immune response for proper regeneration for regulating a variety of processes including extra-cellular matrix remodeling, apoptotic cell clearance, and vascularization (Aztekin et al., 2020; Godwin et al., 2013; Julier et al., 2017; Petrie et al., 2014; Pillay et al., 2013). The precise mechanisms of regulating the immune response remain unclear. We propose that the activity oh EZH2 may serve to dampen expression of genes that are inhibitory to the immune response, particularly genes that prevent macrophage formation. Our data shows that upon EZH2 inhibition regions associated with genes involved in inhibiting myeloid differentiation are accessible, leading to increased gene expression. We also showed that in the regenerating tissue there were fewer macrophages as visualized by neutral red (Figure 3-9). It may be that the total number of macrophages in the animal is decreased; nevertheless, there is a clear dampening of the immune response in the regenerating tissue down stream of inhibition of EZH2 activity.

A recent study in *Xenopus laevis* found that macrophage recruitment to the injury site was upstream of apoptosis (Aztekin et al., 2020). It is not clear exactly how the myeloid lineage regulates apoptosis but one hypothesis is that the myeloid lineage clears apoptotic cells. Our data shows that by 24 hpa loss of EZH2 activity is also causing increased accessibility of genomic regions associated with genes involved in promoting apoptosis, it is unclear if this is a result of EZH2 inhibition, loss of macrophages, or some other mechanism. We also found changes in several candidate genes associated with these changes in genomic accessibility, and an increase in pro-caspase3 in EZH2 inhibited animals 24 hpa. Overall, our data supports the link between the immune response and regulating levels of apoptosis during regeneration and suggests that EZH2 activity and methylation of H3k27me3 is important for regulating gene expression profiles promoting proper immune response (Figure 3-9).

3.5.Conclusions

Taken as a whole, our study presents a highly temporally resolved analysis of global chromatin dynamics of tail regeneration while EZH2 or HDAC activity is inhibited. We showed that inhibition of these enzymes does not serve to globally open chromatin, and that there are distinct targets of HDAC and EZH2 activity during early regeneration. We also showed that early HDAC activity plays a role in regulation of neural regeneration. Finally, we found a role for EZH2 activity in regulation of the early immune response which in turn alters the level of apoptosis later in regeneration (Figure 3-10).

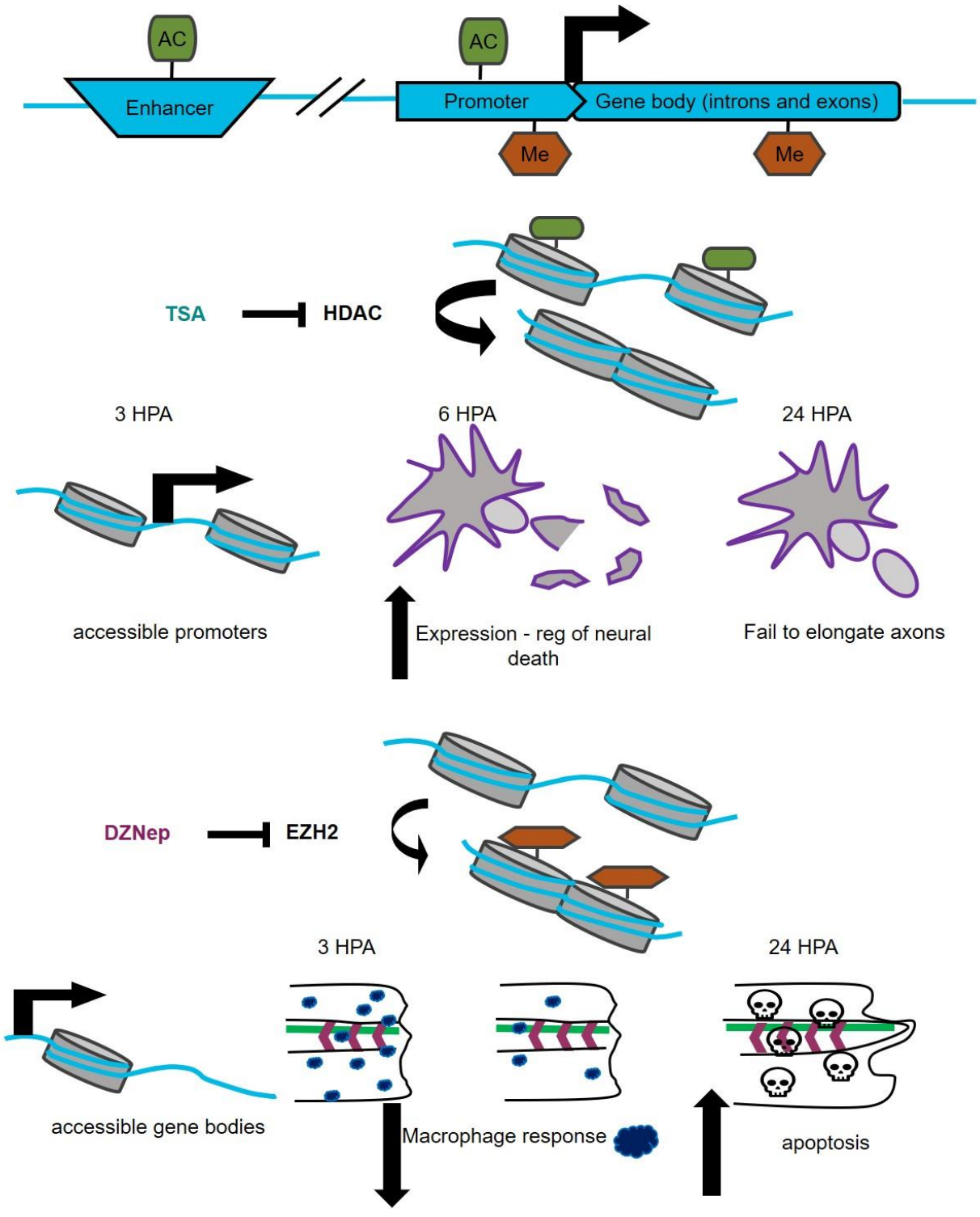

Figure 3-10 Model for the roles of HDAC and EZH2 activity roles in early tail regeneration

3.6.Materials and Methods

3.6.1.Ovulation, in vitro fertilization, and rearing of embryos

Use of *Xenopus tropicalis* was carried out under the approval and oversight of the IACUC committee at UW, an AALAC-accredited institution. Ovulation of adult *X. tropicalis* and generation of embryos by in vitro fertilization according to published methods(Khokha et al., 2002; Sive et al., 2010). Fertilized eggs were de-jellied in 3% cysteine in 1/9x modified frog ringer's solution (MR) for 10-15 minutes. Embryos were reared as described (Khokha et al., 2002)Staging was assessed by Nieuwkoop and Faber (Nieuwkoop and Faber, 1994).

3.6.2.X. tropicalis amputation assay

X. tropicalis tadpoles were reared to stage 4. Tadpoles were anesthetized with 0.05% ms-222 in 1/9x MR and tested for touch prior to amputation. Once anesthetized a sterilized scalpel was used to amputate the most distal 1/3 of the tail. Tadpoles were transferred from anesthetic media into fresh 1/9xMR within 10 minutes post amputation and left to regenerate at a density not greater than 3 tadpoles per 1 mL of media.

3.6.3. Pharmacological inhibitors

Tricostatin A (TSA, Sigma T8552) and 3-Deazaneplanocin (DZNep, Cayman chemical 13828) were suspended in DMSO as a vehicle. For experiments inhibitors were diluted to the following final concentrations in 1/9th MR; TSA 20nM, DZNep 15 uM.

3.6.4.Regeneration measurement

To measure regenerated tail length tadpoles were mounted in agarose wells and imaged with a Lecia M205FA fluorescence Steromicroscope. Using the Lecia imaging software (LasX) measurements were taken from the most posterior point of regenerated tissue to the amputation plane. The amputation plane was identified using morphological features such as disruption of the chevron pattern of somites. For classifying tissue type regeneration, we identified fin (dorsal or ventral) and axial tissues based on

morphological features such as the notochord. We classified animals with a regeneration length less than 15% of wild type regeneration length as no regeneration.

3.6.5. ATAC-seq library preparation

Libraries were prepared as previously described(Kakebeen et al., 2020).

At each timepoint, regenerating tadpoles were anesthetized until non-responsive to touch. A scalpel was used to amputate to the regenerated tail tissue. Regenerated tail tips were collected and spun down at 1000xg. Media was taken off and ~60 tails were resuspended in 200 uL of 0.035 mg/ml liberase in PBS (Roche 05401119001). Tails were left to incubate for 20 min at room temperature. A p-200 was then used to pipet the tails up and down gently and break up tail tissue. Once no visible chunks were apparent, cells were spun down for 3 min at 1000xg. Supernatant was disposed and cells were washed with 180 uL of 1xPBS. Cells were spun down for 3 min at 1000xg, and supernatant was discarded. Cells were resuspended in 15 uL of TN5 reaction mix using the TN5 enzyme, buffer, and water from the Nextera DNA Sample prep kit (Illumina 15028212). Cells were transposed for 1 hr at 37C. Post transposition, cells were removed from 37C and DNA was purified using the Qiagen MinElute kit (Qiagen 28206). DNA was eluted in 10 uL of buffer EB. Purified DNA was then amplified using the 2xNEB PCR Master Mix (NEB M0541L), a universal forward primer, and an indexed reverse primer from the i7 Illumina series (Table 1, File S1). Initial amplification as follows: 72C:5 min, 98C:30 s, then 5 cycles of 98C:10 s, 63C:30 s, 72C:1 min. 5 uL of the initial PCR product was then used for a 15 µl side qPCR reaction to determine how many more cycles to run to stop amplification prior to saturation. The side reaction was carried out as follows: 98C:30 s, then 30 cycles of 98C:10 s, 63C:30 s, 72C:1 min. The number of cycles was determined by taking the range of the starting and ending CT values and dividing that number by 4, then identifying how many cycles the sample had gone through at the derived CT value. The initial PCR reactions were then run for the calculated number of extra cycles and removed from the thermo cycler. Amplified samples were purified with the Qiagen MinElute kit and eluted in 20 uL of buffer EB. 5 uL of purified PCR product were run out on a 5% acrylamide gel in 1xTBE at 100V for ~45 min. Gels were stained with Ethidium Bromide and imaged on the gel imager (BioRad). Samples with sufficient periodic bands, relating to length of DNA to wrap a mono-, di-, tri- nucleosome, were then run out on a bioanalyzer. Library concentrations were taken using the Qubit

high sensitivity dsDNA assay. Libraries were pooled by normalizing library concentrations to the lowest concentration and adding equal volumes of libraries for a minimum of 5 ng of each library (File S1).

Libraries were sequenced on the Illumina Next-Seq platform across one NextSeq 500 High Output Kit v2.5 (150 cycles, Illumina CAT. 20024907) for TSA and respective controls and one Next-seq High output 150 cycle and one Next-seq Mid output 150 cycle kit (150 cycles, Illumina CAT. 20024904) Libraries were sequenced with, paired end, 75 bp reads at the Seattle Genomics facility.

3.6.6. ATAC-Seq analysis pipeline

For software versions and sequencing primer information see table 1, and for sample workflow see appendix A.

Table 1: ATAC-seq software and primer information

Reagent type (species) or resource	Designation	Source or reference	Identifiers	Additional information
Software, algorithm	Trim Galore! (v0.4.4_dev)	Felix Krueger	RRID:SCR_011847	https://github.com/FelixKrueger/TrimGalore
Software, algorithm	Bowtie2 (V2.3.4.1)	PMID: 22388286; PMID: 30020410	RRID:SCR_005476	http://bowtie-bio.sourceforge.net/bowtie2/manual.shtml
Software, algorithm	MACS2 (V2.1.1)	PMID: 18798982	RRID:SCR_013291	https://github.com/taoliu/MACS
Software, algorithm	Picard (v2.18.5)	Broad Institute		https://broadinstitute.github.io/picard/

Software, algorithm	Bedtools (V2.27.1)	PMID: 20110278		https://bedtools.readthedocs.io/en/latest/
Software, algorithm	featureCounts (v1.6.2)	PMID: 24227677		https://rdrr.io/bioc/Rsubread/man/featureCounts.html
Software, algorithm	GenomicRanges	PMID: 23950696		https://bioconductor.org/packages/release/bioc/html/GenomicRanges.html
Software, algorithm	edgeR	PMID: 19910308; PMID: 22287627	RRID:SCR_012802	https://bioconductor.org/packages/release/bioc/html/edgeR.html
Software, algorithm	Gviz	ISBN 978-1-4939-3578-9		https://bioconductor.org/packages/release/bioc/html/Gviz.html
Software, algorithm	HOMER (V4.11.1)	PMID: 20513432	RRID:SCR_010881	http://homer.ucsd.edu/homer/
Sequence-based reagent	PMID: 24097267 : Ad2.1; Nextera barcode 701	PMID: 24097267	library primers	CAAGCAGAAGACGGCATACGAGATTCGCCTTAGTCTCGTGGGCTCGGAGATGT
Sequence-based reagent	PMID: 24097267 : Ad2.2; Nextera barcode 702	PMID: 24097267	library primers	CAAGCAGAAGACGGCATACGAGATCTAGTACGGTCTCGTGGGCTCGGAGATGT

Sequence-based reagent	PMID: 24097267 : Ad2.3; Nextera barcode 703	PMID: 24097 267	library primers	CAAGCAGAAGAC GGCATACGAGAT TTCTGCCTGTCT CGTGGGCTCGG AGATGT
Sequence-based reagent	PMID: 24097267 : Ad2.4; Nextera barcode 704	PMID: 24097 267	library primers	CAAGCAGAAGAC GGCATACGAGAT GCTCAGGAGTCT CGTGGGCTCGG AGATGT
Sequence-based reagent	PMID: 24097267 : Ad2.5; Nextera barcode 705	PMID: 24097 267	library primers	CAAGCAGAAGAC GGCATACGAGAT AGGAGTCCGTCT CGTGGGCTCGG AGATGT
Sequence-based reagent	PMID: 24097267 : Ad2.6; Nextera barcode 706	PMID: 24097 267	library primers	CAAGCAGAAGAC GGCATACGAGAT CATGCCTAGTCT CGTGGGCTCGG AGATGT
Sequence-based reagent	PMID: 24097267 : Ad2.7; Nextera barcode 707	PMID: 24097 267	library primers	CAAGCAGAAGAC GGCATACGAGAT GTAGAGAGGTCT CGTGGGCTCGG AGATGT
Sequence-based reagent	PMID: 24097267 : Ad2.8; Nextera barcode 708	PMID: 24097 267	library primers	CAAGCAGAAGAC GGCATACGAGAT CCTCTCTGGTCT CGTGGGCTCGG AGATGT

Sequence-based reagent	PMID: 24097267 : Ad2.9; Nextera barcode 709	PMID: 24097 267	library primers	CAAGCAGAAGAC GGCATACGAGAT AGCGTAGCGTCT CGTGGGCTCGG AGATGT
Sequence-based reagent	PMID: 24097267 : Ad2.10; Nextera barcode 710	PMID: 24097 267	library primers	CAAGCAGAAGAC GGCATACGAGAT CAGCCTCGGTCT CGTGGGCTCGG AGATGT
Sequence-based reagent	PMID: 24097267 : Ad2.11; Nextera barcode 711	PMID: 24097 267	library primers	CAAGCAGAAGAC GGCATACGAGAT TGCCTCTTGTCT CGTGGGCTCGG AGATGT
Sequence-based reagent	PMID: 24097267 : Ad2.12; Nextera barcode 712	PMID: 24097 267	library primers	CAAGCAGAAGAC GGCATACGAGAT TCCTCTACGTCT CGTGGGCTCGG AGATGT
Sequence-based reagent	PMID: 24097267 : Ad1_noMX	PMID: 24097 267	library primers	AATGATACGGCG ACCACCGAGATC TACACTCGTCGG CAGCGTCAGATG TG

3.6.6.1. Trimming adaptors and alignment

Adapters were trimmed from reads and low-quality sequences (Phred < 33) were removed using Trim Galore! (Krueger, 2021). Reads were aligned to xenTro9 using Bowtie2 (option:–very-sensitive) (Langmead and Salzberg, 2012; Langmead et al., 2019). Duplicate reads were marked using Picard

'MarkDuplicates' (Picard Tools - By Broad Institute). Duplicate reads were removed using SAMtools (Li et al., 2009).

3.6.6.2. Peak calling

Peaks were called using MACS2 (options: --nomodel --shift -100 --extsize 200 -g 1.7e9) (Zhang et al., 2008). Consensus peak set used for differential accessibility was generated by combining all peaks called in all samples, reducing to 400 bp windows centered on peaks, and merging peaks overlapping by 201 bp or more (bedtools merge -d -201) (Quinlan and Hall, 2010).

3.6.6.3.Differential accessibility analysis

Differential accessibility analysis in ATAC-seq peaks. Differential accessibility across ATAC-seq sample groups was determined as detailed in the edgeR users guide (Robinson et al., 2010). A matrix of counts for all samples was then generated using 'featureCounts' in the Subread package (options: -F SAF -p)] in consensus regions as defined above (Liao et al., 2014). The counts matrix was filtered to select rows having at least one count per million in n−one samples to minimize the influence of variability at the threshold for sensitivity on the analysis.

3.6.6.4.Peak annotation

Annotation of ATAC-seq peaks was performed using GenomicRanges (Lawrence et al., 2013), matching each peak to the nearest TSS using Xtropicalisv9.1.Named.primaryTrs.gff3 from Xenbase(Karimi et al., 2018).

3.6.6.5.Genome Ontology analysis

Using differential accessibility flags, we identified regions more accessible in the indicated contrast. The nearest TSS annotation of these regions was used as input for genome ontology. Genomic annotation enrichment analysis was performed using homer annotatePeaks.pl (options: xenTro9 -gsize 1700000000 -genomeOntology) (Heinz et al., 2010).

3.6.6.6.Peak Visualizations

Reads were merged between replicates. Counts per million were visualized in the vicinity of significant peaks using GVis v1.30.3 (Hahne and Ivanek, 2016).

3.6.6.7.Data Visualization

R studio was used for data visualization, using the ggplot2, ggpubr, gplots packages with custom generated color palettes (Galili, 2021; ggplot2 Based Publication Ready Plots; RStudio | Open source & professional software for data science teams).

3.6.7. Quantitative RT-PCR

At each timepoint, regenerating tadpoles were anesthetized until non-responsive to touch. A scalpel was used to amputate to the regenerated tail tissue. Regenerated tail tips were collected and spun down at 1000xg. Media was taken off and tails were suspended in RNA-lysis buffer. Tails were agitated at 42C for 45min until there were no tissue chunks remaining. RNA/DNA were extracted and purified by phenol: chloroform extraction and ethanol precipitation. Samples were DNAse treated to remove DNA. SuperscriptIII reverse transcription kit (ThermoFisher 18080044) was used to make cDNA. Amplifications were carried out with PowerUp SYBR Green master Mix (ThermoFisher A25742) for 40 cycles of 95C:10 s, 57C:30 s after initial 2minutest at 95C.

ap2b1	TTGGTCTCCAATGTGACGTG	TTGGTCTCCAATGTGACGTG
pou4f1	GCAGCGGAGGATCAAGTTAG	AAACCTGCAGATGGTGCTCT
AKT1	CATCTGCCCCTTCCAAATTA	AAGCGCTGGGAACTTGTCTA
wisp1	AGGCTCCTCCTTCTCCTTGA	TGGCAGAGCTCTCTGTAGTGC
erg	TTCCCCAAGGACAATTGAGA	TTCTGAGACCATGCTTTGGA
meis2	CACCGTCACTCGGACACTAA	TCATTTGGTGCAAAGACCAG

inhba	ATGCCATGTTGTCAGTCAGC	TGCAAGGATAGTGCAGAGGA
stk3	CTGTGTGGGAGCAGGGTAGT	GCACACACACAGCACAACTG
thsb1	AGAAGGGTGGATAGCCGAGT	TAGGGTCTTGTGCGGCTATT
fraf1	CTGATCTCGGCAATGGAAAT	ATCCTGCTCTCGCTTCACAT

3.6.8.Immunohistochemistry

X. tropicalis embryos were fixed for 20 minutes in MEMFA at room temperature. Embryos were permeabilized by washing 3X 20 minutes in PBS + 0.01% Triton x-100 (PBT). Embryos were blocked for 1 hour at room temperature in 10% CAS-block (Invitrogen #00-8120) in PBT. Then embryos were incubated in primary antibodies (1:50 neurofilament associated antigen, DSHB 3A10, and 1:100 cleaved caspase 3 cell signaling technologies 9661T) in 100% CAS-block overnight at 4°C. Embryos were then washed 3X 10 minutes at room temperature in PBT and re-blocked for 30 minutes in 10% CAS-block in PBT. Secondary antibodies (1:500 Anti-Mouse Life Technologies A21422, and 1:500 Anti-Rabbit Life Technologies A11008) were diluted in 100% CAS-block and incubated for 2 hours. Embryos were then washed 3X 20 minutes in PBT. Whole embryos or isolated tails were mounted on slides in Vectashield containing DAPI (Vector Laboratories #H-1500). Images were acquired with a Lecia DM 5500 B and ORCA-flash 4.0LT camera.

3.6.9. Quantification of Neurofilament regrowth length

The amputation plane was identified by morphological features such as loss of chevron patterning in somites. Neurofilament length was measured from the amputation plane of the spinal cord to the end of the longest extending axon from the spinal cord using Fiji(Schindelin et al., 2012).

3.6.10. Neutral Red staining and quantification

Neutral red was suspended in rearing media at a concentration of 5mg/ml, tadpoles were incubated in media for 3 hours and washed for 30 minutes in neutral red free media prior to imaging. Tadpoles were imaged live while anesthetized with 0.05% ms-222 in custom made agarose molds. Images were acquired

with a Lecia M205FA fluorescence Steromicroscope. Using Fiji, the amputation plane was identified by morphological features such as loss of chevron patterning in the somites. Neutral red puncta were counted using Fiji's built-in multipoint tool in regions posterior to the amputation plane(Schindelin et al., 2012).

3.6.11.Quantification of cleaved caspase

The amputation plane was identified by morphological features such as loss of chevron patterning in somites. Cleaved caspase puncta were counted using Fiji's multipoint tool in the regenerating tissue and 500um anterior to the amputation plane (Schindelin et al., 2012).

3.7. Acknowledgements

We would like to thank all the members of the Wills lab for their thoughtful discussions of this work. We would also like to thank the UW MF4 and regeneration groups for their feedback, we would like to acknowledge the Reh lab for allowing us to use equipment for library analysis. We thank Xenbase (Karimi et al., 2018) for curation of genomic and literature information used to generate materials and conduct analysis.

3.8.Competing Interests

The authors have not competing interests to report.

3.9.Funding

This work was supported by the National Institutes of Health (R03HD091716 to A.E.W and F31HD09910 to H.E.A.) and by unrestricted funds from the University of Washington.

3.10.Data Availability

Data will be made available on GEO.

CHAPTER 4. CONCLUDING REMARKS AND FUTURE DIRECTIONS

In this thesis, I leveraged the strength of *Xenopus tropicalis* as a model to probe how the structure of the nuclear compartment and its genomic contents affect biological processes. I characterized a previously undescribed elaborate branched nuclear morphology in the tail fin of *Xenopus tropicalis*. I used the easy manipulation and visualization of the early tadpole, as well as the recently developed CRISPR/Cas9 system to perform genome editing to identify two components of the nucleoskeleton involved in maintaining nuclear branches. I also utilized a highly temporally resolved study of chromatin accessibility during the first 24 hours of tail regeneration in *Xenopus tropicalis* to gain insight on direct and indirect consequences of EZH2 activity and HDAC activity during early regeneration. This identified distinct regulatory targets of HDACs and EZH2 during early regeneration. Collectively this work advanced our basic biological understanding of nuclear organization in two ways: (1) providing a model for studying the effects of extreme nuclear morphological variation in a healthy cell type for both tissue biophysics and genome organization and (2) uncovering the differing roles of multiple epigenetic modifications during regeneration. In this final chapter I will reflect on how my studies interface with the broader framework of how nuclear structure and genome organization alter biological processes, and the remaining questions that these studies illicit.

4.1.A new model for extreme nuclear morphology variation

Direct links and mechanisms that explain how alterations in nuclear structure induce enhancing or deleterious effects to cellular function are slowly becoming more prevalent. In models of laminopathies, which have a known mutation on a component of the nuclear lamina, studies have made steps in identifying changes in genome organization both globally and in precise loci (Bertero et al., 2019; Bonne et al., 1999; Chen et al., 2014; Shah et al., 2013; Solovei et al., 2013; Towbin et al., 2012; Zwerger et al., 2013). These advances have also occurred in some developmental contexts, primarily in differentiating cell culture (Dixon et al., 2015; Peric-Hupkes et al., 2010; Perovanovic et al., 2016; Rowat et al., 2013; Solovei et al., 2013). Additionally, neutrophils have been an excellent model for studying how changes in nuclear morphology affect the biophysical properties that alterations in nuclear morphology can impart (Pillay et al., 2013; Rowat et al., 2013).

However, each of these studies leaves open at least one of the following questions of how these alterations to the nuclear lamina affect biophysical properties of tissues, and the dynamics of changes in genome organization that could occur during development, organ, or tissue function, and aging on a global level and in a tissue context. These questions are difficult to answer, however with the advances in imaging and next-generation sequencing technologies getting closer to these questions will be possible. Sequencing methods will enable studies of genome wide dynamics of chromatin structure, and targeted regions and the heterogeneity of their localization and topology can be explored utilizing techniques such as DNA-PAINT (Beliveau, 2015). Such studies would reveal alterations of nuclear structure and genome structure are the tipping point between health and disease, and how changes in the biophysical properties of the nucleus affect tissue function.

In my work I characterized a healthy nuclear morphology in a system that is amenable to studying not only the cell biological origins, maintenance, and function of extreme nuclear branching, but also chromatin structure. Unlike neutrophils which are a migratory cell type, this morphology is also in an epithelial tissue the epidermis. I was able to show that this model was a tractable system for molecular perturbations through small molecule perturbations and genomic manipulation, and that it is a model that is easily imaged both live and fixed tissues. Utilizing what was known from disease states I was able to identify proteins critical for nuclear branching: actin and Laminb1. However, there are many unanswered questions with regards to the specific role these molecules are playing in maintaining nuclear structure. I think understanding the specific functions of actin filaments is crucial to understanding how the nucleoskeleton maintains this structure. The absence of a change in nuclear depth when actin filaments are perturbed suggest that actin is not compressing the nucleus. Limitations on microscopy resolution may contribute to the lack of seeing any actin structures that obviously contribute to nuclear morphology. However, a critical experiment to understanding actin's role is parsing the role that nuclear versus cytoplasmic actin may play in maintain nuclear branches. One way to approach this is to perturb the LINC complex, thereby disconnecting cytoplasmic actin from the nuclear structure. If disrupting the LINC complex resulted in a loss of nuclear branches that indicated that nuclear f-actin, and not cytoplasmic actin are necessary for nuclear branching.

New technologies coming to the field will help advance the understanding of both biophysical consequences of nuclear branching and chromatin structure. The use of tension sensors such as the beads developed in the Campàs lab would enable the study of changes of tissue tension during the development of nuclear branches as well as during their maintenance (Campàs, 2016; Serwane et al., 2017; Zhu et al., 2020). While changes in tension of the extracellular matrix do not change the branching structure of the larger multicellular branching structure of the airway, it is clear that gradients of tensions and stiffness are important during development (Nerger and Nelson, 2020; Serwane et al., 2017; Shyer et al., 2017; Varner et al., 2015; Zhu et al., 2020). One speculative hypothesis is that the epidermis experiences a change in tension forces as the epidermis is pulled as the mesenchymal core migrates to form the tail fin structure thereby modifying its nuclear structure to accommodate the changing tension while maintaining tissue (Tucker and Slack, 2004). Another highly speculative hypothesis is that branches form to distribute the nucleus over a larger surface area, because the nucleus is far stiffer than the cytosol (Kha et al., 2004; Peric-Hupkes et al., 2010). Coupling the tail epidermis system with cutting edge AFM techniques that have been utilized to measure forces in cultured cells could highlight some of the biophysical properties of this tissue (Shibata et al., 2017).

The other large questions to consider are how chromatin is organized within nuclear branches and if genome organization is preserved across cells with branched nuclei. DNA-PAINT and other FISH techniques would enable us to answer this question in a highly quantitative manner (Beliveau, 2015). If organization is not conserved between branches, this opens a whole host of questions on what range of genomic structure is allowable for proper cellular function, and how does that change in different cellular contexts.

4.2. Epigenetic regulation during regeneration

Next-generation sequencing techniques are advancing rapidly enabling the identification of many differentially accessible, expressed, or epigenetically modified genes and genetic loci. From these data sets it seems a lifetime of hypotheses can be generated. In regeneration a variety of genomic techniques have been utilized including microarrays, RNA-seq, ChIP-seq, and ATAC-seq, with each technique and study offering its own benefit and limitation (Aztekin et al., 2019; Ferreira et al., 2018; Gehrke et al., 2019;

Gerber et al., 2018; Harris et al., 2016; Harris et al., 2020; Hayashi et al., 2015; Kakebeen et al., 2020; Lee-Liu et al., 2014; Love et al., 2011; Pai et al., 2016; Siebert et al., 2019; Voss et al., 2019; Wu et al., 2013). For example, when studying changes in epigenetic modifications the most commonly used technique is ChIP-seq to show a gain or loss of a targeted modification, sometimes coupled with RNA-seq or microarray analysis (Ben-Yair et al., 2019; Harris et al., 2016; Harris et al., 2020; Hayashi et al., 2015; Hirose et al., 2013; Voss et al., 2019; Yakushiji et al., 2007). ChIP-seq fails to capture the possible indirect effects that occur when perturbing an epigenetic modification, and RNA-seq is an indirect read-out of changes in epigenetic modifications. In addition, for the most part these studies have had limited temporal resolution focusing on spreading time points over several days of regeneration rather than many time points in a short period of time.

In this work I had two aims. The first was to be able to capture both direct and indirect changes in chromatin structure, and the second was to increase temporal resolution of a specific time-period during regeneration. To this end I used ATAC-seq to capture all changes in chromatin accessibility rather than focusing on identifying changes in one specific epigenetic modification. I also used phenotypic analysis of differing treatment intervals to narrow down a 24-hour time window in which to focus my data collection. This study also compares the action of two different mechanisms of regulating chromatin accessibility via epigenetic modifications which so far has not been studied. Differences between the action of HDAC and EZH2 activity in regeneration was apparent from the phenotypic analysis, where the same treatment interval resulted in different phenotypes.

This study was limited though in that it was a bulk analysis, rather than a tissues specific analysis. An interesting follow-up would be tissue specific ATAC-seq analysis to understand tissue specific effects. The GO analysis already is suggestive of tissue specific effects by calling terms associated with certain tissues types or cellular lineages; however, it would be interesting to see if the primary effects driving changes in cell behavior are due to changes in that cell population or another cell population that may be providing critical signals or structural scaffolds. Another potential approach to determine more specific effects of the action of HDAC and EZH2 activity would be the utilization of a dCAS9 system to target a histone modifying enzyme to a specific locus (one identified in the bulk ATAC-seq), thereby changing only

the epigenetic state or accessibility of one specific region (Peddle et al., 2020; Thakore et al., 2015). This would be highly valuable in a line that could have temporal restriction of expression of the dCas9 and gRNA, and even more advantageous if there was tissue specific spatial restriction (Hsu et al., 2019).

Preliminary characterization of cell types called through GO analysis offers promising avenues of further investigation as well. In the case of HDAC activity and its role in the early phases of neuronal regeneration it appears that axons fail to extend into the regeneration bud. Neural progenitors prioritize differentiation of new neurons early in regeneration rather than producing more neural progenitors (Kakebeen et al., 2020). With my data this suggests the hypothesis that HDAC activity is regulating some of the critical pathways that are inhibiting neuronal differentiation in neuronal progenitors. In this scenario loss of HDAC activity results in persistent accessibility of a region(s) that is inhibitory to differentiation. Lineage tracing of neural progenitors could determine if there is a change in the number that differentiate into neurons when HDAC activity is inhibited. If there is no change that could suggest that cut neurons are extending axons first, and HDACs are regulating that process, or that some other non-neuronal cell type has a previously expressed anti-neuronal secreted signal upon HDAC inhibition.

In the case of EZH2 activity we identified that the myeloid lineage was susceptible to EZH2 inhibition. Several studies have shown that the innate immune response is important for regeneration, but very little is known about the genetic regulation of the coordination of this response (Aztekin et al., 2020; Edwards-Faret et al., 2021; Franchini and Bertolotti, 2011; Julier et al., 2017; Kakebeen and Wills, 2019; Kawasumi et al., 2013; Paré et al., 2017; Paredes et al., 2015). While we saw fewer macrophages recruited to the wound site after EZH2 inhibition, it is unclear if the global number of macrophages decreases, or if some signaling from the wound causes a burst of macrophage maturation that is being inhibited. Alternatively, EZH2 activity could be regulating signaling at the wound site, causing alteration in the expression of pro- or anti- macrophage recruitment factors. To distinguish between these possibilities' macrophages could be sorted and counting to determine if there was a decrease in the global number of macrophages in the whole tadpole suggesting that macrophage maturation is regulated by EZH2 activity and not recruitment to the wound site.

Another area of great interest in vertebrate regeneration is whether damage specific enhancers exist in *Xenopus* as they do in *Drosophila* (Harris et al., 2016; Harris et al., 2020). The large role for both HDAC and EZH2 activity in regulating precise control of gene expression either in maintaining pluripotency or in lineage restriction makes a comparison to developmental work very intriguing. To accomplish this in a comprehensive way ChIP-seq assays would be necessary to identify precise locations of methylation and acetylation sites. Comparing these datasets with ATAC-seq datasets could help determine if developmental promoters and enhancers are reutilized in regeneration or if there are a subset of particular gene networks that are regulated by damage specific regulatory elements. This approach could also identify if changes in accessibility or methylation and acetylation states in gene regulatory regions are not present in the non-regenerative adult frog, perhaps contributing to their non-regenerative injury response.

4.3.Future use of generated datasets

There is no one way to interpret and analyze -omic datasets. The type of analysis one does is driven by the question one wants to answer, and then these analyses can generate new and interesting hypotheses from the data. This is especially useful since as knowledge and mechanisms are more understood, data can be re-analyzed in the context of the new information. In addition to different interpretations of the data, there is a large amount of power in intersecting datasets. In the future one could generate ChIP-seq or RNA-seq datasets under the same conditions and use epigenetic, chromatin accessibility, and genes expression data to inform new hypotheses and make predictions on mechanisms.

4.4.Mile high view

The main goal of my work has been to understand various ways in which nuclear structure and chromatin architecture regulate biological processes. The two contexts in which I breached this vast topic were though characterizing branched nuclear morphology and through studying chromatin accessibility in regeneration. Both of those basic biological systems provide important contributions to understanding human health and disease. Cancers are frequently staged by alterations in nuclear morphology, and

therefore by understanding what changes can cause alterations in nuclear morphology we can better understand why cancer cells may alter their nuclear structure and what advantages that may impart upon cancer cells. Additionally, gaining insight into nuclear regulation of biophysical properties could have implications for tissue engineering, enabling the production of finely tuned tissues with distinct biophysical properties that aid in their function. In terms of regeneration, apart from the liver, blood, palate of the mouth, and skin humans are extremely poor regenerators. Seventeen people die each day in the United States alone waiting for an organ donation (Data - OPTN; Organ Donation Statistics | Organ Donor, 2018). While work on regenerative tadpoles will not jump into humans tomorrow, in the future understanding the pro-regenerative response in regenerative species could help drive regenerative treatments for organ damage rather than needing a transplant.

The main conclusions I have drawn from my work are that dynamic regulation of nuclear structure and its contents are important for imparting an adaptable system to control genetic responses, as well as alter biophysical properties. We were unable to inducing branching in cells that do not already contain nuclear branches, nor were we able to perturb branches in a way that would not eventually be lethal (perturbations of actin) or cause destabilization of tissue mechanics and potential changes in gene regulation (Lamin B1 perturbations). However, we do have a great appreciation of the extent of biological extremes and how understanding these systems can help us gain a better understanding of basic biology translating both into potential future bioengineering applications, but also to comparative studies to diseases with perturbations in nuclear morphology. In regeneration we were able to conclude that HDAC and EZH2 activity have at least partially independent functions. We identified distinct biological processes that were regulated by either EZH2 or HDAC activity. The work in this study also highlighted that the direct effects of the absolute change in acetylation or methylation sites during regeneration are only part of the changes that contribute to the phenotypes that result from loss of either HDAC or EZH2 activity during regeneration. In either inhibited treatment at all time points almost half of all differentially accessible peaks by ATAC-seq had decreased accessibility, which is the opposite of what would be expected. Understanding how alterations in regulation can propagate to farther downstream effects is important for understanding complex biological processes. As technologies emerge targeting of specific loci for epigenetic modifications with high

spatiotemporal resolution will enable highly detailed mechanisms of genomic regulation during regeneration to be parsed at a single cell resolution eventually.

Beyond my own results, developing new models in which to study cell biology in a whole organism and tissue context is important. The rise of organoids is helping to address this need but going back to the animal is an important step and reminder that sometimes reductionist approaches in cell biology yield important but incomplete understanding of a process. Additionally, the need for multidisciplinary approaches and multiple models will be critical for moving basic discoveries in cell biology in regeneration into helpful therapies for humans. Ultimately basic science discoveries drive forward innovation in medicine, and this innovation is only aided through highly collaborative scientific approaches.

CHAPTER 5. REFERENCES

Aboobaker, A. A. (2011). Planarian stem cells: a simple paradigm for regeneration. *Trends Cell Biol* **21**, 304–311.

Afouda, B. A. and Hoppler, S. (2009). Xenopus Explants as an Experimental Model System for Studying Heart Development. *Trends in Cardiovascular Medicine* **19**, 220–226.

Aztekin, C., Hiscock, T. W., Marioni, J. C., Gurdon, J. B., Simons, B. D. and Jullien, J. (2019). Identification of a regeneration-organizing cell in the Xenopus tail. *Science* **364**, 653–658.

Aztekin, C., Hiscock, T. W., Butler, R., De Jesús Andino, F., Robert, J., Gurdon, J. B. and Jullien, J. (2020). The myeloid lineage is required for the emergence of a regeneration-permissive environment following Xenopus tail amputation. *Development (Cambridge)* **147**,.

Baarlink, C., Plessner, M., Sherrard, A., Morita, K., Misu, S., Virant, D., Kleinschnitz, E.-M., Harniman, R., Alibhai, D., Baumeister, S., et al. (2017). A transient pool of nuclear F-actin at mitotic exit controls chromatin organization. *Nature Cell Biology* **19**, 1389–1399.

Bauer, D. V., Huang, S. and Moody, S. A. (1994). The cleavage stage origin of Spemann's Organizer: analysis of the movements of blastomere clones before and during gastrulation in Xenopus. *Development (Cambridge, England)* **120**, 1179–89.

Beck, C. W., Christen, B. and Slack, J. M. W. (2003). Molecular pathways needed for regeneration of spinal cord and muscle in a vertebrate. *Developmental Cell* **5**, 429–439.

Beck, C. W., Belmonte, J. C. I. and Christen, B. (2009). Beyond early development: Xenopus as an emerging model for the study of regenerative mechanisms. *Developmental Dynamics* **238**, 1226–1248.

Beliveau, B. J. (2015). Single-molecule super-resolution imaging of chromosomes and in situ haplotype visualization using Oligopaint FISH probes. *NATURE COMMUNICATIONS* 13.

Ben-Yair, R., Butty, V. L., Busby, M., Qiu, Y., Levine, S. S., Goren, A., Boyer, L. A., Geoffrey Burns, C. and Burns, C. E. (2019). H3K27me3-mediated silencing of structural genes is required for zebrafish heart regeneration. *Development (Cambridge)* **146**,.

Bernstein, B. E., Mikkelsen, T. S., Xie, X., Kamal, M., Huebert, D. J., Cuff, J., Fry, B., Meissner, A., Wernig, M., Plath, K., et al. (2006). A Bivalent Chromatin Structure Marks Key Developmental Genes in Embryonic Stem Cells. *Cell* **125**, 315–326.

Bertero, A., Fields, P. A., Ramani, V., Bonora, G., Yardimci, G. G., Reinecke, H., Pabon, L., Noble, W. S., Shendure, J. and Murry, C. E. (2019). Dynamics of genome reorganization during human cardiogenesis reveal an RBM20-dependent splicing factory. *Nat Commun* **10**, 1538.

Bhattacharya, D., Marfo, C. A., Li, D., Lane, M. and Khokha, M. K. (2015). CRISPR/Cas9: An inexpensive, efficient loss of function tool to screen human disease genes in Xenopus. *Developmental Biology* **408**, 196–204.

Bogdanović, O., Fernandez-Miñán, A., Tena, J. J., Calle-Mustienes, E. de la, Hidalgo, C., Kruysbergen, I. van, Heeringen, S. J. van, Veenstra, G. J. C. and Gómez-Skarmeta, J. L. (2012). Dynamics of enhancer chromatin signatures mark the transition from pluripotency to cell specification during embryogenesis. *Genome Res.* **22**, 2043–2053.

Bonne, G., Schwartz, K., Barletta, M. R. D., Varnous, S., Bécane, H.-M., Hammouda, E.-H., Merlini, L., Muntoni, F., Greenberg, C. R., Gary, F., et al. (1999). Mutations in the gene encoding lamin A/C cause autosomal dominant Emery-Dreifuss muscular dystrophy. *Nature Genetics* **21**, 285–288.

Brangwynne, C. P., Mitchison, T. J. and Hyman, A. A. (2011). Active liquid-like behavior of nucleoli determines their size and shape in Xenopus laevis oocytes. *Proceedings of the National Academy of Sciences* **108**, 4334–4339.

Buenrostro, J. D., Wu, B., Chang, H. Y. and Greenleaf, W. J. (2015). ATAC-seq: A Method for Assaying Chromatin Accessibility Genome-Wide. In *Current Protocols in Molecular Biology*, p. 21.29.1-21.29.9. Hoboken, NJ, USA: John Wiley & Sons, Inc.

Buntrock, L., Marec, F., Krueger, S. and Traut, W. (2012). Organ growth without cell division: somatic polyploidy in a moth, Ephestia kuehniella. *Genome* **55**, 755–763.

Busse, S. M., McMillen, P. T. and Levin, M. (2018). Cross-limb communication during Xenopus hindlimb regenerative response: non-local bioelectric injury signals. *Development* **145**,.

Chang, W., Worman, H. J. and Gundersen, G. G. (2015). Accessorizing and anchoring the LINC complex for multifunctionality. *The Journal of Cell Biology* **208**, 11–22.

Chang, J., Baker, J. and Wills, A. (2017). Transcriptional dynamics of tail regeneration in Xenopus tropicalis. *Genesis* **55**,.

Chen, Z.-J., Wang, W.-P., Chen, Y.-C., Wang, J.-Y., Lin, W.-H., Tai, L.-A., Liou, G.-G., Yang, C.-S. and Chi, Y.-H. (2014). Dysregulated interactions between lamin A and SUN1 induce abnormalities in the nuclear envelope and endoplasmic reticulum in progeric laminopathies. *Journal of Cell Science* **127**, 1792–1804.

Cho, Y. and Cavalli, V. (2014). HDAC signaling in neuronal development and axon regeneration. *Current Opinion in Neurobiology* **27**, 118–126.

Christen, B., Beck, C. W., Lombardo, A. and Slack, J. M. W. (2003). Regeneration-specific expression pattern of three posterior Hox genes. *Dev Dyn* **226**, 349–355.

Coleman, M. (2005). Axon degeneration mechanisms: commonality amid diversity. *Nature Reviews Neuroscience* **6**, 889–898.

Creyghton, M. P., Cheng, A. W., Welstead, G. G., Kooistra, T., Carey, B. W., Steine, E. J., Hanna, J., Lodato, M. A., Frampton, G. M., Sharp, P. A., et al. (2010). Histone

H3K27ac separates active from poised enhancers and predicts developmental state. *PNAS* **107**, 21931–21936.

Czermin, B., Melfi, R., McCabe, D., Seitz, V., Imhof, A. and Pirrotta, V. (2002). Drosophila enhancer of Zeste/ESC complexes have a histone H3 methyltransferase activity that marks chromosomal Polycomb sites. *Cell* **111**, 185–196.

Dahl, K. N., Scaffidi, P., Islam, M. F., Yodh, A. G., Wilson, K. L. and Misteli, T. (2006). Distinct structural and mechanical properties of the nuclear lamina in Hutchinson-Gilford progeria syndrome. *Proceedings of the National Academy of Sciences* **103**, 10271–10276.

Data - OPTN.

Davidson, P. M. and Lammerding, J. (2014). Broken nuclei – lamins, nuclear mechanics, and disease. *Trends in Cell Biology* **24**, 247–256.

Davis, R. L. and Kirschner, M. W. (2000). The fate of cells in the tailbud of Xenopus laevis. *Development* **127**,.

Denais, C. and Lammerding, J. (2014). Nuclear Mechanics in Cancer. In *Advances in experimental medicine and biology*, pp. 435–470.

Dixon, J. R., Selvaraj, S., Yue, F., Kim, A., Li, Y., Shen, Y., Hu, M., Liu, J. S. and Ren, B. (2012). Topological domains in mammalian genomes identified by analysis of chromatin interactions. *Nature* **485**, 376–380.

Dixon, J. R., Jung, I., Selvaraj, S., Shen, Y., Antosiewicz-Bourget, J. E., Lee, A. Y., Ye, Z., Kim, A., Rajagopal, N., Xie, W., et al. (2015). Chromatin architecture reorganization during stem cell differentiation. *Nature* **518**, 331–336.

Dovey, O. M., Foster, C. T. and Cowley, S. M. (2010). Histone deacetylase 1 (HDAC1), but not HDAC2, controls embryonic stem cell differentiation. *PNAS* **107**, 8242–8247.

Dreesen, O., Chojnowski, A., Ong, P. F., Zhao, T. Y., Common, J. E., Lunny, D., Lane, E. B., Lee, S. J., Vardy, L. A., Stewart, C. L., et al. (2013). Lamin B1 fluctuations have differential effects on cellular proliferation and senescence. *The Journal of Cell Biology* **200**, 605–617.

Durand, B. C. (2016). Stem cell-like Xenopus Embryonic Explants to Study Early Neural Developmental Features In Vitro and In Vivo. *J Vis Exp*.

Dutta, A. and Kumar Sinha, D. (2015). Turnover of the actomyosin complex in zebrafish embryos directs geometric remodelling and the recruitment of lipid droplets. *Scientific Reports* **5**, 13915–13915.

Eden, E., Lipson, D., Yogev, S. and Yakhini, Z. (2007). Discovering Motifs in Ranked Lists of DNA Sequences. *PLOS Computational Biology* **3**, e39.

Eden, E., Navon, R., Steinfeld, I., Lipson, D. and Yakhini, Z. (2009). GOrilla: a tool for discovery and visualization of enriched GO terms in ranked gene lists. *BMC Bioinformatics* **10**, 48.

Edwards-Faret, G., González-Pinto, K., Cebrián-Silla, A., Peñailillo, J., García-Verdugo, J. M. and Larraín, J. (2021). Cellular response to spinal cord injury in regenerative and non-regenerative stages in Xenopus laevis. *Neural development* **16**, 2–2.

Esmaeili, M., Blythe, S. A., Tobias, J. W., Zhang, K., Yang, J. and Klein, P. S. (2020). Chromatin accessibility and histone acetylation in the regulation of competence in early development. *Dev Biol* **462**, 20–35.

Ferreira, F., Raghunathan, V., Luxardi, G., Zhu, K. and Zhao, M. (2018). Early redox activities modulate Xenopus tail regeneration. *Nat Commun* **9**, 4296.

Franchini, A. and Bertolotti, E. (2011). Tail regenerative capacity and iNOS immunolocalization in Xenopus laevis tadpoles. *Cell and Tissue Research* **344**, 261–269.

Fraser, J., Ferrai, C., Chiariello, A. M., Schueler, M., Rito, T., Laudanno, G., Barbieri, M., Moore, B. L., Kraemer, D. C. A., Aitken, S., et al. (2015). Hierarchical folding and reorganization of chromosomes are linked to transcriptional changes in cellular differentiation. *Molecular systems biology* **11**, 852–852.

Frost, B., Bardai, F. H. and Feany, M. B. (2016). Lamin Dysfunction Mediates Neurodegeneration in Tauopathies. *Current Biology* **26**, 129–136.

Fu, Y., Chin, L. K., Bourouina, T., Liu, A. Q. and VanDongen, A. M. J. (2012). Nuclear deformation during breast cancer cell transmigration. *Lab on a Chip* **12**, 3774–3774.

Galili, T. (2021). *talgalili/gplots*.

Gdula, M. R., Poterlowicz, K., Mardaryev, A. N., Sharov, A. A., Peng, Y., Fessing, M. Y. and Botchkarev, V. A. (2013). Remodeling of Three-Dimensional Organization of the Nucleus during Terminal Keratinocyte Differentiation in the Epidermis. *Journal of Investigative Dermatology* **133**, 2191–2201.

Gehrke, A. R., Neverett, E., Luo, Y.-J., Brandt, A., Ricci, L., Hulett, R. E., Gompers, A., Ruby, J. G., Rokhsar, D. S., Reddien, P. W., et al. (2019). Acoel genome reveals the regulatory landscape of whole-body regeneration. *Science* **363**,.

Gerber, T., Murawala, P., Knapp, D., Masselink, W., Schuez, M., Hermann, S., Gac-Santel, M., Nowoshilow, S., Kageyama, J., Khattak, S., et al. (2018). Single-cell analysis uncovers convergence of cell identities during axolotl limb regeneration. *Science* **362**,.

ggplot2 Based Publication Ready Plots.

Giarmarco, M. M., Cleghorn, W. M., Sloat, S. R., Hurley, J. B. and Brockerhoff, S. E. (2017). Mitochondria Maintain Distinct Ca 2+ Pools in Cone Photoreceptors. *The Journal of Neuroscience* **37**, 2061–2072.

Gilsbach, R., Schwaderer, M., Preissl, S., Grüning, B. A., Kranzhöfer, D., Schneider, P., Nührenberg, T. G., Mulero-Navarro, S., Weichenhan, D., Braun, C., et al. (2018). Distinct epigenetic programs regulate cardiac myocyte development and disease in the human heart in vivo. *Nature Communications* **9**, 391.

Godwin, J. W., Pinto, A. R. and Rosenthal, N. A. (2013). Macrophages are required for adult salamander limb regeneration. *Proceedings of the National Academy of Sciences of the United States of America* **110**, 9415–9420.

Goldman, R. D., Shumaker, D. K., Erdos, M. R., Eriksson, M., Goldman, A. E., Gordon, L. B., Gruenbaum, Y., Khuon, S., Mendez, M., Varga, R. E., et al. (2004). Accumulation of mutant lamin A causes progressive changes in nuclear architecture in Hutchinson–Gilford progeria syndrome.

Good, M. C., Vahey, M. D., Skandarajah, A., Fletcher, D. A. and Heald, R. (2013). Cytoplasmic volume modulates spindle size during embryogenesis. *Science (New York, N.Y.)* **342**, 856–60.

Grainger, R. M. (2012). Xenopus tropicalis as a Model Organism for Genetics and Genomics: Past, Present and Future. *Methods Mol Biol* **917**, 3–15.

Guelen, L., Pagie, L., Brasset, E., Meuleman, W., Faza, M. B., Talhout, W., Eussen, B. H., de Klein, A., Wessels, L., de Laat, W., et al. (2008). Domain organization of human chromosomes revealed by mapping of nuclear lamina interactions. *Nature* **453**, 948–951.

Guilak, F., Tedrow, J. R. and Burgkart, R. (2000). Viscoelastic Properties of the Cell Nucleus. *Biochemical and Biophysical Research Communications* **269**, 781–786.

Gupta, R., Wills, A., Ucar, D. and Baker, J. (2014). Developmental enhancers are marked independently of zygotic Nodal signals in Xenopus. *Developmental Biology* **395**, 38–49.

Hahne, F. and Ivanek, R. (2016). Visualizing Genomic Data Using Gviz and Bioconductor. In *Statistical Genomics: Methods and Protocols* (ed. Mathé, E.) and Davis, S.), pp. 335–351. New York, NY: Springer.

Harris, R. E., Setiawan, L., Saul, J. and Hariharan, I. K. (2016). Localized epigenetic silencing of a damage-activated WNT enhancer limits regeneration in mature Drosophila imaginal discs. *eLife* **5**,.

Harris, R. E., Stinchfield, M. J., Nystrom, S. L., McKay, D. J. and Hariharan, I. K. (2020). Damage-responsive, maturity-silenced enhancers regulate multiple genes that direct regeneration in Drosophila. *Elife* **9**,.

Hatch, E. M. and Hetzer, M. W. (2016). Nuclear envelope rupture is induced by actin-based nucleus confinement. *The Journal of cell biology* **215**, 27–36.

Hatch, E. M., Fischer, A. H., Deerinck, T. J. and Hetzer, M. W. (2013). Catastrophic nuclear envelope collapse in cancer cell micronuclei. *Cell* **154**, 47–60.

Hayashi, S., Kawaguchi, A., Uchiyama, I., Kawasumi-Kita, A., Kobayashi, T., Nishide, H., Tsutsumi, R., Tsuru, K., Inoue, T., Ogino, H., et al. (2015). Epigenetic modification maintains intrinsic limb-cell identity in Xenopus limb bud regeneration. *Developmental Biology* **406**, 271–282.

Heinz, S., Benner, C., Spann, N., Bertolino, E., Lin, Y. C., Laslo, P., Cheng, J. X., Murre, C., Singh, H. and Glass, C. K. (2010). Simple combinations of lineage-determining transcription factors prime cis-regulatory elements required for macrophage and B cell identities. *Mol Cell* **38**, 576–589.

Hellsten, U., Harland, R. M., Gilchrist, M. J., Hendrix, D., Jurka, J., Kapitonov, V., Ovcharenko, I., Putnam, N. H., Shu, S., Taher, L., et al. (2010). The Genome of the Western Clawed Frog Xenopus tropicalis. *Science* **328**, 633–636.

Hirose, K., Shimoda, N. and Kikuchi, Y. (2013). Transient reduction of 5-methylcytosine and 5-hydroxymethylcytosine is associated with active DNA demethylation during regeneration of zebrafish fin. *Epigenetics* **8**, 899–906.

Ho, D. M. and Whitman, M. (2008). TGF-β signaling is required for multiple processes during Xenopus tail regeneration. *Developmental Biology* **315**, 203–216.

Ho, C. Y., Jaalouk, D. E., Vartiainen, M. K. and Lammerding, J. (2013). Lamin A/C and emerin regulate MKL1–SRF activity by modulating actin dynamics. *Nature* **497**, 507–511.

Hsu, M.-N., Chang, Y.-H., Truong, V. A., Lai, P.-L., Nguyen, T. K. N. and Hu, Y.-C. (2019). CRISPR technologies for stem cell engineering and regenerative medicine. *Biotechnology Advances* **37**, 107447.

Jamaladdin, S., Kelly, R. D. W., O'Regan, L., Dovey, O. M., Hodson, G. E., Millard, C. J., Portolano, N., Fry, A. M., Schwabe, J. W. R. and Cowley, S. M. (2014). Histone deacetylase (HDAC) 1 and 2 are essential for accurate cell division and the pluripotency of embryonic stem cells. *PNAS* **111**, 9840–9845.

Jevtić, P. and Levy, D. L. (2015). Nuclear Size Scaling during Xenopus Early Development Contributes to Midblastula Transition Timing. *Current Biology* **25**, 45–52.

Jevtić, P., Edens, L. J., Li, X., Nguyen, T., Chen, P. and Levy, D. L. (2015). Concentration-dependent Effects of Nuclear Lamins on Nuclear Size in Xenopus and Mammalian Cells. *Journal of Biological Chemistry* **290**, 27557–27571.

Jorstad, N. L., Wilken, M. S., Grimes, W. N., Wohl, S. G., VandenBosch, L. S., Yoshimatsu, T., Wong, R. O., Rieke, F. and Reh, T. A. (2017). Stimulation of functional neuronal regeneration from Müller glia in adult mice. *Nature* **548**, 103–107.

Julier, Z., Park, A. J., Briquez, P. S. and Martino, M. M. (2017). Promoting tissue regeneration by modulating the immune system. *Acta Biomaterialia* **53**, 13–28.

Kakebeen, A. D. and Wills, A. E. (2019). More Than Just a Bandage: Closing the Gap Between Injury and Appendage Regeneration. *Frontiers in physiology* **10**, 81–81.

Kakebeen, A. D., Chitsazan, A. D., Williams, M. C., Saunders, L. M. and Wills, A. E. (2020). Chromatin accessibility dynamics and single cell RNA-seq reveal new regulators of regeneration in neural progenitors. *eLife* **9**,.

Kalendová, A., Kalasová, I., Yamazaki, S., Uličná, L., Harata, M. and Hozák, P. (2014). Nuclear actin filaments recruit cofilin and actin-related protein 3, and their formation is connected with a mitotic block. *Histochemistry and Cell Biology* **142**, 139–152.

Karimi, K., Fortriede, J. D., Lotay, V. S., Burns, K. A., Wang, D. Z., Fisher, M. E., Pells, T. J., James-Zorn, C., Wang, Y., Ponferrada, V. G., et al. (2018). Xenbase: a genomic, epigenomic and transcriptomic model organism database. *Nucleic Acids Res* **46**, D861–D868.

Karmodiya, K., Krebs, A. R., Oulad-Abdelghani, M., Kimura, H. and Tora, L. (2012). H3K9 and H3K14 acetylation co-occur at many gene regulatory elements, while H3K14ac marks a subset of inactive inducible promoters in mouse embryonic stem cells. *BMC Genomics* **13**, 424.

Kawasumi, A., Sagawa, N., Hayashi, S., Yokoyama, H. and Tamura, K. (2013). Wound healing in mammals and amphibians: toward limb regeneration in mammals. *Current topics in microbiology and immunology* **367**, 33–49.

Kaya-Okur, H. S., Wu, S. J., Codomo, C. A., Pledger, E. S., Bryson, T. D., Henikoff, J. G., Ahmad, K. and Henikoff, S. (2019). CUT&Tag for efficient epigenomic profiling of small samples and single cells. *Nature Communications* **10**, 1930.

Keeling, M. C., Flores, L. R., Dodhy, A. H., Murray, E. R. and Gavara, N. (2017). Actomyosin and vimentin cytoskeletal networks regulate nuclear shape, mechanics and chromatin organization. *Scientific reports* **7**, 5219–5219.

Kha, H. N., Chen, B. K., Clark, G. M. and Jones, R. (2004). Stiffness properties for Nucleus standard straight and contour electrode arrays. *Medical Engineering & Physics* **26**, 677–685.

Khokha, M. K., Chung, C., Bustamante, E. L., Gaw, L. W. K., Trott, K. A., Yeh, J., Lim, N., Lin, J. C. Y., Taverner, N., Amaya, E., et al. (2002). Techniques and probes for the study ofXenopus tropicalis development. *Developmental Dynamics* **225**, 499–510.

Kieserman, E. K., Lee, C., Gray, R. S., Park, T. J. and Wallingford, J. B. (2010). High-magnification in vivo imaging of Xenopus embryos for cell and developmental biology. *Cold Spring Harbor protocols* **2010**, pdb.prot5427-pdb.prot5427.

Kim, D.-H. and Wirtz, D. (2015). Cytoskeletal tension induces the polarized architecture of the nucleus. *Biomaterials* **48**, 161–172.

King, M. C. and Lusk, C. P. (2016). A model for coordinating nuclear mechanics and membrane remodeling to support nuclear integrity. *Current opinion in cell biology* **41**, 9–17.

Krueger, F. (2021). *FelixKrueger/TrimGalore*.

Krumm, A. and Duan, Z. (2019). Understanding the 3D genome: Emerging impacts on human disease. *Seminars in Cell & Developmental Biology* **90**, 62–77.

Lammerding, J., Fong, L. G., Ji, J. Y., Reue, K., Stewart, C. L., Young, S. G. and Lee, R. T. (2006). Lamins A and C but Not Lamin B1 Regulate Nuclear Mechanics. *Journal of Biological Chemistry* **281**, 25768–25780.

Langmead, B. and Salzberg, S. L. (2012). Fast gapped-read alignment with Bowtie 2. *Nature Methods* **9**, 357–359.

Langmead, B., Wilks, C., Antonescu, V. and Charles, R. (2019). Scaling read aligners to hundreds of threads on general-purpose processors. *Bioinformatics* **35**, 421–432.

Lawrence, M., Huber, W., Pagès, H., Aboyoun, P., Carlson, M., Gentleman, R., Morgan, M. T. and Carey, V. J. (2013). Software for Computing and Annotating Genomic Ranges. *PLOS Computational Biology* **9**, e1003118.

Lee, J.-Y. and Harland, R. M. (2007). Actomyosin contractility and microtubules drive apical constriction in Xenopus bottle cells. *Developmental Biology* **311**, 40–52.

Lee-Liu, D., Moreno, M., Almonacid, L. I., Tapia, V. S., Muñoz, R., von Marées, J., Gaete, M., Melo, F. and Larraín, J. (2014). Genome-wide expression profile of the response to spinal cord injury in Xenopus laevis reveals extensive differences between regenerative and non-regenerative stages. *Neural Development* **9**, 12.

Lee-Liu, D., Méndez-Olivos, E. E., Muñoz, R. and Larraín, J. (2017). The African clawed frog Xenopus laevis: A model organism to study regeneration of the central nervous system. *Neuroscience Letters* **652**, 82–93.

Lemaitre, J. M., Géraud, G. and Méchali, M. (1998). Dynamics of the genome during early Xenopus laevis development: karyomeres as independent units of replication. *The Journal of cell biology* **142**, 1159–66.

Levy, D. L. and Heald, R. (2010). Nuclear size is regulated by importin α and Ntf2 in Xenopus. *Cell* **143**, 288–98.

Li, H., Handsaker, B., Wysoker, A., Fennell, T., Ruan, J., Homer, N., Marth, G., Abecasis, G., Durbin, R., and 1000 Genome Project Data Processing Subgroup (2009). The Sequence Alignment/Map format and SAMtools. *Bioinformatics* **25**, 2078–2079.

Li, Y., Hassinger, L., Thomson, T., Ding, B., Ashley, J., Hassinger, W. and Budnik, V. (2016). Lamin Mutations Accelerate Aging via Defective Export of Mitochondrial mRNAs through Nuclear Envelope Budding. *Current Biology* **26**, 2052–2059.

Liao, Y., Smyth, G. K. and Shi, W. (2014). featureCounts: an efficient general purpose program for assigning sequence reads to genomic features. *Bioinformatics* **30**, 923–930.

Lin, G. and Slack, J. M. W. (2008). Requirement for Wnt and FGF signaling in Xenopus tadpole tail regeneration. *Dev Biol* **316**, 323–335.

Lin, G., Chen, Y. and Slack, J. M. W. (2007). Regeneration of neural crest derivatives in the Xenopus tadpole tail. *BMC Dev Biol* **7**, 56.

Lis, J. T. (2019). A 50 year history of technologies that drove discovery in eukaryotic transcription regulation. *Nature Structural & Molecular Biology* **26**, 777–782.

Love, N. R., Chen, Y., Bonev, B., Gilchrist, M. J., Fairclough, L., Lea, R., Mohun, T. J., Paredes, R., Zeef, L. A. and Amaya, E. (2011). Genome-wide analysis of gene expression during Xenopus tropicalis tadpole tail regeneration. *BMC Developmental Biology* **11**, 70.

Mattout, A., Cabianca, D. S. and Gasser, S. M. (2015a). Chromatin states and nuclear organization in development — a view from the nuclear lamina. *Genome Biology* **16**, 174–174.

Mattout, A., Aaronson, Y., Sailaja, B. S., Raghu Ram, E. V., Harikumar, A., Mallm, J.-P., Sim, K. H., Nissim-Rafinia, M., Supper, E., Singh, P. B., et al. (2015b). Heterochromatin Protein 1β (HP1β) has distinct functions and distinct nuclear distribution in pluripotent versus differentiated cells. *Genome Biology* **16**, 213–213.

McKenna, T., Rosengardten, Y., Viceconte, N., Baek, J.-H., Grochová, D. and Eriksson, M. (2014). Embryonic expression of the common progeroid lamin A splice mutation arrests postnatal skin development. *Aging Cell* **13**, 292–302.

Mitogawa, K., Makanae, A. and Satoh, A. (2018). Hyperinnervation improves Xenopus laevis limb regeneration. *Developmental Biology* **433**, 276–286.

Moody, S. A. (1987). Fates of the blastomeres of the 16-cell stage Xenopus embryo. *Developmental biology* **119**, 560–78.

Moreau, N. and Boucher, Y. (2020). Hedging against Neuropathic Pain: Role of Hedgehog Signaling in Pathological Nerve Healing. *Int J Mol Sci* **21**,.

Nakayama, T., Fish, M. B., Fisher, M., Oomen-Hajagos, J., Thomsen, G. H. and Grainger, R. M. (2013). Simple and efficient CRISPR/Cas9-mediated targeted mutagenesis in Xenopus tropicalis. *Genesis (New York, N.Y. : 2000)* **51**, 835–43.

Nieuwkoop, P. D. (Pieter D.) and Faber, J. (1994). *Normal table of Xenopus laevis (Daudin) : a systematical and chronological survey of the development from the fertilized egg till the end of metamorphosis*. New York : Garland Pub.

Oda, H., Shirai, N., Ura, N., Ohsumi, K. and Iwabuchi, M. (2017). Chromatin tethering to the nuclear envelope by nuclear actin filaments: a novel role of the actin cytoskeleton in the Xenopus blastula. *Genes to Cells* **22**, 376–391.

Organ Donation Statistics | Organ Donor (2018).

Oulhen, N., Heyland, A., Carrier, T. J., Zazueta-Novoa, V., Fresques, T., Laird, J., Onorato, T. M., Janies, D. and Wessel, G. (2016). Regeneration in bipinnaria larvae of the bat star Patiria miniata induces rapid and broad new gene expression. *Mech Dev* **142**, 10–21.

Pai, V. P., Martyniuk, C. J., Echeverri, K., Sundelacruz, S., Kaplan, D. L. and Levin, M. (2016). Genome-wide analysis reveals conserved transcriptional responses downstream of resting potential change in Xenopus embryos, axolotl regeneration, and human mesenchymal cell differentiation. *Regeneration (Oxf)* **3**, 3–25.

Pajerowski, J. D., Dahl, K. N., Zhong, F. L., Sammak, P. J. and Discher, D. E. (2007). Physical plasticity of the nucleus in stem cell differentiation. *Proceedings of the National Academy of Sciences* **104**, 15619–15624.

Paré, J.-F., Martyniuk, C. J. and Levin, M. (2017). Bioelectric regulation of innate immune system function in regenerating and intact Xenopus laevis. *NPJ Regen Med* **2**, 15.

Paredes, R., Ishibashi, S., Borrill, R., Robert, J. and Amaya, E. (2015). Xenopus: An in vivo model for imaging the inflammatory response following injury and bacterial infection. *Dev Biol* **408**, 213–228.

Peddle, C. F., Fry, L. E., McClements, M. E. and MacLaren, R. E. (2020). CRISPR Interference-Potential Application in Retinal Disease. *Int J Mol Sci* **21**,.

Peric-Hupkes, D., Meuleman, W., Pagie, L., Bruggeman, S. W. M., Solovei, I., Brugman, W., Gräf, S., Flicek, P., Kerkhoven, R. M., van Lohuizen, M., et al. (2010). Molecular maps of the reorganization of genome-nuclear lamina interactions during differentiation. *Molecular cell* **38**, 603–13.

Perovanovic, J., Dell'Orso, S., Gnochi, V. F., Jaiswal, J. K., Sartorelli, V., Vigouroux, C., Mamchaoui, K., Mouly, V., Bonne, G. and Hoffman, E. P. (2016). Laminopathies disrupt epigenomic developmental programs and cell fate. *Science translational medicine* **8**, 335ra58-335ra58.

Petrie, T. A., Strand, N. S., Tsung-Yang, C., Rabinowitz, J. S. and Moon, R. T. (2014). Macrophages modulate adult zebrafish tail fin regeneration. *Development* **141**, 2581–2591.

Pfefferli, C., Müller, F., Jaźwińska, A. and Wicky, C. (2014). Specific NuRD components are required for fin regeneration in zebrafish. *BMC Biology* **12**, 30–30.

Phipps, L. S., Marshall, L., Dorey, K. and Amaya, E. (2020). Model systems for regeneration: Xenopus. *Development* **147**,.

Picard Tools - By Broad Institute.

Pillay, J., Tak, T., Kamp, V. M. and Koenderman, L. (2013). Immune suppression by neutrophils and granulocytic myeloid-derived suppressor cells: similarities and differences. *Cellular and Molecular Life Sciences* **70**, 3813–3827.

Plessner, M., Melak, M., Chinchilla, P., Baarlink, C. and Grosse, R. (2015). Nuclear F-actin formation and reorganization upon cell spreading. *The Journal of biological chemistry* **290**, 11209–16.

Poss, K. D., Shen, J., Nechiporuk, A., McMahon, G., Thisse, B., Thisse, C. and Keating, M. T. (2000). Roles for Fgf signaling during zebrafish fin regeneration. *Dev Biol* **222**, 347–358.

Prokopuk, L., Stringer, J. M., Hogg, K., Elgass, K. D. and Western, P. S. (2017). PRC2 is required for extensive reorganization of H3K27me3 during epigenetic reprogramming in mouse fetal germ cells. *Epigenetics & chromatin* **10**, 7–7.

Quinlan, A. R. and Hall, I. M. (2010). BEDTools: a flexible suite of utilities for comparing genomic features. *Bioinformatics* **26**, 841–842.

Rada-Iglesias, A., Bajpai, R., Swigut, T., Brugmann, S. A., Flynn, R. A. and Wysocka, J. (2011). A unique chromatin signature uncovers early developmental enhancers in humans. *Nature* **470**, 279–283.

Ramdas, N. M. and Shivashankar, G. V. (2015). Cytoskeletal Control of Nuclear Morphology and Chromatin Organization. *Journal of Molecular Biology* **427**, 695–706.

Rao, A. and LaBonne, C. (2018). Histone deacetylase activity has an essential role in establishing and maintaining the vertebrate neural crest. *Development* **145**,.

Rastelli, L., Chan, C. S. and Pirrotta, V. (1993). Related chromosome binding sites for zeste, suppressors of zeste and Polycomb group proteins in Drosophila and their dependence on Enhancer of zeste function. *EMBO J* **12**, 1513–1522.

Robinson, M. D., McCarthy, D. J. and Smyth, G. K. (2010). edgeR: a Bioconductor package for differential expression analysis of digital gene expression data. *Bioinformatics* **26**, 139–140.

Rowat, A. C., Jaalouk, D. E., Zwerger, M., Ung, W. L., Eydelnant, I. A., Olins, D. E., Olins, A. L., Herrmann, H., Weitz, D. A. and Lammerding, J. (2013). Nuclear Envelope Composition Determines the Ability of Neutrophil-type Cells to Passage through Micron-scale Constrictions. *Journal of Biological Chemistry* **288**, 8610–8618.

RStudio | Open source & professional software for data science teams.

Schindelin, J., Arganda-Carreras, I., Frise, E., Kaynig, V., Longair, M., Pietzsch, T., Preibisch, S., Rueden, C., Saalfeld, S., Schmid, B., et al. (2012). Fiji: an open-source platform for biological-image analysis. *Nature Methods* **9**, 676–682.

Schirmer, E. C., Guan, T. and Gerace, L. (2001). Involvement of the lamin rod domain in heterotypic lamin interactions important for nuclear organization. *The Journal of cell biology* **153**, 479–89.

Schöchlin, M., Weissinger, S. E., Brandes, A. R., Herrmann, M., Möller, P. and Lennerz, J. K. (2014). A nuclear circularity-based classifier for diagnostic distinction of desmoplastic from spindle cell melanoma in digitized histological images. *Journal of pathology informatics* **5**, 40–40.

Schoft, V. K., Beauvais, A. J., Lang, C., Gajewski, A., Prüfert, K., Winkler, C., Akimenko, M.-A., Paulin-Levasseur, M. and Krohne, G. (2003). The lamina-associated

polypeptide 2 (LAP2) isoforms beta, gamma and omega of zebrafish: developmental expression and behavior during the cell cycle. *Journal of cell science* **116**, 2505–17.

Schwarz, D., Varum, S., Zemke, M., Schöler, A., Baggiolini, A., Draganova, K., Koseki, H., Schübeler, D. and Sommer, L. (2014). Ezh2 is required for neural crest-derived cartilage and bone formation. *Development (Cambridge, England)* **141**, 867–77.

Sedzinski, J., Hannezo, E., Tu, F., Biro, M. and Wallingford, J. B. (2016). Emergence of an Apical Epithelial Cell Surface In Vivo. *Developmental cell* **36**, 24–35.

Shah, P. P., Donahue, G., Otte, G. L., Capell, B. C., Nelson, D. M., Cao, K., Aggarwala, V., Cruickshanks, H. A., Rai, T. S., McBryan, T., et al. (2013). Lamin B1 depletion in senescent cells triggers large-scale changes in gene expression and the chromatin landscape. *Genes & Development* **27**, 1787–1799.

Siebert, S., Farrell, J. A., Cazet, J. F., Abeykoon, Y., Primack, A. S., Schnitzler, C. E. and Juliano, C. E. (2019). Stem cell differentiation trajectories in Hydra resolved at single-cell resolution. *Science* **365**,.

Sive, H. L., Grainger, R. M. and Harland, R. M. (2007). Xenopus laevis Keller Explants. *CSH Protoc* **2007**, pdb.prot4749.

Sive, H. L., Grainger, Robert. and Harland, R. M. (2010). *Early development of Xenopus laevis : a laboratory manual*. Cold Spring Harbor Laboratory Press.

Skene, P. J. and Henikoff, S. (2017). An efficient targeted nuclease strategy for high-resolution mapping of DNA binding sites. *eLife* **6**,.

Slack, J. M. W., Beck, C. W., Gargioli, C. and Christen, B. (2004). Cellular and molecular mechanisms of regeneration in Xenopus. In *Philosophical Transactions of the Royal Society B: Biological Sciences*, pp. 745–751. Royal Society.

Slack, J. M. W., Lin, G. and Chen, Y. (2008). Molecular and Cellular Basis of Regeneration and Tissue Repair. *Cellular and Molecular Life Sciences* **65**, 54–63.

Solovei, I., Kreysing, M., Lanctôt, C., Kösem, S., Peichl, L., Cremer, T., Guck, J. and Joffe, B. (2009). Nuclear Architecture of Rod Photoreceptor Cells Adapts to Vision in Mammalian Evolution. *Cell* **137**, 356–368.

Solovei, I., Wang, A. S., Thanisch, K., Schmidt, C. S., Krebs, S., Zwerger, M., Cohen, T. V., Devys, D., Foisner, R., Peichl, L., et al. (2013). LBR and lamin A/C sequentially tether peripheral heterochromatin and inversely regulate differentiation. *Cell* **152**, 584–98.

Srivatsan, S. R., McFaline-Figueroa, J. L., Ramani, V., Saunders, L., Cao, J., Packer, J., Pliner, H. A., Jackson, D. L., Daza, R. M., Christiansen, L., et al. (2020). Massively multiplex chemical transcriptomics at single-cell resolution. *Science* **367**, 45–51.

Stergachis, A. B., Neph, S., Reynolds, A., Humbert, R., Miller, B., Paige, S. L., Vernot, B., Cheng, J. B., Thurman, R. E., Sandstrom, R., et al. (2013). Developmental Fate and Cellular Maturity Encoded in Human Regulatory DNA Landscapes. *Cell* **154**, 888–903.

Storer, M. A., Mahmud, N., Karamboulas, K., Borrett, M. J., Yuzwa, S. A., Gont, A., Androschuk, A., Sefton, M. V., Kaplan, D. R. and Miller, F. D. (2020). Acquisition of a Unique Mesenchymal Precursor-like Blastema State Underlies Successful Adult Mammalian Digit Tip Regeneration. *Dev Cell* **52**, 509-524.e9.

Suzuki, M., Yakushiji, N., Nakada, Y., Satoh, A., Ide, H. and Tamura, K. (2006). Limb regeneration in Xenopus laevis froglet. *TheScientificWorldJournal* **6**, 26–37.

Swift, J., Ivanovska, I. L., Buxboim, A., Harada, T., Dingal, P. C. D. P., Pinter, J., Pajerowski, J. D., Spinler, K. R., Shin, J.-W., Tewari, M., et al. (2013). Nuclear Lamin-A Scales with Tissue Stiffness and Enhances Matrix-Directed Differentiation. *Science* **341**, 1240104–1240104.

Taniguchi, Y., Watanabe, K. and Mochii, M. (2014). Notochord-derived hedgehog is essential for tail regeneration in Xenopus tadpole. *BMC Developmental Biology* **14**,.

Tariq, Z., Zhang, H., Chia-Liu, A., Shen, Y., Gete, Y., Xiong, Z.-M., Tocheny, C., Campanello, L., Wu, D., Losert, W., et al. (2017). Lamin A and microtubules collaborate to maintain nuclear morphology. *Nucleus* **8**, 433–446.

Taylor, A. J. and Beck, C. W. (2012). Histone deacetylases are required for amphibian tail and limb regeneration but not development. *Mechanisms of development* **129**, 208–18.

Thakore, P. I., D'Ippolito, A. M., Song, L., Safi, A., Shivakumar, N. K., Kabadi, A. M., Reddy, T. E., Crawford, G. E. and Gersbach, C. A. (2015). Highly specific epigenome editing by CRISPR-Cas9 repressors for silencing of distal regulatory elements. *Nature Methods* **12**, 1143–1149.

Towbin, B. D., González-Aguilera, C., Sack, R., Gaidatzis, D., Kalck, V., Meister, P., Askjaer, P. and Gasser, S. M. (2012). Step-Wise Methylation of Histone H3K9 Positions Heterochromatin at the Nuclear Periphery. *Cell* **150**, 934–947.

Tseng, A.-S. S., Carneiro, K., Lemire, J. M. and Levin, M. (2011). HDAC Activity Is Required during Xenopus Tail Regeneration. *PLoS ONE* **6**, e26382–e26382.

Tucker, A. S. and Slack, J. M. W. (2004). Independent induction and formation of the dorsal and ventral fins inXenopus laevis. *Developmental Dynamics* **230**, 461–467.

VandenBosch, L. S., Wohl, S. G., Wilken, M. S., Hooper, M., Finkbeiner, C., Cox, K., Chipman, L. and Reh, T. A. (2020). Developmental changes in the accessible chromatin, transcriptome and Ascl1-binding correlate with the loss in Müller Glial regenerative potential. *Sci Rep* **10**, 13615.

Vergnes, L., Peterfy, M., Bergo, M. O., Young, S. G. and Reue, K. (2004). Lamin B1 is required for mouse development and nuclear integrity. *Proceedings of the National Academy of Sciences* **101**, 10428–10433.

Versaevel, M., Grevesse, T. and Gabriele, S. (2012). Spatial coordination between cell and nuclear shape within micropatterned endothelial cells. *Nature Communications* **3**, 671–671.

Verstraeten, V. L. R. M., Ji, J. Y., Cummings, K. S., Lee, R. T. and Lammerding, J. (2008). Increased mechanosensitivity and nuclear stiffness in Hutchinson–Gilford progeria cells: effects of farnesyltransferase inhibitors. *Aging Cell* **7**, 383–393.

Vishavkarma, R., Raghavan, S., Kuyyamudi, C., Majumder, A., Dhawan, J. and Pullarkat, P. A. (2014). Role of actin filaments in correlating nuclear shape and cell spreading. *PloS one* **9**, e107895–e107895.

Voss, S. R., Ponomareva, L. V., Dwaraka, V. B., Pardue, K. E., Baddar, N. W. A. H., Rodgers, A. K., Woodcock, M. R., Qiu, Q., Crowner, A., Blichmann, D., et al. (2019). HDAC Regulates Transcription at the Outset of Axolotl Tail Regeneration. *Scientific Reports* **9**,.

Wallingford, J. B. (2010). Low-Magnification Live Imaging of Xenopus Embryos for Cell and Developmental Biology. *Cold Spring Harbor Protocols* **2010**, pdb.prot5425-pdb.prot5425.

Wallingford, J. B. (2019). We Are All Developmental Biologists. *Developmental Cell* **50**, 132–137.

Wallingford, J. B. (2021). Aristotle, Buddhist scripture and embryology in ancient Mexico: building inclusion by re-thinking what counts as the history of developmental biology. *Development* **148**,.

Wang, Z., Zang, C., Rosenfeld, J. A., Schones, D. E., Barski, A., Cuddapah, S., Cui, K., Roh, T.-Y., Peng, W., Zhang, M. Q., et al. (2008). Combinatorial patterns of histone acetylations and methylations in the human genome. *Nature Genetics* **40**, 897–903.

Wang, M. H., Wu, C. H., Huang, T. Y., Sung, H. W., Chiou, L. L., Lin, S. P. and Lee, H. S. (2019). Nerve-mediated expression of histone deacetylases regulates limb regeneration in axolotls. *Developmental Biology* **449**, 122–131.

Webster, M., Witkin, K. L. and Cohen-Fix, O. (2009). Sizing up the nucleus: nuclear shape, size and nuclear-envelope assembly. *Journal of Cell Science* **122**, 1477–1486.

Wiggan, O., Schroder, B., Krapf, D., Bamburg, J. R. and DeLuca, J. G. (2017). Cofilin Regulates Nuclear Architecture through a Myosin-II Dependent Mechanotransduction Module. *Scientific reports* **7**, 40953–40953.

Wu, C. H., Tsai, M. H., Ho, C. C., Chen, C. Y. and Lee, H. S. (2013). De novo transcriptome sequencing of axolotl blastema for identification of differentially expressed genes during limb regeneration. *BMC Genomics* **14**,.

Wühr, M., Güttler, T., Peshkin, L., McAlister, G. C., Sonnett, M., Ishihara, K., Groen, A. C., Presler, M., Erickson, B. K., Mitchison, T. J., et al. (2015). The Nuclear Proteome of a Vertebrate. *Current Biology* **25**, 2663–2671.

Yakushiji, N., Suzuki, M., Satoh, A., Sagai, T., Shiroishi, T., Kobayashi, H., Sasaki, H., Ide, H. and Tamura, K. (2007). Correlation between Shh expression and DNA methylation status of the limb-specific Shh enhancer region during limb regeneration in amphibians. *Developmental biology* **312**, 171–82.

Yang, S. H., Chang, S. Y., Yin, L., Tu, Y., Hu, Y., Yoshinaga, Y., de Jong, P. J., Fong, L. G. and Young, S. G. (2011). An absence of both lamin B1 and lamin B2 in keratinocytes has no effect on cell proliferation or the development of skin and hair. *Human Molecular Genetics* **20**, 3537–3544.

Yi, S., Tang, X., Yu, J., Liu, J., Ding, F. and Gu, X. (2017). Microarray and qPCR Analyses of Wallerian Degeneration in Rat Sciatic Nerves. *Front. Cell. Neurosci.* **11**,.

Zhang, Y., Liu, T., Meyer, C. A., Eeckhoute, J., Johnson, D. S., Bernstein, B. E., Nussbaum, C., Myers, R. M., Brown, M., Li, W., et al. (2008). Model-based Analysis of ChIP-Seq (MACS). *Genome Biology* **9**, R137–R137.

Zwerger, M., Jaalouk, D. E., Lombardi, M. L., Isermann, P., Mauermann, M., Dialynas, G., Herrmann, H., Wallrath, L. L. and Lammerding, J. (2013). Myopathic lamin mutations impair nuclear stability in cells and tissue and disrupt nucleo-cytoskeletal coupling. *Human molecular genetics* **22**, 2335–49.

APPENDIX A: ATAC-SEQ PIPELINE WORKFLOW

#read trimming and initial qc

trim_galore --paired --phred33 --fastqc --trim1 --nextera ../fastq/G001_SG_Wills_08_WhT41_S1_R1_001.fastq.gz ../fastq/G001_SG_Wills_08_WhT41_S1_R2_001.fastq.gz --output_dir ../fastq/trimmed/ --fastqc_args "--outdir ../fastq/trimmed/fastqc/"

#alignment and bam generation

bowtie2 --very-sensitive -x /gscratch/hpc/crbraden/genomes/xenTro9/bowtie2/xenTro9 -X 2000 2>> ../BAM/bowtie_log.txt -p 2 -1 ../fastq/trimmed/G001_SG_Wills_08_WhT41_S1_R1_001_val_1.fq.gz -2 ../fastq/trimmed/G001_SG_Wills_08_WhT41_S1_R2_001_val_2.fq.gz | samtools view -Sb - | samtools sort - -o ../BAM/G001_SG_Wills_08_WhT41_S1_R.bam

#make bigwig

Rscript bam2rpm.r -b /gscratch/hpc/crbraden/Wills/2019_ATACseq_HEA/scripts/../fastq/../BAM -bw /gscratch/hpc/crbraden/Wills/2019_ATACseq_HEA/scripts/../fastq/../bigwig -rdir /gscratch/hpc/crbraden/Wills/2019_ATACseq_HEA/scripts/../fastq/../bigwig/rdir >> /gscratch/hpc/crbraden/Wills/2019_ATACseq_HEA/scripts/../fastq/../bigwig/rdir/bam2rpm_log.txt

#duplicate read marking with picard

picardtools="java -XX:ParallelGCThreads=8 -jar /gscratch/hpc/crbraden/python_env/picard.jar"

picard_markdup () {

    local arg=$1

    echo "removing duplicates from $arg, writing to ${arg%.bam}.markdup.bam"

    $picardtools MarkDuplicates I=$arg O="${arg%.bam}.markdup.bam" M="${arg%.bam}.markdup.metrics"

```
#collect alignment metrics

picardtools="java -jar /gscratch/hpc/crbraden/python_env/picard.jar"

picard_metrics () {

	local arg=$1

	echo "collecting metrics for $arg, writing to ${arg%.bam}.metrics"

	$picardtools CollectAlignmentSummaryMetrics R=/gscratch/hpc/crbraden/genomes/xenTro9/Sequence/DNA/xenTro9.fa.$

}



#remove duplicates, maybe unmapped and discordant

filterdup () {

	    local arg=$1

	echo "removing duplicates from $arg, writing to ${arg%.markdup.bam}.rmdup.bam"

	samtools view -q 20 -F 1804 -@ 8 -b -h $arg > "${arg%.markdup.bam}.rmdup.bam"

}



#per-sample peak calling

macs2 callpeak -t /gscratch/hpc/crbraden/Wills/2019_ATACseq_HEA/HEA_MHD_combine/scripts_shared//../BAM/01_SG_Wills_07_WT_Whole-Tail_0hpa_Run01_S1_R.rmdup.bam --nomodel --shift -100 --extsize 200 -g 1.7e9 -n 01_SG_Wills_07_WT_Whole-Tail_0hpa_Run01_S1_R.rmdup --outdir /gscratch/hpc/crbraden/Wills/2019_ATACseq_HEA/HEA_MHD_combine/scripts_shared//../BAM/../bed/
```

```
#unified peak set generation

cat ../bed/*_summits.bed > ../peak_merge/all.summits.bed

sort -k1,1 -k2,2n ../peak_merge/all.summits.bed > ../peak_merge/all.summits.sorted.bed

awk -v OFS="\t" '$2<200 {print $1,"0",$2+200,$4,$5;next};{print $1,$2-199,$2+200,$4,$5}' ../peak_merge/all.summits.so$

#it may be important to decide whether the -d setting on bedtools merge below is really what we want

bedtools merge -d -201 -i ../peak_merge/all.summits.sorted.window.bed > ../peak_merge/all.summits.window.merged.bed

awk -v OFS="\t" 'BEGIN {print "GeneID","Chr","Start","End","Strand"} {print "Peak_"NR,$1,$2,$3,"."}' ../peak_merge/al$

featureCounts -F SAF -T 16 -p\

    -a ../peak_merge/all.summits.window.merged.saf \

    -o ../peak_merge/summit_window_merged_counts.txt \

    ../BAM/*.bam



#peak annotation, per sample: on Chris's local environment

source ~/miniconda3/etc/profile.d/conda.sh

conda activate motifs



anno () {

        local file=$1

        mkdir "homer_out/${file%.homerpeak}"

        annotatePeaks.pl $file xenTro9 -gsize 1700000000 -genomeOntology "homer_out/${file%.homerpeak}" > "homer_out/${file%.homerpeak}.log" 2>&
```

VITA

Hannah Arbach grew up in a family with a parent serving as an active-duty officer in the US Airforce. This provided them with the privilege to live at one of the alternate NASA space shuttle landing sites in Edwards Airforce Base, CA where they watched two shuttle landings, which helped spark their love of science. Hannah graduated in 2015 with a B.A. *cum laude* in biochemistry from Mount Holyoke College where they were a four-year varsity athlete on the rowing team and two-year team captain. While at Mount Holyoke College Hannah was encouraged by their academic advisor Dr. Wei Chen to try laboratory research before fully committing to being a pre-med student. Hannah met with their eventual research advisor Dr. Kathryn McMenimen whose lab focused on chemical biology and studying small heat-shock proteins and fell in love with having their job be to ask new questions and discover things no one else had before. Hannah's work in Katie's lab culminated in a first author paper. Hannah moved across the country immediately after graduating to begin their PhD at UW. They made the leap from a biochemistry heavy lab to developmental biology in Dr. Andrea Wills' lab. They became a passionate microscopist at the Woods Hole advanced *Xenopus* imaging course and a card-carrying developmental biologist at the Embryology course also at Woods Hole. When not in lab Hannah enjoys cooking, a good beer, good whiskey, adventurous cocktails, snuggles with their cats, going on nature adventures with their wife.